Universitetet i Stavanger

FACULTY OF SCIENCE AND TECHNOLOGY

MASTER'S THESIS

Study program / Specialization: MSc Petroleum Engineering / Reservoir Engineering	Spring semester, 2017 Open
Author: Daisy Siti Aisyah	…… (signature of author)
Supervisor(s): Dr. Pål Østebø Andersen Co-Supervisor: Kenny Walrond, M.Sc	
Title of master's thesis: **Modelling of co-current spontaneous imbibition – improved understanding of reservoir flow physics**	
Credits: 30 ECTS	
Keywords: Naturally Fractured Reservoir Spontaneous Imbibition Co-Current Imbibition Counter-Current Imbibition Capillary Back Pressure Viscosity Ratio Capillary Pressure Relative Permeability	Number of pages: 101 + supplemental material/other: 1 CD Stavanger, 15 June 2017

Modelling of Co-current Spontaneous Imbibition – Improved Understanding of Reservoir Flow Physics

---

Master Thesis by Daisy Siti Aisyah

University of Stavanger

Spring 2017

Acknowledgements

First and Foremost, I would like to say Alhamdulillah, praise be to Allah, the Almighty, for bestowing upon me strength and determination to do my thesis.

Secondly, my deepest appreciation and gratitude goes to my supervisor, Dr. Pål Østebø Andersen and co-supervisor, Kenny Walrond, MSc for their excellent guidance, advice, and quick specific review while writing my thesis. It has been an inspiring and a great experience writing my thesis since lots of knowledge and insight that I obtained from them, specifically knowledge in a simulation and model-build. Owing to that, I have developed my technical skills. Furthermore, I would like to thank Arild Lohne at IRIS who help me to get into his software, IORCoreSim (Version 1.2) to build the model for this thesis.

Furthermore, I would especially like to express my sincere appreciation and acknowledgment to my parents, Ir. Solechudin and Esih, W. M.Pd, for their prayers, loves, and continuous support during my study abroad and to my brother and sisters: Haqiki, A. M.Sc, Yahya J. M.Sc, and especially Stiffi Zukhrufany who always motivate, encourage, and support me during my thesis. Last but not least, thanks go out for my fellow students and my Indonesian friends who help and support me during my study.

Abstract

Study of recovery mechanism in naturally fractured reservoir (NFRs), such as spontaneous imbibition has high interest in the oil industry to enhance oil production. Many studies of spontaneous imbibition such as counter-current and co-current imbibition have been carried out by researchers to understand more about the physical process of oil displacement from the matrix to the fracture. Understanding parameters influencing the spontaneous imbibition is a fundamental stage to obtain optimum oil recovery in NFRs.

To develop that understanding, the generated model from the successful spontaneous imbibition experiment is required. Experimental setup D has been chosen from spontaneous imbibition experiment with arbitrary fluid viscosity that was conducted by Haugland, H.K (2016). This type of experimental setup represent two ends open free spontaneous imbibition (TOEFSI) boundary condition where the inlet of imbibition tube is contact in with water, while the other side is oil-saturated outlet. As the result of five experiments from this setup, oil production mostly occurred by co-current flow for all experiments, while poor counter-current oil production was determined in one of these experiments.

Assuming horizontal homogeneous 1D model is generated from that setup D with applying TEOFSI boundary condition and allowing both co-current and counter-current imbibition to happen in this model. Corey-type Relative permeability and J-function capillary pressure correlation is used for developing the flow. Assuming atmospheric condition for the model which correspond to the condition of the experiment. Various of the imbibition tube length, viscosity ratio, relative permeability, the shape of capillary pressure curve, and the capillary back pressure are applied during simulation to investigate the change of controller parameters effect on the oil recovery and, analysis and understand the behaviour behind it.

As the result, high co-current or total (co + counter current) oil recovery is obtained when oil mobility is increased (i.e. high viscosity ratio (μ_w/μ_o)) with a reduction of tube length. These results are satisfied with the Haugland, H.K's (2016) experimental result for viscosity ratio effect and another conducted experiment by Zhang, et al. (1996) for the increase of the core length effect. High imbibition rate that is induced from those parameters leads to oil to produce co-currently and vice versa.

The capillary pressure shape that affects the co-current production has been discovered during this parameter study. The combination of concave up and down-negative slope of capillary pressure curve can increase oil production co-currently. It might be due to high level of capillary back pressure shown in that shape restricts high oil pressure to overcome it. The various capillary back pressure is investigated by changing boundary water pressure. From the simulation result, counter-current production occurs when the boundary water pressure (Pcbw) is lower than the oil pressure inside the model. The reason is high oil pressure overcomes this type of pressure. On the other hand, the counter-current decreases as the Pcbw is higher than the oil pressure. Both counter-current and co-current production occurs if those pressure are equal.

Table Of Contents

List of figure

List of Table

Abbreviation

1D	- One – Dimensional
HM	- History Matching
kr	- Relative Permeability
NFRs	- Naturally Fractured Reservoir
Pc	- Capillary Pressure
Pcbw	- Boundary Water Pressure
OEO	- One-end Open
TEOFSI	- Two-ends Open Face Spontaneous Imbibition

1. INTRODUCTION

1.1.Background

Improvement of oil recovery from naturally fractured reservoir (NFRs) has high interest in the oil industry to fulfil the energy demand and consumption. This type of reservoir has been discovered throughout the world and contains more than 20% of the world's oil and gas reserves (Saidi, 1983). Most of oil is stored in a matrix which has low permeability but high porosity. Several studies of NFRs recovery mechanism such as spontaneous imbibition has been carried out by researchers to understand more about the physical process of fluid displacement from the matrix to the fracture. Spontaneous water imbibition in oil saturated core is commonly used to investigate and study a such displacement. Most of the spontaneous imbibition experiments were conducted for counter-current flow condition since the assumption were made that counter current flow is dominated during displacement (Norman R Morrow & Mason, 2001). In addition, the co-current flow is also being of interest for researcher to be analysed these days since oil production from the matrix block in the fractured reservoir is dominated by gravity force generating the co-current flow condition (Haugen, Fernø, Mason, & Morrow, 2014).

The process of spontaneous imbibition occurs when the non-wetting fluid (water) imbibes into porous medium and displace the non-wetting phase (oil) by the action of capillary pressure (Norman R Morrow & Mason, 2001). Counter-current and co-current flow in the spontaneous imbibition can be generated by specifying their boundary condition (Bernard J. Bourbiaux & Kalaydjian, 1990). All faces open (AFO) (Mason, Fischer, Morrow, & Ruth, 2009) and one-end-open (OEO) boundary condition are commonly applied to generate counter-current flow, while two-ends open free spontaneous imbibition (TEOFSI) is used for co-current flow with some degree of counter-current flow (Dong, Dullien, & Zhou, 1998). Counter-current imbibition occurs as only one-end face open for oil and water to produce and invade in, respectively, in an opposite direction. On the other hand, oil and water can flow in the same direction if the matrix block is partially water-contacted-one-end open face and the other is in contact with oil.

The complexity process in the spontaneous imbibition is caused by many factors affect that process. Understanding the factors that affect spontaneous imbibition is a fundamental stage to figure out this process and obtain the optimum oil recovery in NFRs afterwards. Two example study in spontaneous imbibition experiment, which is more dominating in co-current flow, with

arbitrary fluid viscosity was conducted by Haugland, H.K. (2016) and Vabø, T. (2016) from University of Bergen to investigate the effect of various viscosity on the front behaviour, imbibition rate, oil recovery in sand and glass beads. By using the imbibition tube which was saturated with 100% oil and immerse it into the water bath, the spontaneous imbibition successfully occurred in their experiment.

In this thesis, study of spontaneous imbibition will be focused only in Haugland's experiment, especially in one of the experimental setup that involved the paper filter in the inlet of the tube which governs the counter-current flow in TEOFSI boundary condition. By modelling this type of experimental setup, the flow behaviour and the oil recovery from counter-current and co-current can be predicted with various viscosity, capillary back pressure, various the imbibition tube length, and saturation-dependent capillary pressure and relative permeability during imbibition in numerical simulation. The behaviour of the paper filter that involved the capillary back pressure in the inlet will be observed as well with those parameters in the sensitivity analysis. Since the high complex of fluid flow in the NFRs, the simplified model is needed to interpret characteristics of this system. One-dimensional horizontal homogeneous model of spontaneous imbibition is going to build with initial and boundary condition of experimental setup by considering the domination of co-current flow takes place during the displacement and gives possibility also for counter current flow to occur. For simplicity, the oil displacement in the model is only governed by capillary force and neglecting the advection transport and influenced gravity forces. Finally, the model is thus simulated to satisfy the simulation result with the experimental result.

1.2. Objectives

The main objective of this thesis is to study one-dimensional spontaneous imbibition and its relation to provided experimental results. Studying co-current spontaneous imbibition that has been experimented by Haugland, H.K (2016) and the effect of counter-current production in the one-dimensional model with TEOFSI boundary condition, where water only imbibes at the inlet and allow oil to produce at the both side of model (inlet and outlet). Moreover, to observe and get understanding the behaviour of adjusted parameters that affect an amount of co-current oil production and counter current production during imbibition, and how the production profile in the simulation result will be matched with the experimental result.

1.3. Scope

- Interpretation of experimental data by selecting one experimental setup that involves the capillary back pressure and consists of several successful experiments as a data input for modelling.
- Build-up 1D model of co-current flow spontaneous imbibition using IOR Core Sim based on the initial and boundary condition of experimental setup.
- Describe the mathematical model of spontaneous imbibition – co-current and counter current- flow.
- Describe the numerical model and solve of the equations given in the IOR Core Sim.
- Do sensitivity analysis by changing parameter of fluid and imbibition tube properties to investigate the effect on oil recovery counter-current and co-currently
- Match the simulation result with the experimental result.

1.4. Outlines

In the introduction, it will describe about the background of this thesis which describes the reason of this thesis is high interested and necessary to investigate, some introduction about the theoretical aspect behind it, plan to do to achieve of goal of this thesis, objective of this thesis and the scope of work during the thesis. For literature review part, it will summarize and review fundamental that is related to this topic of thesis, some experiment that related to this thesis which has been successfully conducted, and introduce the software that used for building the model in the end of this chapter. In the chapter 3, mathematical model of co-current and counter-current imbibition will be expressed, and the description of flow modelling that occur in the model in the section of numerical model. This chapter will be followed by the parameter study for relative permeability, capillary pressure, viscosity ratio, and the imbibition tube length, and do manual history matching in the section of result and analysis. Last but not least, the thesis will be end up by conclusion from all discussion in the chapter 4.

2. FUNDAMENTALS

2.1. Wettability

According to the Ahmed (2009), degree of wetting, known as wettability, is the ability of fluid to adhere on a solid surface in presence of another fluid (Ahmed, 2009). The fluid adheres to the solid surface is denoted as wetting phase, while the fluid which is non-solid-preference is defined as a non-wetting phase. The strong attraction between fluid molecules-solid surface is more dominated by adhesive force than cohesive force. If the rock surface is water-wet-preference, the attractive force lead water to occupy the smallest pores, while the oil will reside the largest pores owing to the repulsive force between the oil and the surface. The adherence of wetting phase on the surface will displace another immiscible fluid by covering the surface. Spread of wetting phase on the surface is varied depending on the magnitude of the contact angle which is illustrated in the Figure 2-1.

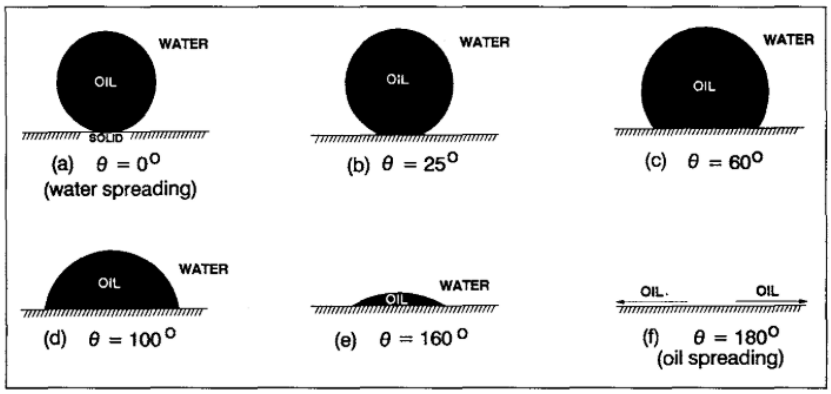

Figure 2-1 Contact Angles from Strongly Water Wet to Strongly Oil Wet (Norman R. Morrow, 1990)

Anderson, W.G. (1986) classified the wettability based on the contact angle, such as it ranges from strongly water-wet to strongly oil wet, neutral wettability (no preference to either oil or water) and fractional wettability where the total surface area in the reservoir has heterogenous wettability (Brown & Fatt). In addition, Salathiel, R.A (1973) introduced mixed wettability as a sort of fractional wettability where water occupies the small pores and large pores are occupied by the oil. Wettability controls the oil and water distribution in the reservoir. When an oil-saturated water-wetted-core is immersed into a water bath, water will imbibe spontaneously and displace the oil from the solid surface. It is obviously convinced that the capillary pressure depends fully on the wettability. In addition, the movement of two immiscible fluid is relied on the wettability, that means the wettability gives an effect to the relative permeability.

2.1.1. The Wettability Effect on The Capillary Pressure

Capillary pressure exists in the presence of two immiscible fluid occupying the same reservoir pores. The capillary pressure is pressure difference across the fluid interface (Donnez, 2012) which is illustrated at the curved interface which is caused by the pressure above the interface pushes down and exceeds the pressure on the across side (see Figure 2-3). The convex-concave-shaped curve at the interface is formed by the contact of two immiscible fluids with the contact angles at the surface (Figure 2-2). The curve of the interface hence depends on the interfacial tension and wettability.

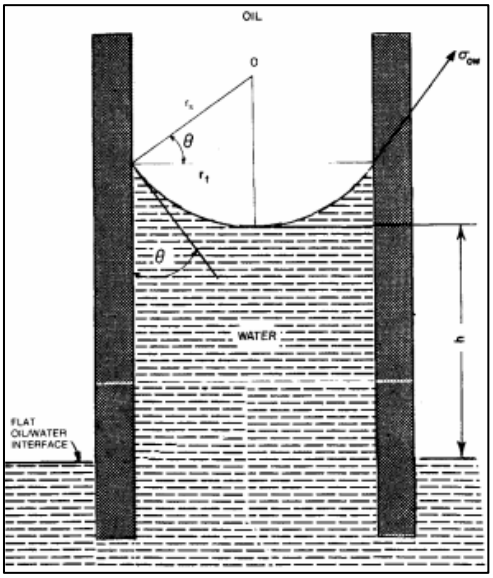

Figure 2-2 Oil-Water Interface in a Capillary Tube (Anderson, 1987)

The capillary pressure is defined as

$$P_c = P_{nw} - P_w \qquad 2\text{-}1$$

where P_{nw} = non-wetting pressure and P_w = wetting pressure.

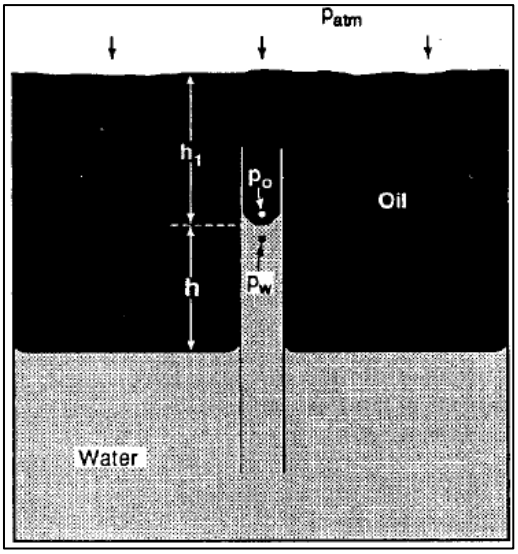

Figure 2-3 Pressure Difference in The Capillary Tube. The Wetting Phase is Water and Non-Wetting Phase is Oil (Green & Willhite, 1997)

In the capillary tube radius, the capillary forces are governed by the curvature radii of the interface which is generated by the contact angle, the fluid saturation, the pore geometry, and the interfacial force. A general expression for capillary pressure as a function of interfacial tension and curvature radii is given by the Laplace's equation as follows (Anderson, 1987),

$$P_c = P_o - P_w = \sigma(\frac{1}{r_1} + \frac{1}{r_2}) \qquad 2\text{-}2$$

where σ = interfacial tension, Pc = capillary pressure, r_1 and r_2 is curvature radii of the interface. Because of the fluid saturation is related to the curvature radii, the capillary pressure, hence, depends on the fluid saturation which wets the porous medium. Anderson, W.G. (1987) expressed that by the definition of the capillary pressure in the equation 2-1, the capillary pressure is, either positive or negative is determined by the positive or negative value of the curvature radii in the non-wetting and wetting phase (Anderson, 1987).

There are two type of fluid displacement in the reservoir that is controlled by capillary pressure, such as drainage and imbibition process. Drainage is the process of non-wetting phase (oil) displaces the wetting phase (water) due to the mobility of oil is higher than water as the oil saturation increases. Oil invades the 100%-water-saturated reservoir as the minimum capillary pressure, known as threshold pressure, is reached. Oil invasion needs higher oil pressure than water pressure to displace water from the largest pores. During water displacement by oil, capillary pressure rises at decreasing water saturation until reach the residual water saturation (S_{wr}) where the capillary pressure goes to infinity. This process is defined as the primary drainage.

On the other hand, the imbibition is the process of fluid flow where the wetting phase saturation increases. When oil pressure reduces gradually which results in a decrease of the high positive capillary pressure to the zero, the water will imbibe spontaneously the reservoir and displaces the oil until the capillary pressure reach zero. At the point where oil pressure is equal to water pressure, the saturation of spontaneous water imbibition (S_{wp}) is attained. This process called spontaneous imbibition. The imbibition of water displace oil is continued as the water saturation rises, generated by a negative capillary pressure due to a surge water pressure over the oil pressure. The displacement stops when a negative infinity of capillary pressure arrives at the residual oil saturation (S_{or}). This process called forced imbibition. Morrow, R Norman (1990) illustrated those process in the capillary pressure for mixed wet (Figure 2-4).

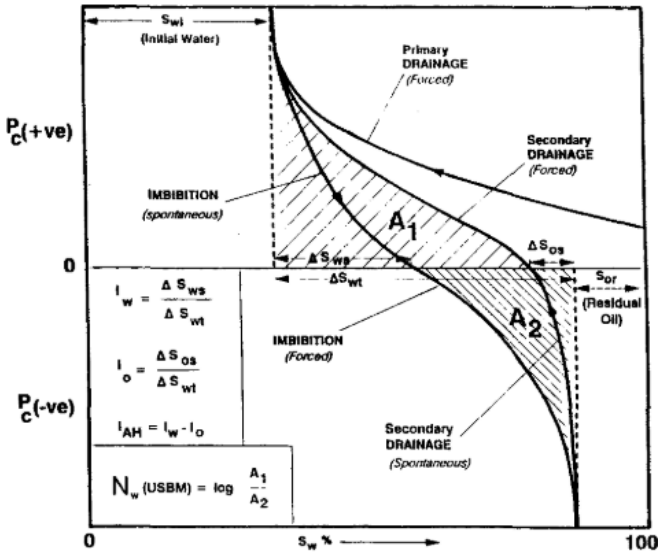

Figure 2-4 Capillary Pressure Curve on Mixed-Wettability System (Norman R. Morrow, 1990)

It can be seen in the Figure 2-4, a decrease in imbibition capillary pressure shows a different value with the drainage capillary pressure at the constant water saturation. An area between them is given by the effect of capillary hysteresis. The capillary hysteresis exists because of contact angle and heterogeneity pores cross section. The contact angle effect on the capillary pressure can be seen in the Figure 2-5 where those capillary pressure curves are measured by Killins, et.al (1953) on strongly wetted system using a porous-plate apparatus (Killins, Nielsen, & Calhoun, 1953). In the strongly water-wet core, a decrease of capillary pressure with increasing water saturation is defined as the spontaneous imbibition process (curve 2). A high positive value of capillary pressure initially in the strongly water-wet core decreases and provides for water to imbibe until capillary pressure reach the residual oil saturation where the capillary pressure is equal to zero.

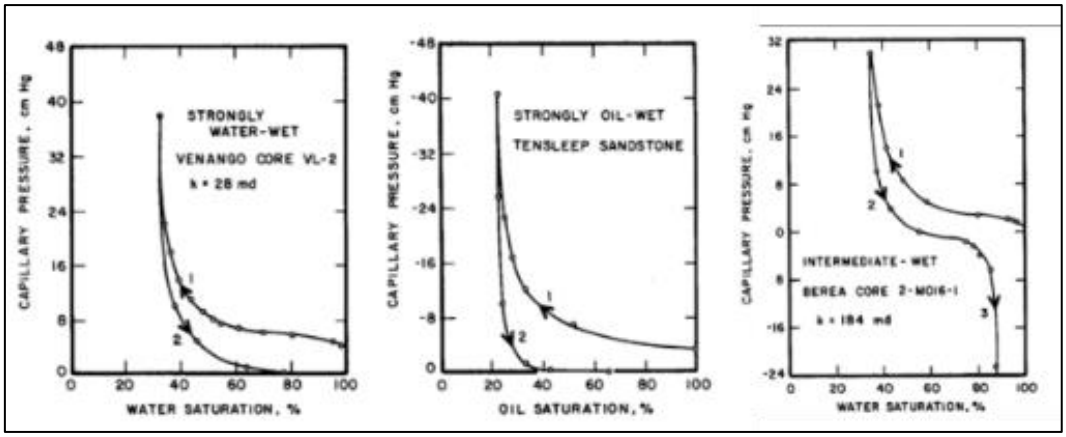

Figure 2-5 Capillary Pressure Curve of Different Wet Rock (Killins et al., 1953)

If the oil is still in continuous path when capillary pressure is zero, the saturation at this capillary pressure is not defined as the residual oil saturation. Since the hydraulic continuity of oil still exists due to continuous oil path, the forced imbibition thus occurs from zero-capillary pressure to the negative value which lead to the additional oil production (see curve 3 in Figure 2-5 for intermediate-wet). Once the vertical capillary pressure curve is reached where the oil hydraulic continuity is diminished, the forced imbibition would stop at the residual oil saturation.

Furthermore, Morrow (1976) measured the capillary pressure curve based on the true contact angle and advancing contact angle (Norman R. Morrow, 1976). He plotted several experiments with different true contact angle and advancing contact angle to investigate the effect of contact angle on the imbibition capillary pressure curve in the Figure 2-6 where the zero-contact angle is equivalent to the reference phase of heptane with true contact angle (θ_T) is equal to 22^o. It is, then shown that capillary pressure curve for strongly water-wet is given at dash lines (----).

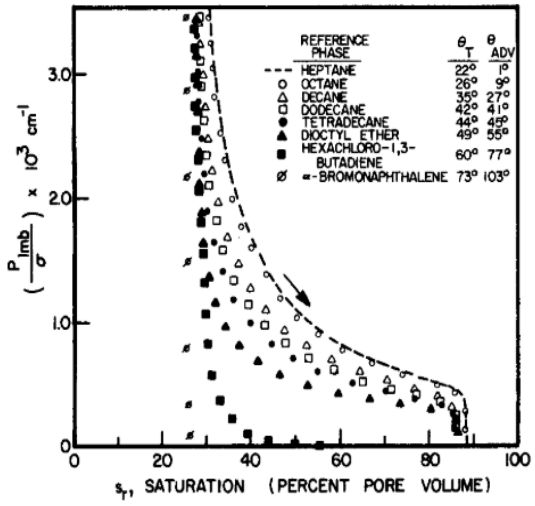

Figure 2-6 Capillary Pressure on The Contact Angle Effect (Norman R. Morrow, 1976)

2.1.2. The Wettability Effect on the Relative Permeability

The relative permeability expresses a flow capability in the presence of 2 phase flow in the reservoir, which is defined such as

$$k_{kri} = \frac{k_i}{k} \qquad 2\text{-}3$$

where i is oil and water, k_i is fluid effective permeability, and k is absolute permeability. 2 constraint in oil-water relative permeability curve which is mentioned by (Craig, 1971):

a) Permeability to water at 100% water saturation.

b) Permeability to oil at irreducible water saturation.

An example oil-water relative permeability curve is given by Lyons (1996) with the process of drainage and imbibition (Figure 2-7)

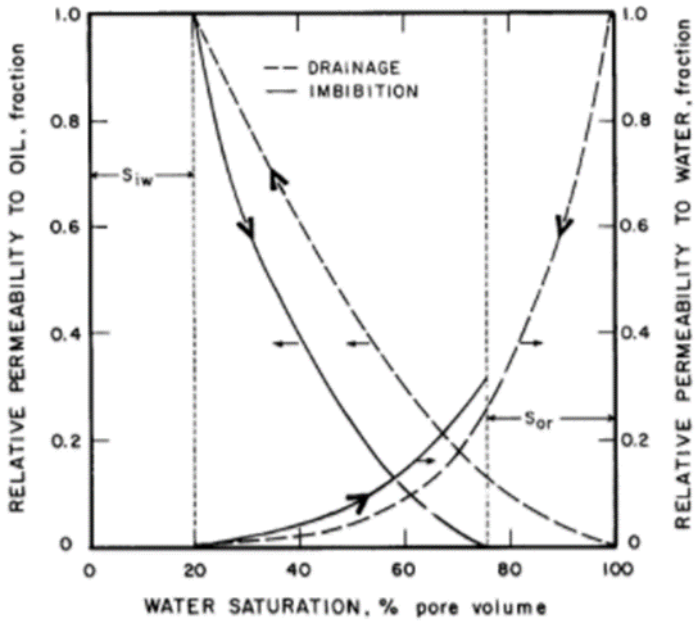

Figure 2-7 Relative Permeability for Drainage and Imbibition (Lyons, 1996)

Wettability on the relative permeability curve governs the imbibition process in the core that lead to controlled oil production at the outlet of core. To generate the relative permeability curve, the constrained end-point values must be determined. A different wet core has different constrained values of the curve. Craig, Forrest F (1971) has classified the limitation of end-point relative permeability curves based on the wettability which is shown in the figure 2.8 (Craig, 1971). He also suggested several rules of thumb in the Table 2-1 to characterize the effect of wettability in the relative permeability.

Table 2-1 Rule of Thumb for Oil-Water Relative Permeability Characterization (Craig, 1971)

	Strongly Water-Wet	Strongly Oil-Wet
Connate water saturation.	Usually greater than 20% to 25% PV.	Generally less than 15% PV, frequently less than 10%.
Saturation at which oil and water relative permeabilities are equal.	Greater than 50% water saturation.	Less than 50% water saturation.
Relative permeability to water at maximum water saturation; i.e., floodout.	Generally less than 30%.	Greater than 50% and approaching 100%.

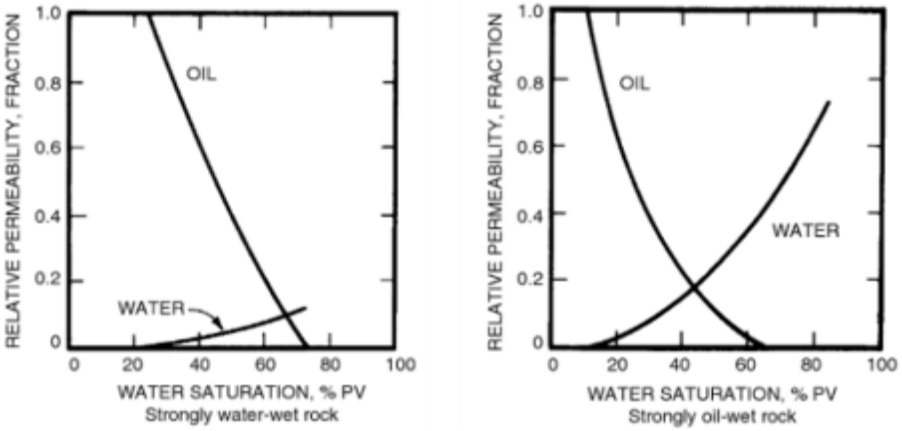

Figure 2-8 Relative Permeability Curves for Strongly Wetting (Craig, 1971)

The effect of wettability in the relative permeability influences the fluid distribution and flow in porous medium. As Figure 2-8 is shown, the oil relative permeability is more concave than the strongly water-wet. In strongly wetting, the oil relative permeability decreases while the water relative permeability increases as the wettability alters to more oil-wet. In partially wetting (mixed wet system), the continuous oil-wet path alters the relative permeability.

2.2. Capillary Pressure Leverett J-function

For correlation objective and modelling, the capillary pressure can be expressed by dimensional capillary pressure, Leverett-J function. Since core properties such as porosity and permeability influences the capillary pressure, Leverett defines empirical J-function to correct these impact as follows (Leverett, 1941):

$$J\,(S_w) = \frac{P_c}{\sigma \cos\theta_c}\sqrt{\frac{k}{\varphi}} \qquad 2\text{-}4$$

where c is constant, P_c is capillary pressure, σ is the interfacial tension between the two phases and k is absolute permeability, ϕ is the porosity of the rock, cos θ = 1 for water-wet core.

2.3. The Fluid Pressure Effect on The Imbibition Capillary Pressure

The magnitude of pressure of non-wetting phase (oil) and wetting phase (water) is the most influencing part of capillary pressure determination referring to the equation 2-1. Interface of oil-water which is represented by the curve-shaped interface induces the brine imbibition in the core and forces the oil toward the outlet of core. As the two-phases interface is moved, the capillary pressure would be developed. In this thesis, the modelling is established by referring to the co-current imbibition experiment. Since the experiment was conducted at the atmospheric condition, the generated magnitude of capillary pressure will be less than one bar. It is similar and related to Handy L.L (1960) experimental result that carried out the imbibition experiment of consolidated sandstone for three cores at the atmospheric condition where a non-wetting phase (air) was displaced by wetting phase (water) (Handy, 1960). During imbibition, the non-wetting phase (air) in the core has a pressure greater than atmospheric pressure, while the water pressure is equal to one atmosphere. Owing to that, the range of capillary pressure is lower than one atmosphere which is resulted in the following figure.

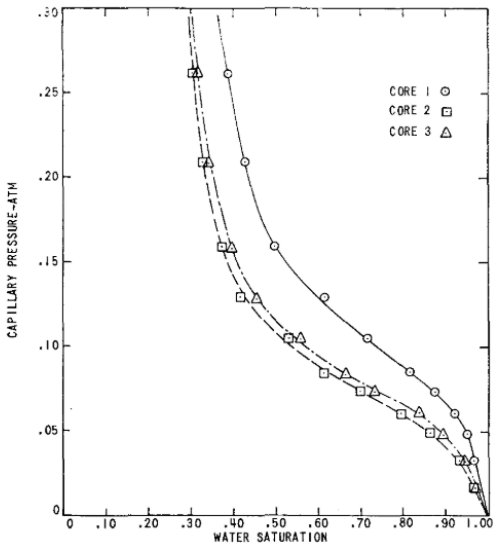

Figure 2-9 Capillary Pressure Curve Result For Fired Cores at Atmospheric Condition (Handy, 1960)

2.4. Relative Permeability Correlation

2.4.1. Corey-type Relative Permeability

Simplified relative permeability model can be generated based on the experiment data by simulating for series water saturation within constrained end-point values (S_{wirr} and S_{or}). Corey et al. (1956) generated simplified imbibition relative permeability correlation and this is generally valid for unconsolidated sands applying various empirical exponents (Honarpour, Koederitz, & Herbert, 1986). Corey's equation for water and oil relative permeability are expressed as follows (Corey, 1954):

$$k_{rw} = k_{rew} (S_{wn})^{n_w} \quad 2\text{-}5$$

$$k_{ro} = k_{reo} (1 - S_{wn})^{n_o} \quad 2\text{-}6$$

where k_{rew} and k_{reo} are end-point water and oil relative permeability, respectively, n_w and n_o are respectively water and oil Corey exponent, and normalized water saturation (S_{wn}) is given by,

$$S_{wn} = \frac{(S_w - S_{wi})}{(1 - S_{wi} - S_{or})} \quad 2\text{-}7$$

where S_{wi} and S_{or} represent initial water saturation and residual oil saturation.

Normalized relative permeability is developed by Corey exponent as a function of normalized water saturation. The oil and water Corey exponent correspond to the rock wettability determining the value of end-point of relative permeability for a certain wet system. The consistency of these Corey exponent with the wettability is necessary. McPhee et.al (2015) generally correlated those Corey exponents with the wettability that shown in the Table 2-2.

Table 2-2 Oil Water Corey Exponent with Wettability (McPhee, Reed, & Zubizarreta, 2015)

Wettability	No (kro)	Nw (krw)
Water-wet	2–4	5–8
Intermediate-wet	4–6	3–5
Oil-wet	6–8	2–3

Another correlation of Corey exponent with various wettability are shown in the Table 2-3. Stiles (2013) applied the Corey exponent correlation in its analytical to examine the quality of the relative permeability after the experiment (Stiles, 2013). Agnia et al. (2014) showed the result of

the implementation of Stiles's method on data from the North Sea in their paper. (Agnia, Algdamsi, & Al-Mossawy, 2014).

Table 2-3 Another Oil Water Corey Exponent versus Wettability (Stiles, 2013)

Wettability	N_o	N_w	$k_{rw\ end\text{-}point}$
Strongly Water-Wet	2 to 3	4 to 6	0.1 to 0.4
Mixed Wettability	3 to 5	2 to 4	0.5 to 0.9

2.4.2. LET-type Relative Permeability

Another sort of relative permeability correlation that is used in special core analysis and reservoir simulation is given by (Lomeland, Ebeltoft, & Thomas, 2005) that expressed a new adjustable 3 parameters correlation, such as L, E, T in water and oil relative permeability as

$$k_{rw} = k_{rew} \frac{(S_{wn})^{L_w^o}}{(S_{wn})^{L_w^o} + E_w^o (1 - S_{wn})^{T_w^o}} \quad 2\text{-}8$$

$$k_{row} = k_{reo} \frac{(1 - S_{wn})^{L_o^w}}{(1 - S_{wn})^{L_o^w} + E_o^w (S_{wn})^{T_o^w}} \quad 2\text{-}9$$

where k_{rew} and k_{row} are end-point water and oil relative permeability, respectively and normalized water saturation (S_{wn}). L in the empirical parameter, L_w^o and L_o^w, describes the lower part of the curve. T shows in the parameter, T_o^w and T_w^o, represents the upper part of the curve, while E in the parameter, E_w^o and E_o^w, describes the slope elevation of the curve. Compared to the Corey Exponent, these three empirical parameters generate a better fit to experimental data and build up a magnitude of flexibility (Lomeland et al., 2005).

2.5. Characterization and Recovery Mechanism of NFRs

"Fractures exist mostly and are omnipresent virtually in outcrop of sedimentary rocks. The fractures in outcrop are the result of surface and subsurface conditions. Fractured - sedimentary rocks which consist of hydrocarbon can be treated as a fractured reservoir" (Nelson, 2001). The reservoir is classified as the fractured reservoir when these fractures affect the fluid flow behaviour in the reservoir (Bernard Jean Bourbiaux, 2009). The fractured reservoir is more challenge to deal with than a conventional reservoir due to complexity of the fractured reservoir, which is characterized by matrix and fractures.

Generally, the fracture which has high permeability-low porosity can be act as a flow path for production and injection and the low permeability-high porosity in the matrix provides

the place for oil to be stored. However, Allan and Sun (2003) classified the fractured reservoir into 4 groups based on the function of porosity and permeability such as (Allan & Sun, 2003):

1) Type I reservoir

   The reservoir has little matrix porosity and permeability. Hence, the fractures provide both storage capacity and fluid-low pathways.

2) Type II reservoir

   The reservoir has low matrix porosity and low permeability. Hence, the matrix provides some storage capacity and the fractures act as the fluid-flow pathways.

3) Type III reservoir (microporous)

   The reservoir has high porosity and low permeability in the matrix. Therefore, the matrix act as the storage capacity and the fractures provide the flow path.

4) Type IV (macroporous)

   The reservoir has high matrix porosity permeability. Thus, the matrix acts both as the storage capacity and the flow path, while fractures solely improve the permeability.

The naturally fractured reservoir commonly exists in Type II and III, where the reservoir contains of high-permeable fracture and low-permeable matrix. The different properties of fracture and matrix contribute the oil recovery mechanism. The flow-path-fracture affect advection flow play a dominating role on oil displacement and bypasses the oil-storage, matrix. On the other hand, the capillary action and gravity forces are the main parameter for oil sweep in the matrix to fracture.

One of the important recovery mechanism in the naturally fractured reservoir is spontaneous imbibition. The fluid flow in this recovery mechanism is governed mainly by capillary action. One of the example of the spontaneous imbibition is conducting the waterflood in water-wet core system. The wetting phase, in this case is water, entry the matrix when the capillary pressure is positive and displaces non-wetting fluid in the matrix towards the fracture. The spontaneous imbibition involves counter current and co-current flow relatively in the fractured reservoir where those flow occur depending on the geometry of boundary condition and the magnitude of gravity to capillary forces (Bernard J. Bourbiaux & Kalaydjian, 1990).

2.5.1. Counter Current Imbibition

Counter current imbibition is the mechanism of wetting fluid displace non-wetting fluid in the opposite direction. A negligible gravity force compared to capillary force in a small block or core is mainly originator for counter-current flow to happen (Haugen et al., 2014). The counter current flow shows two types of direction in the boundary of block one-end-open face system (OEO) where the one end face and the surface of block are closed while the other one end face is open for water invades and oil produces in the same door. Qasem, et al. (2008) illustrated the schematic of the counter-current imbibition as shown in the Figure 2-10.

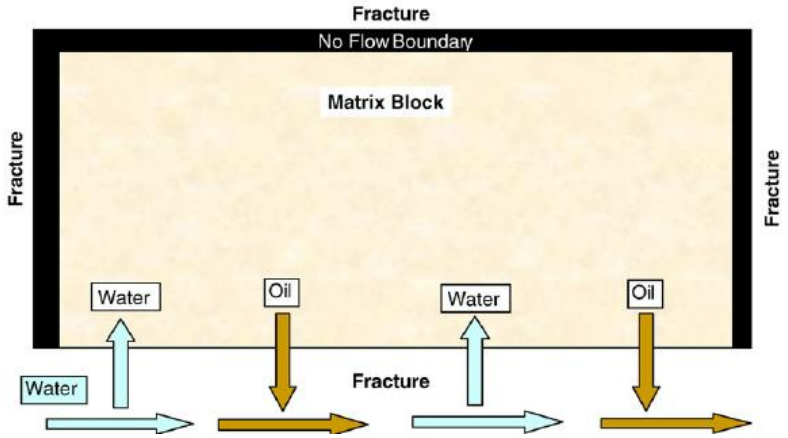

Figure 2-10 Main Sytem Image of Counter Current - Spontaneous Imbibition (Qasem, Nashawi, Gharbi, & Mir, 2008).

During the counter-current spontaneous imbibition, for instance, in the OEO system, the amount of oil production is in proportion to the amount of water imbibes the core. The oil displacement in counter-current is much less efficient than co-current due to the low fluid mobility induced by more viscous non-wetting phase near core's inlet area. Low fluid mobility could happen because the higher viscosity ratio between the wetting and non-wetting phase that causes a reduced the relative permeability in the counter-current (Bernard J. Bourbiaux & Kalaydjian, 1990). Furthermore, the less productive of oil to produce counter currently induced as well by the play role of capillary back pressure which is explained further in the next sub-section.

2.5.2. The Play Role of Capillary Back Pressure in Counter-Current Production

This type of capillary pressure has the same meaning with the definition of capillary pressure in the sub-section 2.1.1, that defines as difference pressure, particularly at the location which is the end-open face of the core. To generate counter-current production, the imbibition capillary pressure must exceed the capillary back pressure and produce oil out of the largest pore

(Haugen et al., 2014). A continuous oil filament must snap-off and form a droplet in the inlet area. According to Unsal et. al (2009), a formed droplet at the largest pore in the end-open face generates the capillary back pressure and since this droplet may take some time to form, the capillary back pressure is thus a function of time (Evren Unsal, Mason, Morrow, & Ruth, 2009).

The occurrence of oil snap off which lead to the oil droplet at the inlet boundary depends on the water saturation at the inlet boundary. This means the existence of the capillary back pressure relies upon the applied water saturation in the inlet boundary (Foley, Nooruddin, & Blunt, 2017). For a strongly water-wet rock with OEO boundary condition, the capillary entry pressure will be low for the non-wetting phase (oil) to flow. A formation of droplet by the capillary back pressure has a similar process with the primary drainage process. The process of counter-current oil production by water in the imbibition tube can be illustrated in the similar process which is describe in the following paragraph.

Unsal et al. (2007a) described an experimental horizontal cell to show capillary process in the small and large capillary tubes which directly investigate the process of counter-current production. Represented in the figure 2.11, the air initially saturated the capillary tubes until the oil invades in to the tubes. Note that the production in this experiment is generated by a movement of two-phase interface in the tubes with the square root of time. The picture shows the two-phases interface in the large tube has the least curve and this interface always lead over the other curve in the small tube (E Unsal, Mason, Morrow, & Ruth, 2007). The dead-end pressure in the Figure 2-11 represent pressure at the outlet boundary of air-filled tube.

In theoretical analysis, Unsal, et al. (2007a) expressed when the air-filled end tube is closed and the other end-face, which is saturated by oil is opened, the counter-current imbibition will occur. This adjusted boundary condition leads to oil imbibes in the small tube, pushing air towards the large tube, and bubbles out at the centre of the oil-end-large tube. The air production will cease at the tube centre when the oil is reached the end of the small tube. Note that the air-oil interface curvature which is close by the oil-end of the large tube is nearly proportionate to the bubbled air curvature at the large tube centre and this bubbled air will snap-off if these two curvatures go beyond each other (E Unsal et al., 2007).

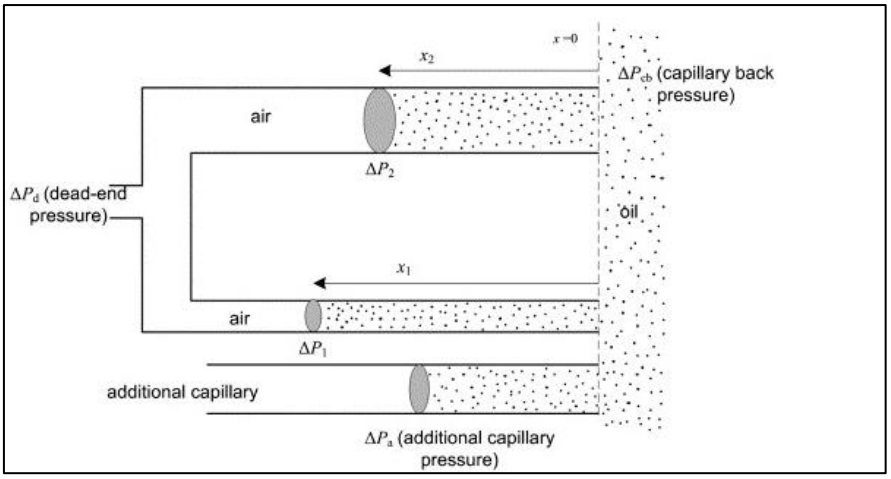

Figure 2-11 Process of the Oil/Air Menisci in The Capillaries (E Unsal et al., 2007)

The process of counter-current imbibition in the Figure 2-11 is described mathematically by Unsal, et al (2007a) in the following sentences. For counter current flow in this experiment, the laminar flow is assumed with the average velocity (u) in terms of volumetric flow rate Q and the capillary cross-sectional area (A) as,

$$\bar{u} = \frac{k}{\mu}\delta^2\frac{\Delta P}{x} \qquad 2\text{-}10$$

where δ is a dimension correlated with the capillary tube, μ is fluid viscosity, k is shape factor, x is the length of the tube, and ΔP is driven flow - pressure difference.

In the small tube (tube 1 in the figure 2.11), the pressure driving is expressed as,

$$[\Delta P_1 - \Delta P_a - \Delta P_d] \qquad 2\text{-}11$$

while the pressure driving in the large tube (tube 2) is described as,

$$\Delta P_2 = \Delta P_d + \Delta P_a - \Delta P_{cb} \qquad 2\text{-}12$$

where ΔP_1 and ΔP_2 are respectively the pressure difference in the small and large tube, ΔP_d is dead-end pressure where it is pressure difference between atmospheric condition in the outside outlet and that in the outlet (in the dead end), ΔP_a is additional capillary pressure, and ΔP_{cb} is capillary back pressure in tube 2. If all air is bubbled out the end-large tube that induces non-existence of oil-air interface, the pressure ΔP_{cb} must be lower than ΔP_2. However, when the bubbled air is snap-off, then pressure ΔP_{cb} will be equal to ΔP_2 due to a presence of oil-water interface ($x_2 > 0$). Hence, the volumetric flow rate (Q) for counter-current flow in the small tube (tube 1) and the large tube (tube 2) are

$$Q_1 = \frac{k_1}{\mu}\,\delta_1^2 A_1 \frac{\Delta P_1 - \Delta P_a - \Delta P_d}{x_1} \quad (2\text{-}13)$$

$$Q_2 = \frac{k_2}{\mu}\,\delta_2^2 A_2 \frac{\Delta P_d + \Delta P_a - \Delta P_{cb}}{x_2} \quad (2\text{-}14)$$

where $Q_1$and Q_2 are the volumetric flow rate in the small and large tube, respectively, and x_1 and x_2 are the location of the interfaces in the tubes.

For counter-current flow, the oil that imbibes in the small tube flow in the opposite direction as the interface travels along the large tube. This induces the volumetric flow rates are equal (Q_1= Q_2). Since then, the equation 2-13 and 2-14 will be,

$$\frac{K_1}{K_2}\frac{A_1}{A_2}\frac{x_2}{x_1}[\Delta P_1 - \Delta P_a - \Delta P_d] = [\Delta P_d + \Delta P_a - \Delta P_{cb}] \quad (2\text{-}15)$$

If ΔP_{cb} is equal to ΔP_2, ΔP_d can be vanished from flow equation 2-14 in the large tube by assuming,

$$\Delta P_d = \frac{B\left({}^{x_2}/_{x_1}\right)\Delta P_1 + \Delta P_{cb}}{1 + B\left({}^{x_2}/_{x_1}\right)} - \Delta P_a \quad (2\text{-}16)$$

Where

$$B = \frac{K_1}{K_2}\frac{A_1}{A_2} \quad (2\text{-}17)$$

$$K_{1,2} = k_{1,2}\,\delta_{1,2}^2 \quad (2\text{-}18)$$

then, the equation 2-14 is resulted in,

$$Q_2 = \frac{d_{x_2}}{d_t} = \frac{K_2 A_2}{\mu x_2}\left[\left[\frac{B\left({}^{x_2}/_{x_1}\right)\Delta P_1 + \Delta P_{cb}}{1 + B\left({}^{x_2}/_{x_1}\right)} - \Delta P_a\right]\Delta P_a - \Delta P_2\right] \quad (2\text{-}19)$$

and ended up as,

$$\frac{1}{2}Bx_2^2 - \frac{1}{2}\frac{A_1}{A_2}x_1^2 = Dt \quad (2\text{-}20)$$

by assuming a constant parameter D as

$$D = \frac{K_1 A_1}{\mu}(\Delta P_1 - \Delta P_2) \quad (2\text{-}21)$$

and the total volumetric flow rate in both capillary pressure is equal to zero,

$$Q_1 = -Q_2 = A_1 dx_1 = -A_2 dx_2 \qquad 2\text{-}22$$

2.5.3. Co-Current Imbibition

The co-current displacement is the process of both wetting and non-wetting phase flow in the same direction. This kind of the system occurs when the boundary condition of the core is TEO (two-ends-open) face system where the inlet core is in contact with the wetting phase (water) while the other ends is contact with the oil as non-wetting phase. The process of co-current imbibition is equivalent with the counter current. Positive capillary pressure develops the oil displacement where it is induced by the advance of interface of oil-water causes the oil produce and water invades. Since the penetration of water in the system (e.g. oil-filled tube) is influenced by wettability, the flow resistance is subjected to water during displacement. Qasem, et al. (2008) illustrated the schematic of the co-current imbibition as shown in the following figure.

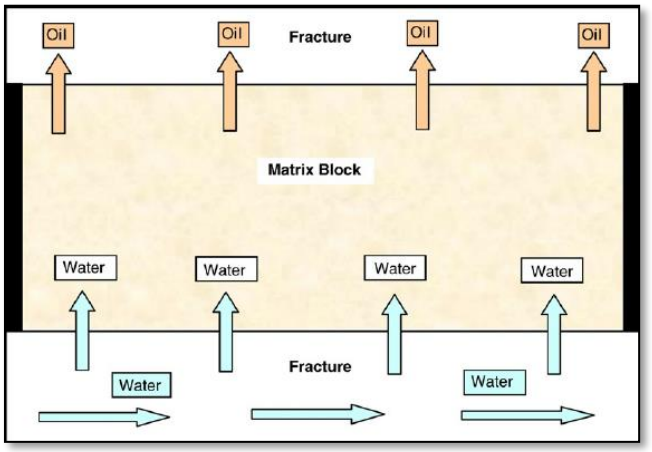

Figure 2-12 Schematic of Co-Current Imbibition (Qasem et al., 2008)

In the core analysis, the process of co-current imbibition is influenced by the velocity of the advanced two-phases meniscus of two phases. Since in the spontaneous imbibition, all the flow resistance exist in the wetting phase (water), the velocity of interface thus depends on the length tube of behind the front (Haugen et al., 2014). That means depending on how long of the length tube has been imbibed by water behind the front. This velocity of the interface is expressed by Washburn equation with the assumption a finite tube (Washburn, 1921).

Haugen, et al (2014) shows the Washburn equation of oil displacement in tube which partially in contact with water and oil at the both open ends in the following paragraph (Haugen et al., 2014). Assuming single capillary tube which is saturated initially with oil and immersed the tube in the water bath and the wet condition is strongly water-wet ($\theta = 0^o$). Capillary pressure is developed by the interface curvature, where using the equation 2-34 and apply the contact angle for strongly water-wet which results in

$$P_c = \frac{2\sigma}{r} \qquad 2\text{-}23$$

Displacement front flow co-currently along the length capillary tube is described mathematically by using Poiseuille equation and assuming an additional driving pressure ($\Delta P_{applied}$) as follows (Haugen et al., 2014),

$$\frac{2\sigma}{R} + \Delta P_{applied} = Q\left(\frac{8\mu_{nw}}{\pi R^4}(L_{tube} - L) + \frac{8\mu_w}{\pi R^4}L\right) \qquad 2\text{-}24$$

Since the velocity of the interface depends on the volumetric flow rate (Q) and the cross-sectional area (A) and then, by integrating the equation (21) from initial condition (L=0, and t=0) and after to L and t, the equation 2-24 will be,

$$\mu_{nw}L_{tube}L - \frac{1}{2}(\mu_{nw} - \mu_w)L^2 = \frac{1}{8}\left(\frac{2\sigma}{R} + \Delta P_{applied}\right)R^2 t \qquad 2\text{-}25$$

When the interface reaches the end of the tube, the equation 2-25 is normalized as,

$$\frac{1}{2}(\mu_{nw} + \mu_w)L_{tube}^2 = \frac{1}{8}\left(\frac{2\sigma}{R} + \Delta P_{applied}\right)R^2 t_{end} \qquad 2\text{-}26$$

The equation 2-26 shows the interface velocity is a function of the tube radius and the resistance flow is a function of square root of the tube radius. Dividing equation 2-25 by equation 2-26 and assume that $\mu_{nw}$is zero, the length parameter in the equation 2-26 will be proportional to the square root of time and the additional driving pressure ($\Delta P_{applied}$) is diminished. Thus, the equation 2-26 yields

$$\frac{t}{t_{end}} = \frac{1}{\mu_{nw} + \mu_w}\left(2\mu_{nw}\frac{L}{L_{tube}} - (\mu_{nw} - \mu_w)\frac{L^2}{L_{tube}^2}\right) \qquad 2\text{-}27$$

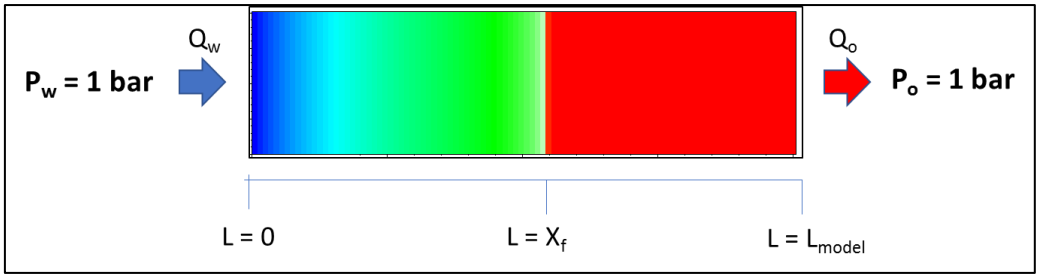

Figure 2-13 Oil Displacement by Water in Perfectly Wetted 1D Model

As the interface travels along the tube the pressure distribution of co-current flow in the generated one-dimensional model (Figure 2-13) can be described mathematically by Haugen et.al (2014) as, (Haugen et al., 2014)

$$\frac{P_{nw,f}}{\left(\left(\frac{2\sigma}{R}\right) + \Delta P_{applied}\right)} = \frac{1}{1 + \left(\frac{\mu_w}{\mu_{nw}}\right)\left(\frac{1}{\left(\left(L_{tube}/L\right) - 1\right)}\right)} \qquad 2\text{-}28$$

The equation 2-28 shows the distribution of non-wetting phase pressure. When the water imbibes the model, the water pressure at the inlet of the model decreases initially and the non-wetting phase (oil) ahead of the front has high pressure. As the interface travels toward the outlet, the oil pressure decreases and reaches zero when the interface reaches the end of the tube.

Furthermore, the viscosity ratio (μ_w/μ_{nw}) in the equation 2-28 determines the imbibition rate. Figure 2-14 shows a various production profile with different viscosity ratio as the result of equation 2-28. The acceleration of interface velocity increases as the oil has a higher viscosity than the water (i.e. low viscosity ratio). On the other hand, a constant velocity if oil and water viscosity is equal, while it deaccelerates when the water viscosity is getting higher. Hence, the interface velocity depends on the imbibition rate that is determined by the viscosity ratio.

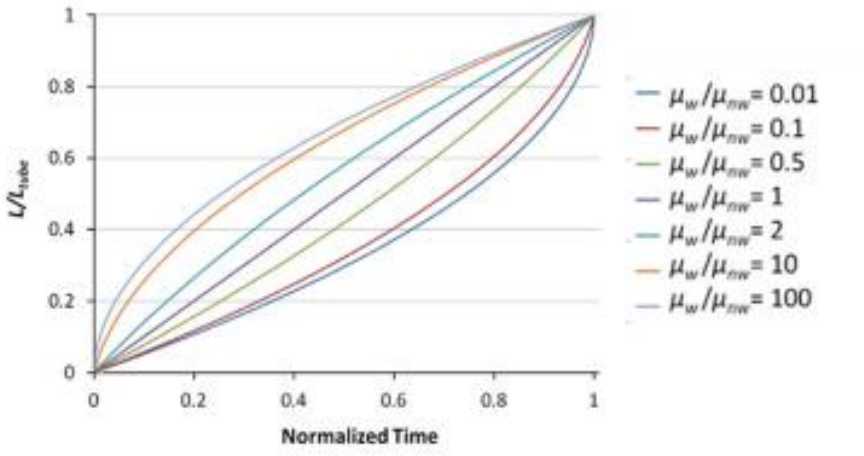

Figure 2-14 Normalized Distance versus Normalized Time with Different Viscosity Ratio (Haugen et al., 2014)

2.6. Scaling Group of Spontaneous Imbibition

Spontaneous imbibition is a complicated process that relies on the many factors affect it (Shouxiang, Morrow, & Zhang, 1997), such as the boundary condition, the fluid viscosity, the length of the core, the relative permeability, and the capillary pressure. Study of these parameter would be high necessary to understand about those effect on the oil recovery and predict the effect on the production rate.

2.6.1. Boundary Condition Effect

A specific boundary condition is very essential to be applied in the spontaneous imbibition system to obtain the continuum equation solution of oil displacement. There are four type of boundary conditions that re-captured by Morrow & Mason (2001) from several conducted experiments (Figure 2.15), such as all faces open (AFO), one end open (OEO), two-ends-open (TEO), and two ends closed system (TEC). The boundary condition of AFO and OEO were used by (Mattax & Kyte, 1962), TOE boundary condition is used by (Hamon & Vidal, 1986), TEC boundary condition was used by (Zhang, Morrow, & Ma, 1996).

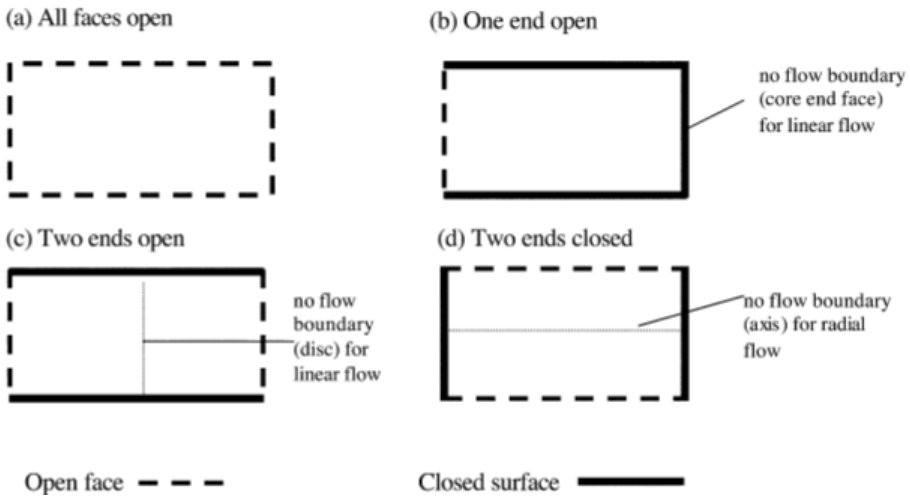

Figure 2-15 Type of Boundary Condition (Norman R Morrow & Mason, 2001)

Each boundary condition generates a different two-immiscible phase flow that contribute to the oil recovery. In this thesis, only TEO is specified for modelling co-current spontaneous imbibition. However, description of OEO is required as well due to understand in what way the counter-current imbibition can happen.

a. One End Open (OEO)

According to Mason and Morrow paper (2013), OEO is represented as the filled-non-wetting phase core is sealed on all faces except the one side and immersed in the wetting phase (Mason & Morrow, 2013). The wetting-phase imbibes to the one-end-open face, disperses throughout the core and displaces non-wetting fluid uniformly by imbibed wetting phase in the opposite direction. This flow mechanism is called counter-current imbibition. As the wetting phase saturation increases at the front, the non-wetting phase is more produced.

b. Two-Ends-Open (TEO)

This condition describes the one-end of the core is in contact with the wetting phase while the other end-face is in contact with the non-wetting phase at the same pressure for both side. Initially, the TEO boundary condition in the experiment was limited by the no-flow boundary in the middle of core resulting the counter-current imbibition for both ends face. However, the opposite results came up from two experimental data of Mason et al. (2010) that produce the asymmetrical of non-wetting production by symmetrical imbibed wetting phase, which means the no-flow boundary in the middle of the core does not function anymore as the non-wetting phase flow through it (Mason et al., 2010).

This asymmetrical production is caused by insignificant difference of capillary back pressure that is generated due to non-uniform of pore size distribution. As the front advances throughout the core, the saturation of wetting phase at the inlet side (one-end-face in contact with wetting phase) gradually increases with decreasing rate of counter-current imbibition rate. Hence, less oil is produced counter currently at the initial time of imbibition and followed by co-current oil production at latter time. The Haugen et al (2014) expressed that the data of oil production from this boundary condition can exhibit the information of the relation of relative permeability and capillary pressure (Haugen et al., 2014)

2.6.2. Viscosity Ratio

Change of viscosity ratio essentially affects the imbibition rate. Evaluating the change in imbibition rate with different viscosity ratio has been investigated by Ma et al. (1999). In the Figure 2-16, their experimental result shows that imbibition rate decreases with increasing oil viscosity where it leads to the high ultimate recovery (Ma, Morrow, & Zhang, 1999). By increasing the oil viscosity, there is extended distinction of water saturation with unclear front (Blair, 1964). The effect of viscosity ratio on the production rate is expressed as,

$$t_D = Ct\sqrt{k/\varphi}\,(\sigma/\mu_w)\sqrt{\mu_w/\mu_{nw}}\left(1/L_c^2\right) \qquad 2\text{-}29$$

where t_D is dimensionless time, C is the unit conversion factor that is equal to 0.018849 if time (t) is in minute, k is permeability [md], φ is fractional porosity, σ is interfacial tension [dynes/cm], μ_w and μ_{nw} are the wetting and non-wetting phase viscosity [cp], and L_c is characteristic length [cm] (Ma et al., 1999).

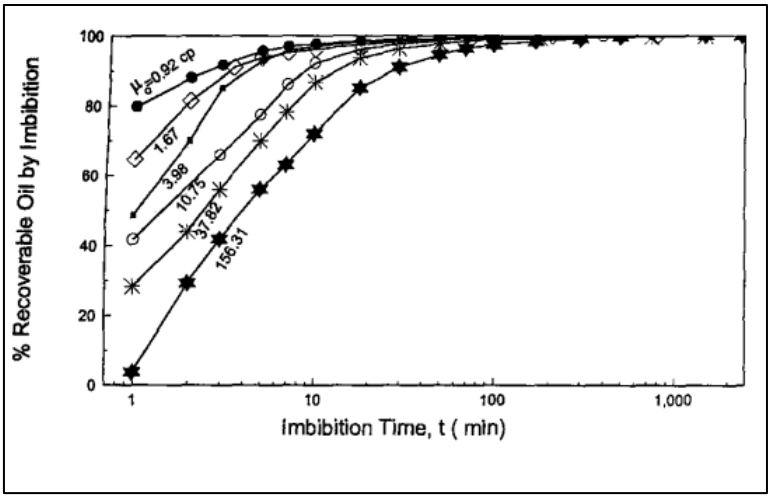

Figure 2-16 Oil Viscosity Effect on Imbibition Rate and Oil Recovery (Ma et al., 1999)

2.6.3. Core Length

The two set of data that considered the viscosity ratio effect, given by Mattax and Kyte (Mattax & Kyte, 1962) were used for characteristic length (L_c) investigation (Kazemi, Gilman, & Elsharkawy, 1992). The relationship between the core length (L) and the characteristic length (L_c) is given by (Zhang et al., 1996),

$$L_c = \frac{Ld}{2\sqrt{d^2 + 2\,L^2}} \qquad 2\text{-}30$$

where d is diameter [cm]. Zhang et al (1996) evaluated the effect of different AFO-core lengths on the oil recovery. This investigation is resulted in the Figure 2-17 (top) that shown by increasing the length of the core, the imbibition rate reduces, then reduces the oil recovery (Zhang et al., 1996). This effect also is corresponded with the characteristic length (L_c) (Figure 2-17 below).

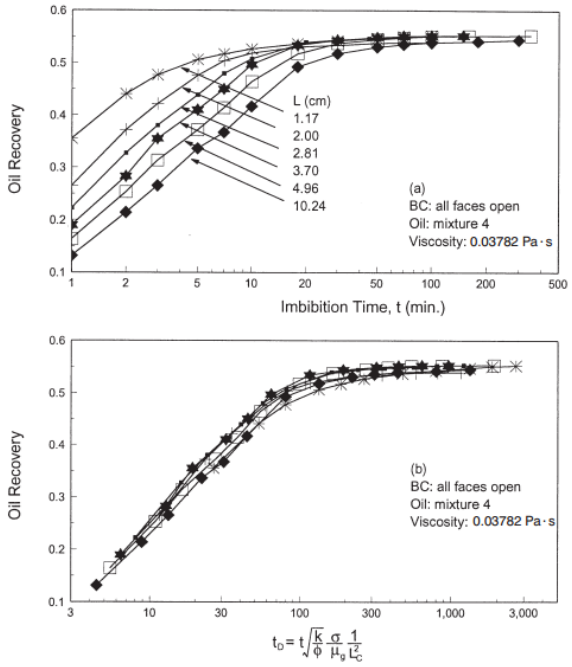

Figure 2-17 An Effect of Different Core-Length on Oil Recovery. Top Figure: The Effect of Core-Length is correlated by the Length (L). Below Figure: The Effect of Core-Length is correlated by the Characteristic Length (L_c) (Zhang et al., 1996)

2.7. IORCoreSim Software (BugSim Version 1.2)

In this thesis, IORCoreSim software is used for building one-dimensional model based on experimental data to investigate spontaneous imbibition process in numerical simulation. This type of software is a second version of MEOR simulator *Bugsim* that has been developed by Arild Lohne for the purpose to investigate oil recovery mechanism at laboratory and in small-field-scale model (Lohne, 2013). Many simulations of spontaneous imbibition have been investigated using this software. There are some specific keyword in this software, such as *wimb* and *wprod* for generating model with certain boundary condition that determines to what type of spontaneous imbibition that will flow in this model (Lohne, 2013). For developing spontaneous imbibition in the model, the main affecting parameters such as capillary pressure and relative permeability must be specified in input data.

2.7.1. Capillary Pressure Correlation in IORCoreSim Software (BugSim Version 1.2)

Capillary pressure correlation that is used in this software as input data of model is J-function capillary pressure. The capillary pressure is built based on the equation from the manual of IORCoreSim which is shown as follow,

$$J_{ow} = C_{L1}\,(S_w - S_{L1})^{-E_{L1}} - C_{R1}\,(S_{R1} - S_w)^{-E_{R1}} + C_{01} \quad \text{2-31}$$

$$P_{cow} = P_o - P_w = J_{ow}\sqrt{\frac{\varphi}{K_{abs}}} \quad \text{2-32}$$

$$C_{01} = C_{L1}\,(1 - S_{or} - S_{L1})^{-E_{L1}} - C_{R1}\,(S_{R1} - 1 - S_{or})^{-E_{R1}} \quad \text{2-33}$$

where J_{ow} is J-function for oil-water, S_w is water saturation, C_{L1} and C_{R1} are capillary pressure parameter, S_{L1} and S_{R1} are minimum and maximum saturation parameters, respectively, E_{L1} and E_{R1} are respectively first and second capillary pressure exponent, and lastly, C_{01} is capillary pressure constant (Lohne, 2013).

2.7.2. Relative Permeability Correlation in IORCoreSim Software (BugSim Version 1.2)

For relative permeability correlation, the Corey-type relative permeability is used in the IORCoreSim to generate flow in the model. The model Corey's equation that is expressed in the manual of IORCoreSim has the same formula as the original Corey's formula in the equation (5) and (6). However, the notation of Corey's equation in the IORCoreSim is different (e.g. in the notation of Corey exponent) that is expressed as follows,

$$k_{rj} = k_{rej}\,(\frac{S_j - S_{rj}}{1 - S_{rj}})^{E_j} \quad \text{2-34}$$

where j is for oil, water, and gas. k_{rj} is fluid relative permeability and k_{rej} is the end-point fluid relative permeability. $S_j$is fluid saturation and S_{rj} is residual fluid saturation. E_j is fluid Corey exponent (Lohne, 2013).

3. Mathematical and Numerical Model Description

3.1.Mathematical Model of Counter Current and Co-Current Imbibition

A mathematical model of counter-current has been described by Evje, Steinar and for the co-current imbibition has been described by Andersen, et.al (2017), respectively. The approach of counter-current model is based on the work of Tavassoli, Zimmerman, and Blunt (Tavassoli, Zimmerman, & Blunt, 2005). Both mathematical model are expressed in the following paragraph. Let consider transport equation for water and oil in 1D homogeneous incompressible reservoir rock with incompressible fluid as follows:

$$\varphi \frac{\partial Sw}{\partial T} + \frac{\partial Uw}{\partial x} = 0 \qquad 3\text{-}1$$

$$\varphi \frac{\partial So}{\partial T} + \frac{\partial Uo}{\partial x} = 0 \qquad 3\text{-}2$$

where S_w and S_o is water and oil saturation respectively. The two phases flow is dominated by Darcy's velocity where the water enters the open face with its velocity (U_w) and oil with its velocity (U_o) flow counter currently to the same open face. The Darcy's velocity for each phase (i = o,w) are expressed by absolute permeability (K) and pressure gradient as (Cheng et al. 2006),

$$U_i = -K\lambda_i (P_i)_x \qquad 3\text{-}3$$

where the gravity is neglected and the fluid mobility (λ_i) is defined as,

$$\lambda_i = \frac{kr_i}{\mu_i} \qquad 3\text{-}4$$

where kr_i is fluid relative permeability and μ_i is fluid viscosity.

Summing both oil and water mass conservation results in water pressure change per unit length of reservoir, $(Pw)_x$

$$(Pw)_x = -\frac{\lambda o}{\lambda_T} (Pc)_x \qquad 3\text{-}5$$

by assuming the fluid saturation is constrained by the mass balance for counter-current and co-current flow,

$$S_w + S_o = 1 \qquad 3\text{-}6$$

in which it generates the assumption of counter-current flow that express a constant total velocity (U_T) as

$$U_T = U_o + U_w = 0 \qquad 3\text{-}7$$

where the counter current flow is induced,

$$U_w = -U_o \qquad 3\text{-}8$$

and fluid pressure is defined by imbibition capillary pressure that is a function of water saturation where capillary pressure is positive value (Pc > 0),

$$P_c\,(S_w) = P_o - P_w \qquad 3\text{-}9$$

Then, substitute equation (13) to the equation (11) and (9) and ends up in water transport equation with another parameter for counter-current flow which is given as follows:

$$\varphi \frac{\partial Sw}{\partial T} + \frac{\partial}{\partial x}\left(K \frac{\lambda_w \lambda_o}{\lambda_T} \frac{\partial P_c(Sw)}{\partial x}\right) = 0 \qquad 3\text{-}10$$

where the total fluid mobility is expressed by,

$$\lambda_T = \lambda_w + \lambda_o \qquad 3\text{-}11$$

For co-current flow, the assumption is described by Andersen, et al. (2017), which expressed by (Andersen, 2017),

a. Introducing total velocity (U_T) as:

$$U_T = U_o + U_w \qquad 3\text{-}12$$

b. The capillary pressure constraint:

$$P_c\,(S_w) = P_o - P_w \qquad 3\text{-}13$$

and produces the water transport equation which include fractional water flow parameter as follows (Chen, Huan, & Ma, 2006):

$$\varphi \frac{\partial Sw}{\partial T} + \frac{\partial}{\partial x}\left(U_T\, f_w + K\, \lambda_o\, f_w \frac{\partial P_c(Sw)}{\partial x}\right) = 0 \qquad 3\text{-}14$$

Where the fractional water flow is,

$$f_w = \frac{\lambda_w}{\lambda_T} \qquad 3\text{-}15$$

And the total fluid mobility is expressed by,

$$\lambda_T = \lambda_w + \lambda_o \qquad 3\text{-}16$$

3.1.1 Initial and Boundary Condition of Counter Current Imbibition

a) Initial condition is specified as follows:

$$S_w(x,0) = S_{w,o}(x) \qquad 3\text{-}17$$

$$P_w(x,0) = P_{w,o}(x) \qquad 3\text{-}18$$

b) Boundary condition is determined as no flux condition at the outlet (x = 1) and let the both oil and water flow at the inlet (x=0) such as

$$S_x(1,t) = 0 \qquad 3\text{-}19$$

where there is no oil is produced at the outlet and,

$$S(0,t) = 1 \qquad 3\text{-}20$$

where water is 100% saturated at the inlet.

3.1.2 Initial and Boundary Condition of Counter Current Imbibition

a) Initial condition is specified as follows:

$$S_w(x,0) = S_{w,o}(x) \quad 3\text{-}21$$

$$P_w(x,0) = P_{w,o}(x) \quad 3\text{-}22$$

b) Boundary condition at the inlet (x = 0) is in contact with water and the flow water is governed by water pressure (P_w) such as

$$S(0,t) = 0 \quad 3\text{-}33$$

If the oil is not allowed to be produced at the inlet (pure co-current oil production), hence, the fractional water flow at the inlet will be:

$$f_w(0,t) = 1 \quad 3\text{-}34$$

At the outlet (x=L), only oil is in contact with and produces at the outlet and the controlled oil pressure (P_o) influence the oil displacement,

$$S(L,t) = 0 \quad 3\text{-}35$$

$$P_w(L,t) = P_o\,(t) - P_c(S_w(L,t)) \quad 3\text{-}36$$

$$f_w(L,t) = 0 \quad 3\text{-}37$$

3.2. Numerical Model

3.2.1. Grid Model

In this thesis, the model is built in the cartesian coordinates that divides the length of model which approximately 48.3 cm in x direction with 100 grid blocks. For simplicity, one-dimensional model is built, the cartesian coordinates will be 100 x 1 x 1 in x, y, and z-direction respectively. To imitate the experimental setup, initially the model is assumed to be saturated with 100% oil and using the TEOFSI boundary condition, let the water to be in contact at the open-inlet and the oil is in contact with the open-outlet. Since experimental setup used the cylindrical tube, the cross-sectional area in the tube must be the same as in 1D cartesian grid model is required. The correction of radius tube for constant cross-sectional area is described in the sub-section 4.5 in the chapter 4. The residual oil saturation for all experiment is approximately in the range of 0.15-0.20. The average fractional porosity and the residual oil saturation for all experiment is mentioned in the Table 3-1. The detail of the input data for building the model is shown in the Appendix A and the built model is shown in the Figure 3-1.

Table 3-1 The Grid Properties Model

Purpose	Grid Properties of Model								
	Sandpack Length [cm]	Corrected Width of Tube [cm]	x	y	z	Fractional Porosity (ϕ)	k [mD]	S_{wi}	S_{or}
For Sensitivity Analysis	48.3	1.8078	1-100	1	1	0.39	14500	0	0.8
History Matching	48.3	1.8078	1-100	1	1	0.39	14500	0	0.85

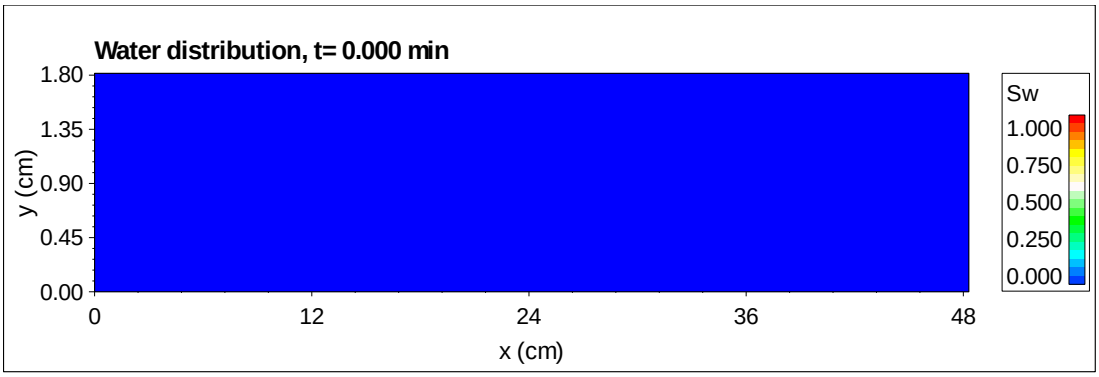

Figure 3-1 The Cartesian Grid Model that Used for Simulation with Initial Condition

3.2.2. Flow Modeling

One-dimensional model is built using IORCoreSim software that generated by Lohne, A. (2013). Referred to the manual of this software, "wimb" and "wprod" keywords are the main controller to generate the boundary condition in the model to be two-ends open free spontaneous imbibition TEOFSI (Lohne, 2013). "wimb" keyword defines the imbibing fluid and "wprod" keyword defines the fluid that want to be produced. Since the model allows for both counter-current and co-current flow to occur, those keywords are thus specified in the input data. Referred to this software, the flow equation in the model, which is described by Lohne, A. (2013) express as follow:

There are two flow occurs at the inlet mode, such as counter-current and co-current flow. Counter-current flow push the oil to produce through the inlet, while co-current flow force water to imbibe the model. These flow equations expressed by,

$$Q_{k,o,prod} = -T_{w,k}\,\lambda_{k,o}(P_{w,k} + P_{cb,o} - P_{i,o} + d_{hz}\gamma_o) \quad 3\text{-}38$$

$$Q_{k,w,inj} = T_{w,k}\,\lambda_{k,t}(P_{w,k} - P_{i,w} + d_{hz}\gamma_w) \quad 3\text{-}39$$

where $Q_{k,o,prod}$ and $Q_{k,w,inj}$ is volumetric flow rate of displaced phase (oil) and the imbibing phase (water) for interval k connected to cell i, respectively. λ_l is fluid mobility, and $\gamma_l = \rho_l g$. d_{hz} defines the height difference between the boundary connection k and the center of cell i. $P_{cb,o}$is additional boundary capillary pressure. $P_{w,k}$is water pressure in the connection k. $P_{i,l}$ is fluid pressure in the center of i. $T_{w,k}$ is the transmissibility or connection factors with flow in x-direction for open face condition that is given by

$$T_{w,k} = \frac{2k_x \Delta y_i \Delta z_i}{\Delta x_i} \quad 3\text{-}40$$

By referring the concept of capillary back pressure in the sub-section 2.5.2 (chapter 2), the equation (52) shows the counter-current production occurs as the oil pressure in the center of cell i is lower than oil pressure in the interval k and oil boundary pressure,

$$P_{i,o} < (P_{w,k} + P_{cb,o}) \quad 3\text{-}41$$

This type of production starts to cease if the oil is snap off in the inlet and hard to form the droplet. Once the counter-current production is stopped, hence, the additional oil boundary pressure is equal to the oil pressure in the center of cell i ,

$$P_{cb,o} = P_{i,o} \quad 3\text{-}42$$

Note that the imbibition process uses downstream total mobility, λ_t, while the production uses upstream fluid mobility, λ_l. At the production boundary, only flow out of the model is allowed. Since only oil is produced, then the oil flow equation will be,

$$Q_{k,o,prod} = -T_{w,k}\, \lambda_{k,o}(P_{w,k} + P_{cb,o} - P_{i,o} + d_{hz}\gamma_o) \quad 3\text{-}43$$

4. INTERPRETATION DATA

Data input to run a simulation for this thesis is taken from experiment result of master's thesis student from University of Bergen, Håkon Kyte Haugland which his thesis is entitled *spontaneous imbibition in sand - viscosity effects on oil recovery and flow using polymer and glycerol*. The experiments are conducted in collaboration with Vabø (2016). There are 4 types of conducted experimental setup with different properties. However, only one experiment setup would be chosen for the simulation. The following paragraph will be consisting of information about an imbibition tube properties, fluid properties, and fluid preparation of the experiment to the selected experimental result.

4.1. Imbibition Tube Properties

Glass tube is used to investigate the imbibition front with glass thread (GL25) at each end. The glass tube properties are given in the table Table 4-1. The tube is printed 40 cm long a centimeter scale starting from the filter. Paper filter is used in the end tube, which was in capillary contact with the sand in the tube. The pore size of the paper filter was not measured. The imbibition glass tube is captured in the Figure 4-1

Table 4-1 Imbibition Glass Tube Properties

Glass Tube Properties		
Tube Length [cm]	Inner Diameter of Tube [cm]	Inner Diameter of Glass Threads [cm]
50	2.04	1.8

Figure 4-1 An imbibition tube with glass threads on each end side and glass filter type 2 inside the inlet tube (Haugland, 2016)

4.2.Fluid Preparation

4.2.1. Oil Properties

There are three different type of oil that were used to conduct this experiment. These oil does not contain of the surface active component. In order word, the polar component has been removed from the mineral oil to prevent wettability alteration during imbibition. The following table is the properties of different oil act as a non-wetting phase during the imbibition experiment.

Table 4-2 The Mineral Oil Properties for Experiments (Haugland, 2016)

Oil	Density, ρ (g/cm3)	Viscosity, μ (cP)
Decane 95%	0.726	0.96
Marcol 82	0.844	32.6
DTE FM 32	0.851	73.2

4.2.2. Brine and Polymer Properties

The following table is the properties of different brine and polymer act as a non-wetting phase during the imbibition experiment. Polymer and glycerol was added to the brine to study the effects of viscosity ratio on spontaneous imbibition. The polymer used was a hydrolyzed polyacrylamide (HPAM). The fluids properties are described in the table Table 4-3.

Table 4-3 The Brine and Polymer Properties for Experiments (Haugland, 2016)

Brine	Density, ρ (g/cm3)	Viscosity, μ (cP)
0 wt% glycerol	1.034	1.15
70 wt% glycerol	1.203	28.3

4.3.Experimental Setup

Experimental setup D from Haugland's Thesis (Haugland, 2016) is selected as the most representative and successful in spontaneous imbibition experiment to build the model. This sort of experimental setup describes an imbibition tube was immersed into the water bath. There were five imbibition tubes that immersed into the water bath and produced the oil. All the inlet of imbibition tube was attached the paper filter to prevent the sand would be produced out. This paper was also restricted the counter-current flow to occur. At the outlet of the imbibition tube,

the end tube was connected to the male-male Swagelok that lead for the outlet is in contact with oil and air outside the tube. A measuring tube is saturated with wetting phase and was resided above the inlet side to measure the counter-current production. At some time, oil droplets would produce on the top of the inlet end piece and float into the measuring tube during the experiment.

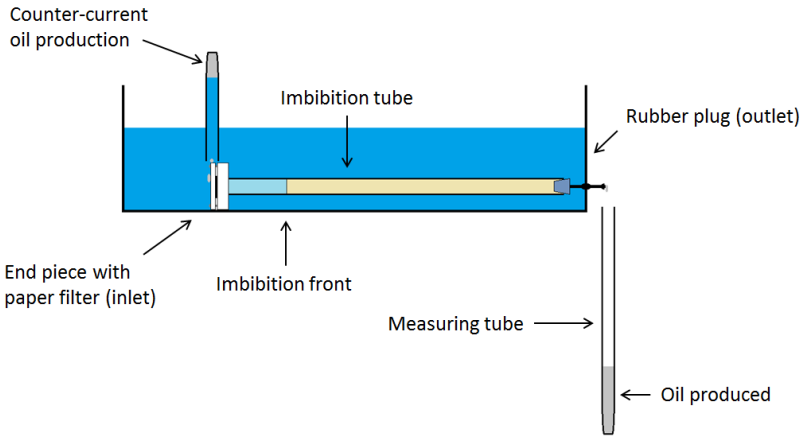

Figure 4-2 Schematic of Experimental Setup D (Haugland, 2016)

4.4.Experimental Result

Table 4-4 Summary of Experimental Setup D Result

Experiment	Oil viscosity [cP]	Water Viscosity [cP]	Porosity [fraction]	Oil Recovery After Breakthrough [fraction]			Oil Recovery at Breakthrough [fraction]		
				Counter current	Co current	Total	Counter current	Co current	Total
SP2	0.96	1.15	0.394	0.103	0.74	0.84	0.103	0.704	0.807
SP3	32.6	1.15	0.377		0.84	0.84		0.83	0.83
SP4	73.2	1.15	0.399		0.74	0.74		0.69	0.69
SP 6	0.96	29.09	0.393		0.77	0.77		0.76	0.76
SP 7	0.96	28.3	0.385		0.82	0.82		0.81	0.81

From all the experiments that conducted by Haugland (2016), the experimental setup D was successfully carried out the spontaneous imbibition process in the sand-pack. This process achieved piston-like displacement for most experiments except experiment SP 5, which is ignored due to there is a retention polymer occurs during imbibition. Following the successful experimental setup D result, a series of experiments where oil with different oil viscosity as the non-wetting phase was displaced by water and the various water viscosity displaces the oil. The oil recovery result for all experiment in the table 5.4 are plotted against the time that shown in the Figure 4-3 for viscous oil-water displacement and in the Figure 4-4 for oil-viscous water displacement.

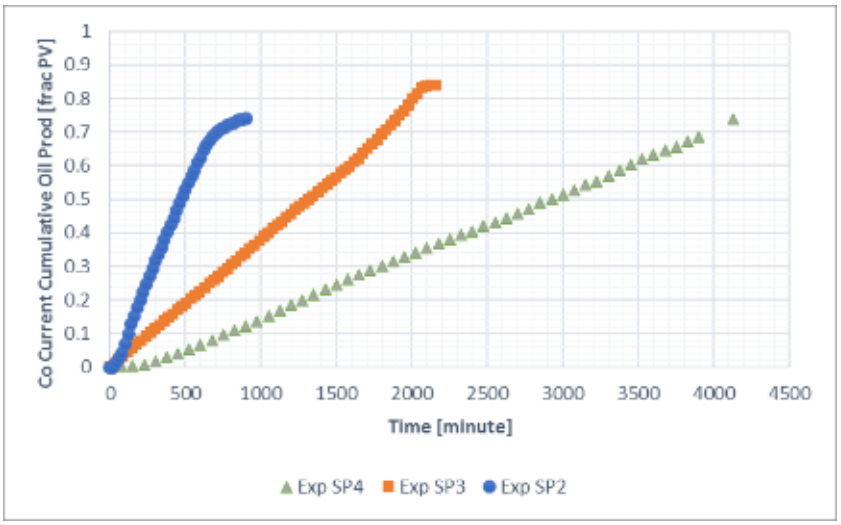

Figure 4-3 Co-Current Oil Recovery from Experiment SP2 to SP4 (Haugland, 2016)

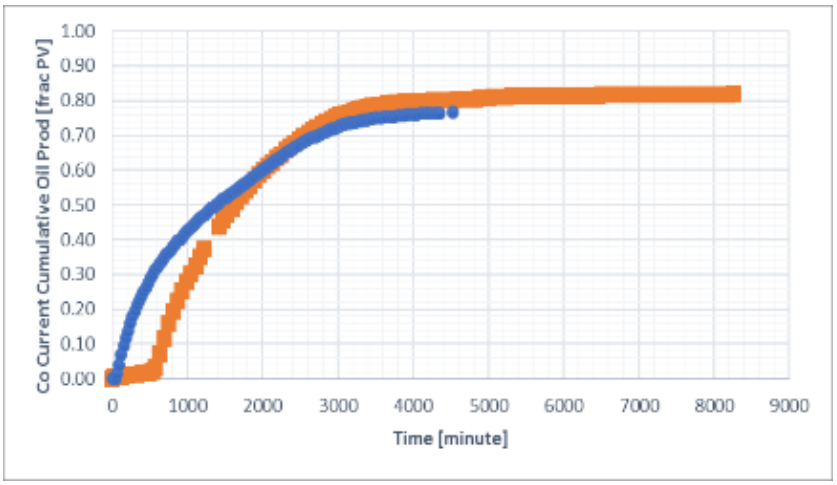

Figure 4-4 Co-Current Oil Recovery of Experiment SP6 and SP7 (Haugland, 2016)

4.5. Interpretation Data for Input Model

All the imbibition properties are identical except for fractional porosity that vary for each experiment. For building the model, the average porosity is required which resulted in the Table 4-5.

Table 4-5 Average Imbibition Tube Properties Based on The Experimental Result

Properties of Imbibition Tube			
Length Sand Pack [cm]	**Inner Diameter of Tube [cm]**	**k [mD]**	**φ**
48.3	2.04	14500	0.39

For simplicity, the cartesian grid is used for model geometry. Thus, the correction of cross section area for 2 phases flow is required. The area of surface area of cylinder tube is (by assuming π = 3.14153)

$$Area_{circle} = \frac{\pi}{4} D^2 = \frac{3.14153}{4} (2.04\ cm)^2 = 3.268\ cm^2$$

Assume a circle is inscribed in a square, the circle diameter is equal to the side length of the square. To obtain the equal cross section area, the square side length (s) should be:

$$s_{square} = \sqrt{Area_{circle}} = \sqrt{(3.268\ cm^2)} = 1.8078\ cm$$

Hence, the correction for width and height for cartesian grid as follows:

Table 4-6 Average Model Properties Based on The Experimental Result

Properties of Imbibition Tube			
Length Sand Pack [cm]	**Inner Diameter of Tube [cm]**	**k [mD]**	**φ**
48.3	2.04	14500	0.39

The assumption for model simplicity:

1) 1D horizontal incompressible porous medium.
2) Immiscible 2-phase flow of incompressible fluid.
3) Porous medium is 100% oil saturated ($S_{wr} = 0$) and strongly water-wet ($\theta = 0^o$).
4) Pc > 0 to initiate spontaneous imbibition.
5) Neglecting the play role of porous disc or paper filter in the system to allow counter-current production.
6) Boundary condition is two ends open (TEO) by the inlet side is in contact with water (wetting phase) and the other side is in contact with oil (non-wetting phase)

5. RESULT AND ANALYSIS

5.1. Sensitivity Analysis

After satisfying the physics of co-current spontaneous imbibition using numerical simulation, a parametric study was carried out to evaluate the influence of relative permeability, viscosity ratio, imbibition tube length, capillary pressure, and capillary back pressure on the production rate and the oil recovery (counter-current and co-current production).

This investigation can also improvement the coherence of production profile with experimental result during manual history matching.

5.1.1. Reference Capillary Pressure for Sensitivity Analysis and Curve Match.

Reference capillary pressure curve is built based on the equation from IORCoreSim that expressed in the section 1.7 (chapter 2). The following table is those parameter values forming capillary pressure curve, which is illustrated in the Figure 5-1.

Table 5-1 Parameter Values Forming Reference Capillary Pressure Curve

Parameter Capillary Pressure Curve								
C_{L1}	C_{R1}	C_{01}	E_{L1}	E_{R1}	S_{L1}	S_{R1}	ϕ [fraction]	k,absolute [mD]
0.008	0.010	0.995	3.000	5.000	1.000	-0.340	0.390	14500

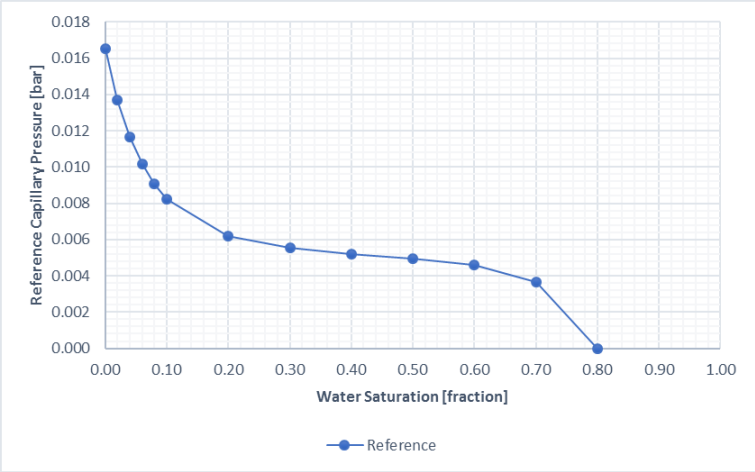

Figure 5-1 The Reference Capillary Pressure Curve

5.1.2. Reference Relative Permeability for Sensitivity Analysis and Curve Match.

Reference relative permeability curve is formed relied on Corey's equation in the IORCoreSim that expressed in the section 2.7.2 (chapter 2). Since the model is assumed to be only strongly water-wet, only one saturation table will be generated. The values of water and oil Corey exponent in the Table 5-2 are referred to the table Table 2-3 (chapter 2) for strongly water-wet.

Table 5-2 Parameter Value Forming Reference Relative Permeability Curve

Parameter Relative Permeability Curve			
k_{rew}	0.2621	n_w	6
k_{reo}	1	n_o	2

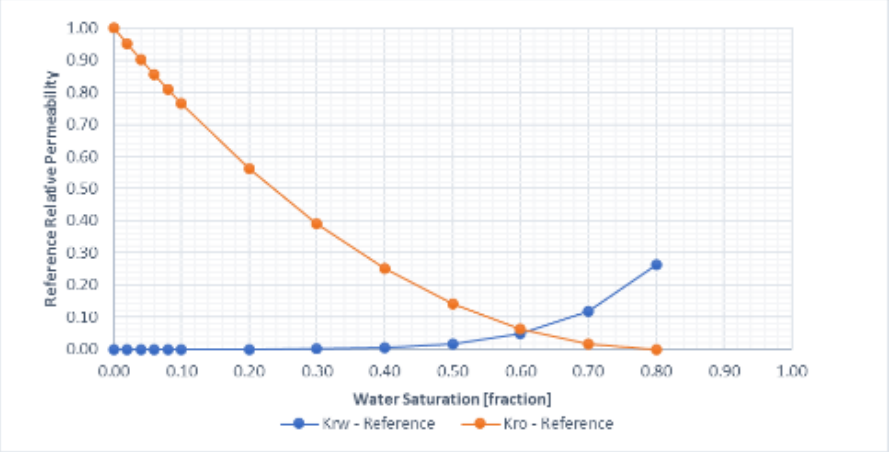

Figure 5-2 Reference Relative Permeability Curve

5.1.3. Parameter Study of Relative permeability

In co-current spontaneous imbibition which involves immiscible two-phase flow system, the relative permeability correlation of Corey exponent is applied. Since the two-phase flow in the model is constrained with the residual oil saturation, the choice of Corey exponent for relative permeability correlation is considerably straightforward. Using of Corey exponent instead of LET-type relative permeability is because of simplicity. To analysis parameter study, Corey exponent for water and oil are adjusted to investigate a change of water breakthrough time which lead to the change of the oil recovery. There are 2 cases will be analysed in the model, such as:

1) Case A: Change of oil recovery with increasing n_w with constant n_o for viscosity ratio (μ_w/μ_o) = 1.20.

In this case, water Corey exponent (n_w) is adjusted from the reference relative permeability to investigate the change of oil recovery. The altered water Corey exponent lead to the modified end-point of water relative permeability that are presented in the Figure 5-3. Note that oil relative permeability is kept constant during the parameter study due to the model is 100% oil saturated at irreducible water saturation (S_{wr}=0).

Table 5-3 Parameter of Relative Permeability for Case A (an increase of water Corey exponent)

μ_w/μ_o = 1.20 (μ_o = 0.96 & μ_w = 1.15)			
	Case A1	Reference	Case A2
n_w	2	7	10
k_{rew}	0.640	0.262	0.107
n_o	2		
k_{reo}	1		

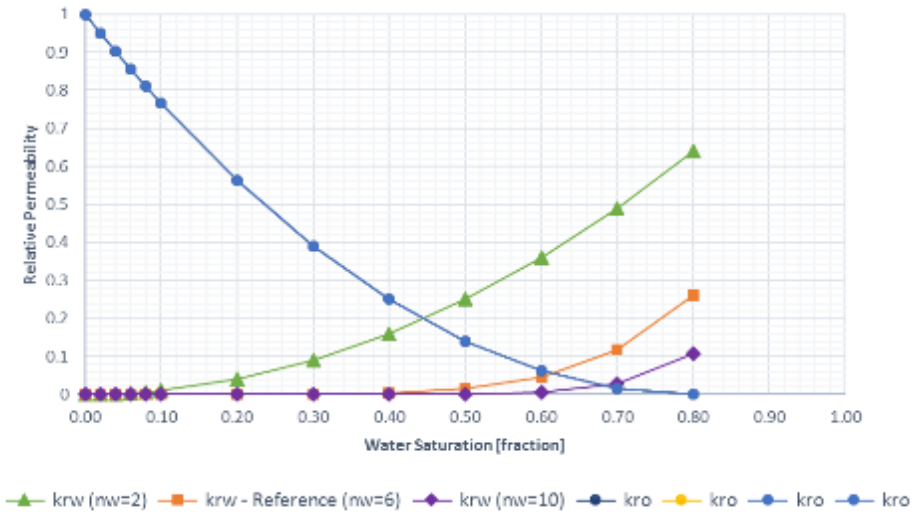

Figure 5-3 Relative Permeability Curves - Case A (An Increase of Water Corey Exponent).

TheFigure 5-3 shows that the relative permeability curve shifts to the right with the end-point of water relative permeability decreases as water Corey exponent increases. As the various relative permeability curves are generated, the parameter study is analyzed by investigating the impact of those different relative permeability on the oil recovery. The results are given as follows

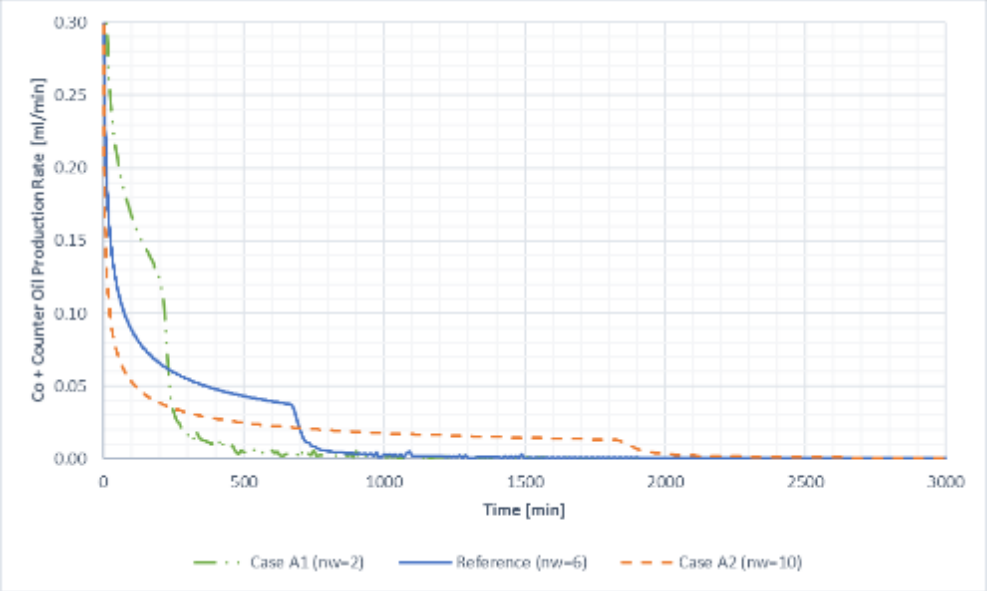

Figure 5-4 Total (Co-Current + Counter-Current) Oil Producation Rate - Case A (an increase of water Corey exponent)

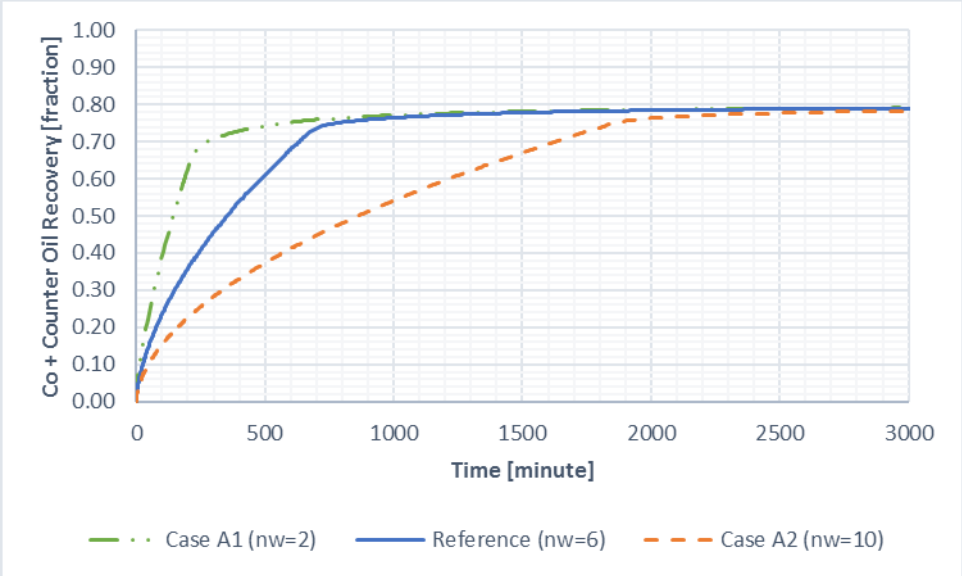

Figure 5-5 Total (Co-Current + Counter-Current) Oil Recovery - Case A (an increase of water Corey exponent)

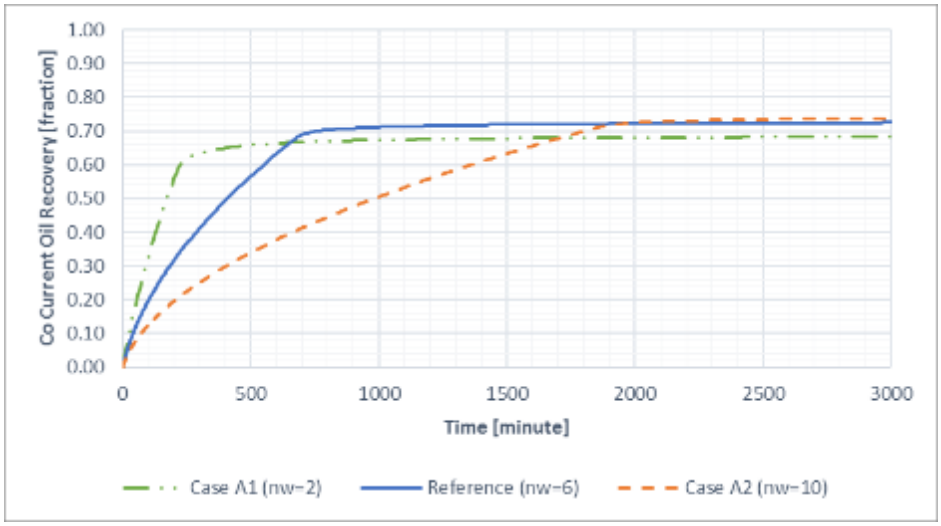

Figure 5-6 Co-Current Oil Recovery - Case A (an increase of water Corey exponent)

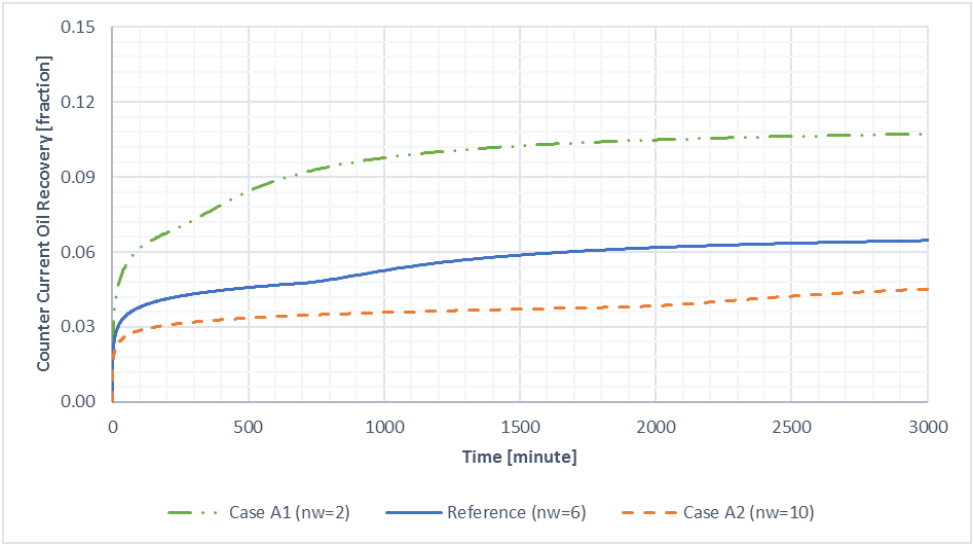

Figure 5-7 Counter Current Oil Recovery - Case A (an increase of water Corey exponent)

Figure 5-4 shows a delay of oil production rate to fall off with increasing water Corey exponent. A surge of water Corey exponent induces a reduction of water relative permeability end-point. As water relative permeability end-point decreases, the oil production rate declines slowly. It implies that the drop of oil production rate is influenced by the water relative permeability. Comparison between Figure 5-4 and Figure 5-5 show that water breakthrough corresponds to the drop of oil production rate. The more water breakthrough is postponed, the more oil is recovered.

As the water relative permeability decreases due to an increase of water Corey exponent, the oil mobility will be higher than water. The higher oil mobility increases the imbibition rate

and thus achieve the high oil recovery in total and co-current production at the breakthrough as it is captured in the Figure 5-5 and Figure 5-6. On the other hand, the counter-current production is reduced as the water is less mobile (see Figure 5-7).

In the Table 5-4, after the breakthrough, the total oil recovery still increases until reaches the maximum oil recovery at the residual oil saturation which is 80% of pore volume. Note that water breakthrough in this thesis defines as the water has reached the outlet or the producer, instead of water production, because of capillary effect. The water front is built up at the producer as water saturation increases and does not affect the oil production after breakthrough. In addition, the oil recovery is plotted against the square root of time in Figure 5-8 shows a linear trendline of oil recovery curve with increasing water Corey exponent. The linear trendline of the curve indicates the all the flow resistance is in the wetting phase (water).

Table 5-4 The Change of Oil Recovery with Increasing water Corey Exponent

	Break-through Time [min]	**Oil Recovery at the Breakthrough [fraction]**				**Oil Recovery after the Breakthrough [fraction]**			
		Counter Current	**Co Current**	**Total**	**Ratio of Counter / Co-current**	**Counter Current**	**Co Current**	**Total**	**Ratio of Counter / Co-Current**
Case A1 ($n_w = 2$)	225	0.069	0.601	0.670	0.103	0.112	0.688	0.800	0.163
Reference ($n_w = 6$)	762	0.048	0.700	0.749	0.065	0.070	0.730	0.800	0.095
Case A2 ($n_w = 10$)	1916	0.038	0.719	0.757	0.050	0.053	0.747	0.800	0.071

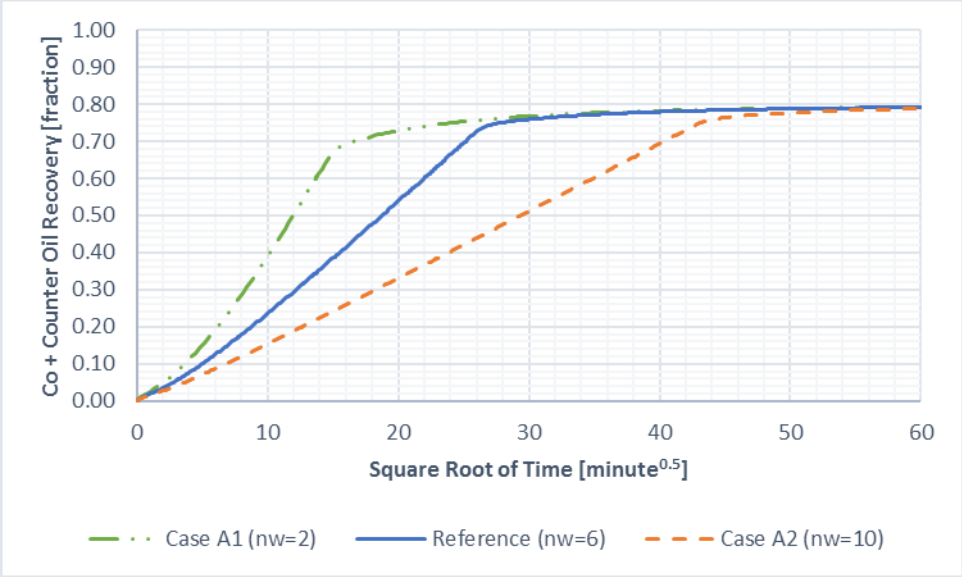

Figure 5-8 Total (Co-Current + Counter Current) Oil Recovery with Square Root of Time- Case A (an increase of water Corey exponent)

2) Case B: Change of oil recovery with increasing n_o with constant n_w for viscosity ratio (μ_w/μ_o) = 1.20.

For case B, oil Corey exponent is only parameter that adjusted from reference relative permeability for oil recovery investigation. Once again, the oil relative permeability end-point is kept constant due to the initial condition of the model. The alteration of oil Corey exponent does not give an impact for another parameter, unlike the change of water Corey exponent that was described in the point 1. The following table contains of values of oil Corey exponent change.

Table 5-5 Parameter of Relative Permeability for Case B (an increase of oil Corey exponent)

μ_w/μ_o = 1.20 (μ_o = 0.96 & μ_w = 1.15)			
	Reference	Case B1	Case B2
n_o	2	4	6
k_{reo}	1		
n_w	6		
k_{rew}	0.26		

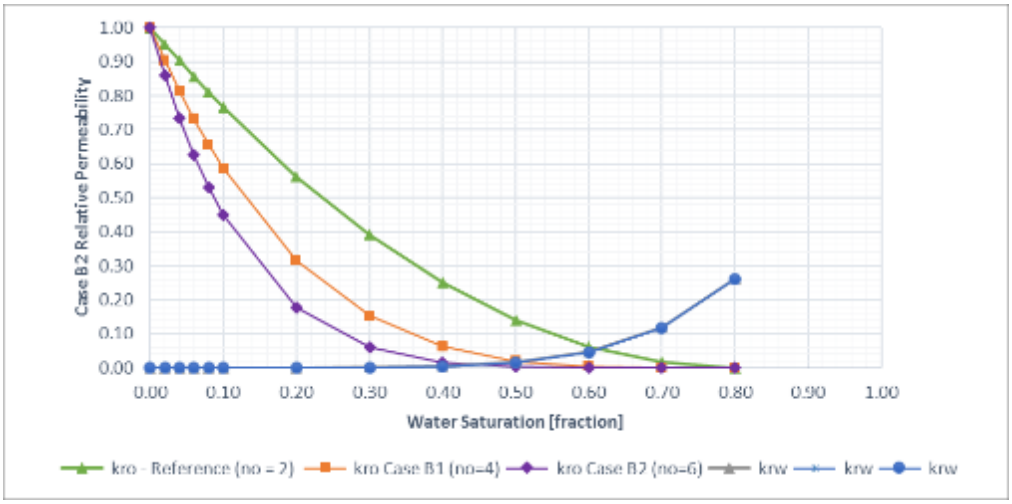

Figure 5-9 Relative Permeability Curves - Case B (an increase of oil Corey exponent)

The Figure 5-9 shows that the relative permeability curve shifts to the left with increasing oil Corey exponent causes the shape of oil relative permeability is more concave up. Nothing's change for the end point of water and oil relative permeability. As the various relative permeability curves are generated, the parameter study is analyzed by investigating the impact of the difference relative permeability on the oil recovery. The results are given as follows

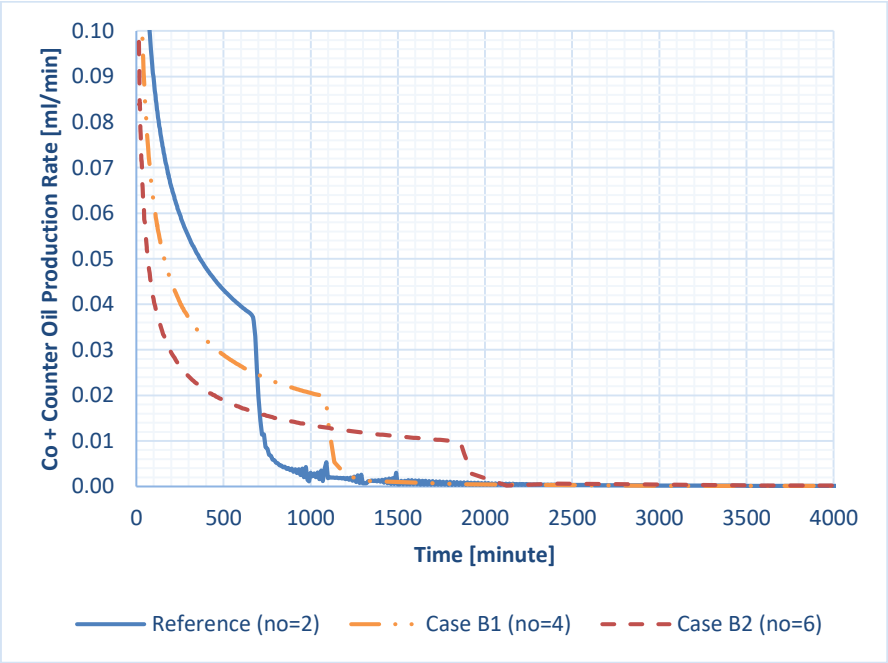

Figure 5-10 Total (Co-Current + Counter-Current) Oil Producation Rate - Case B (an increase of oil Corey exponent)

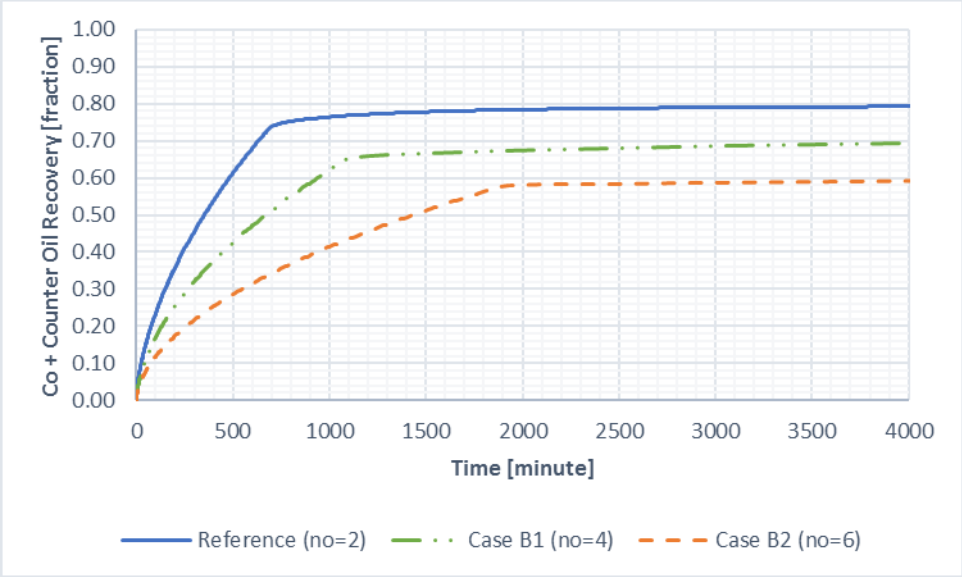

Figure 5-11 Total (Co-Current + Counter Current) Oil Production Rate - Case B (an increase of oil Corey exponent)

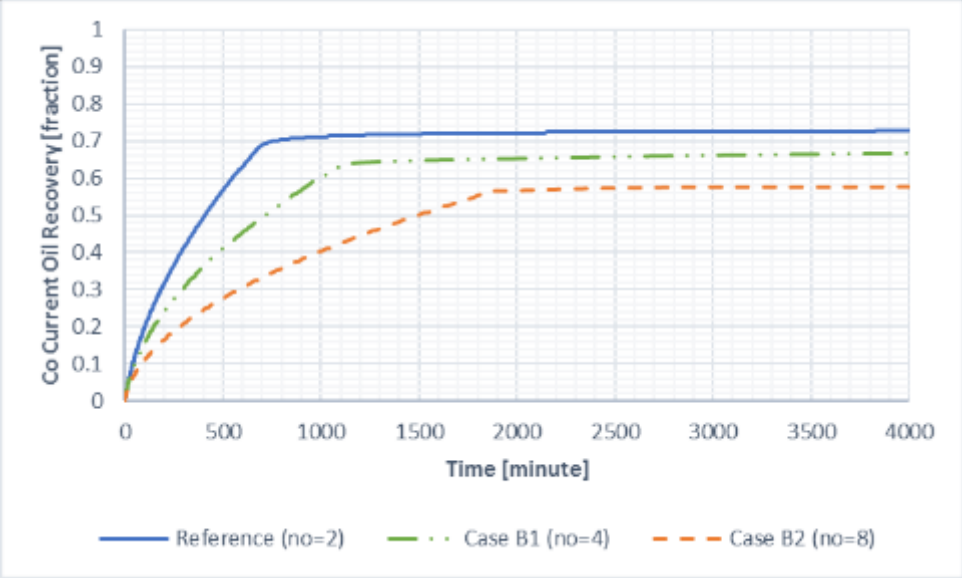

Figure 5-12 Co-Current Oil Recovery - Case B (an increase of oil Corey exponent)

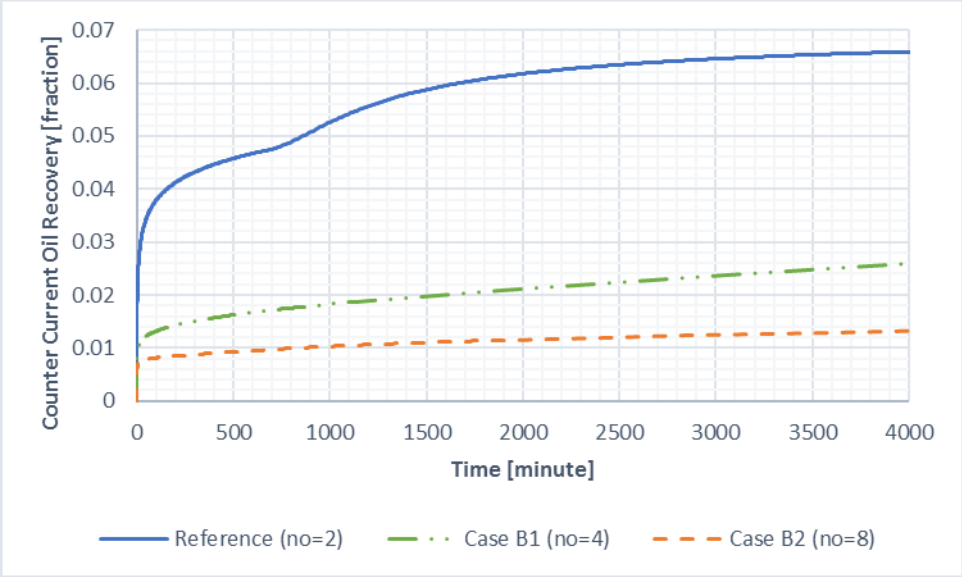

Figure 5-13 Counter Current Oil Recovery - Case B (an increase of oil Corey exponent)

The same result as the case A in the Figure 5-4, which is a delay of production rate drop that it thus postpones the water to reach the outlet as oil Corey exponent is increased (Figure 5-10 and Figure 5-11). However, in the case A, the co-current production increase with increasing water Corey exponent. In the case B, the co-current production reduces, while the counter-current oil recovery rises with increasing oil Corey exponent. In spite of that, the co-current oil production always dominates the flow modeling as it can be seen in the Table 5-6. A surge of oil Corey exponent affects the oil mobility is less mobile. This causes the imbibition rate might be slower than for strongly water-wet. Thus, before breakthrough the all the oil production decreases as imbibition progresses (see Figure 5-11, Figure 5-12, Figure 5-13). It implies that the downfall of production rate is influenced by the oil relative permeability.

Table 5-6 The Change of Oil Recovery with Increasing Oil Corey Exponent

	Break-through Time [min]	**Oil Recovery at breakthrough [fraction]**				**Oil Recovery after breakthrough [fraction]**			
		Counter Current	**Co Current**	**Total**	**Ratio of Counter / Co-current**	**Counter Current**	**Co Current**	**Total**	**Ratio of Counter / Co-current**
Reference ($n_o = 2$)	762	0.048	0.700	0.749	0.069	0.070	0.730	0.800	0.10
Case B1 ($n_o = 4$)	1200	0.019	0.641	0.660	0.030	0.077	0.723	0.800	0.11
Case B2 ($n_o = 6$)	1924	0.011	0.567	0.578	0.020	0.110	0.690	0.800	0.16

After the breakthrough, the co-current production still reduces, while the counter current production enhances with increasing oil Corey exponent as shown in the Figure 5-13 and Table 5-6. Less oil mobile which is triggered by an increase of oil Corey exponent causes the counter-current production to rise. In addition, in the Figure 5-14, the oil recovery is plotted against the square root of time shows a somewhat linear trendline of production curve with increasing oil Corey exponent. The linear trendline of production curve indicate the resistance to flow is in the wetting phase (water).

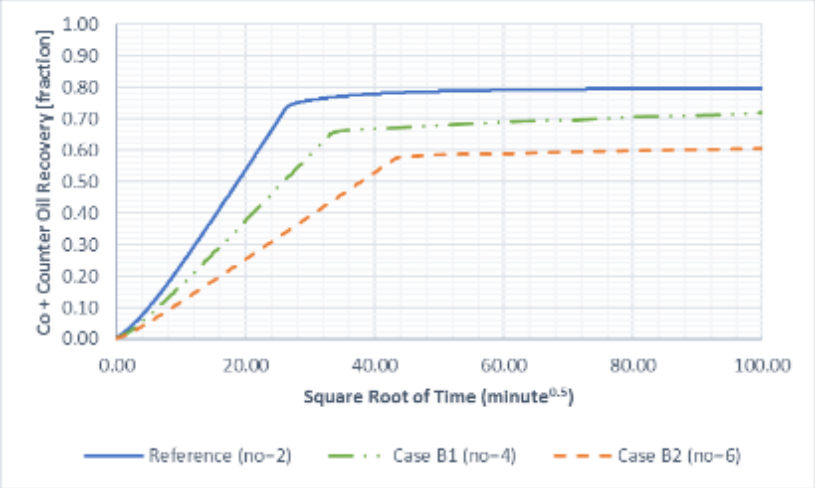

Figure 5-14 Total (Co-Current + Counter-Current) Oil Recovery with Square Root of Time - Case B (an increase of oil Corey exponent)

5.1.4. Parameter Study of Viscosity Ratio

For oil and water viscosity that are used for parameter study of viscosity ratio is taken from experimental data in the Table 4-4 (chapter 4). The viscosity ratio for each case are summarized in the Table 5-7.

Table 5-7 Various of Viscosity Ratio for Increasing Oil Viscosity

	Oil viscosity (cP)	Water Viscosity (cP)	Viscosity Ratio (μ_w/μ_o)
Reference Case	0.96	1.15	1.20
Case 1	32.6	1.15	0.04
Case 2	73.2	1.15	0.02

By using the reference capillary pressure and relative permeability into those experimental input data in the simulator, it thus gives effect of different viscosity ratio on the oil recovery and oil production rate will be resulted in the following graphs.

Figure 5-15 Total (Co-Current + Counter Current) Oil Production Rate for Decreasing Viscosity Ratio

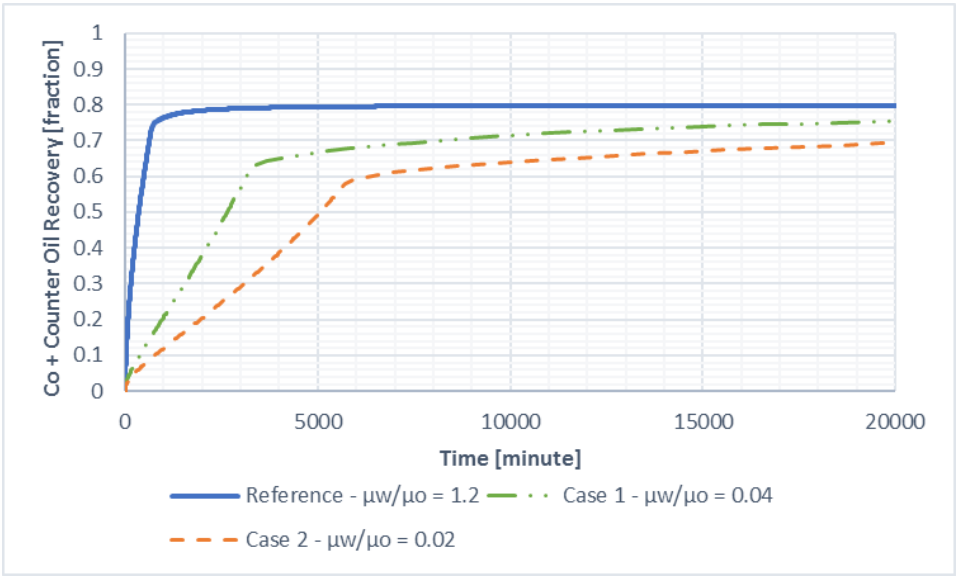

Figure 5-16 Total (Co-Current + Counter Current) Oil Recovery for Decreasing Viscosity Ratio

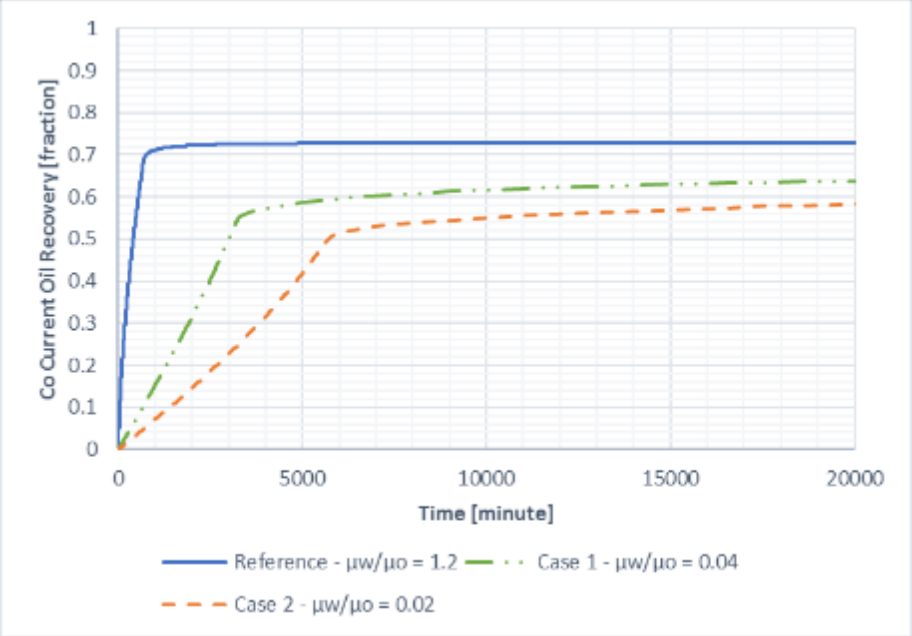

Figure 5-17 Co-Current Oil Recovery for Decreasing Viscosity Ratio

Figure 5-15 shows the latest time of production rate to drop off occurs for low viscosity ratio (case 2). The longer time of production to decline, the longer time for water to reach the producer (water breakthrough) as it illustrated in the Figure 5-16. The reduction of the viscosity ratio due to an increase of oil viscosity leads to a decrease of imbibition rate. Hence, it decreases the total oil recovery as shown up in the Figure 5-16.

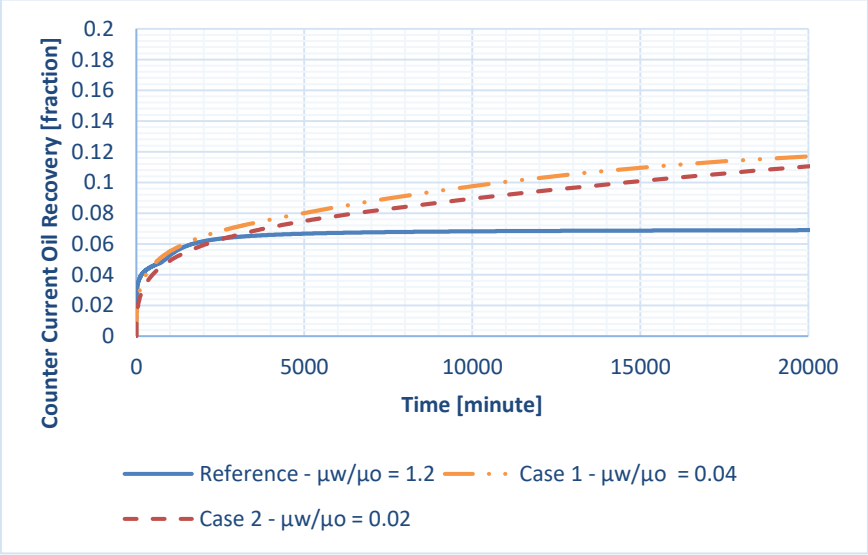

Figure 5-18 Counter Current Oil Recovery for Decreasing Viscosity Ratio

As the oil viscosity increases, the counter current production will be increased, while the co-current production decreases at and after the breakthrough as shown in the Figure 5-17 and Figure 5-18. This case is similar with the case B in the relative permeability parameter study that is shown with reducing oil mobility, the oil tends to produce counter-currently. The reason is the because high oil pressure is needed to water imbibes the viscous-oil-saturated porous medium, the oil pressure might overcome the capillary back pressure and hence, the counter-current production occurs in the inlet. The Table 5-8 shows the an increase of counter-current production over the counter-current oil recovery.

Table 5-8 Result of Decrease Viscosity Ratio Effect on Oil Recovery

	Break-through Time [min]	**Oil Recovery at Breakthrough [fraction]**				**Oil Recovery after Breakthrough [fraction]**			
		Counter Current	**Co Current**	**Total**	**Ratio Counter / Co-current**	**Counter Current**	**Co Current**	**Total**	**Ratio Counter / Co-current**
Reference - μ_w/μ_o = 1.20	762	0.048	0.700	0.749	0.069	0.070	0.730	0.800	0.095
Case 1 - μ_w/μ_o = 0.04	3305	0.073	0.553	0.626	0.131	0.140	0.660	0.800	0.212
Case 2 - μ_w/μ_o = 0.02	5925	0.078	0.512	0.590	0.153	0.163	0.637	0.800	0.255

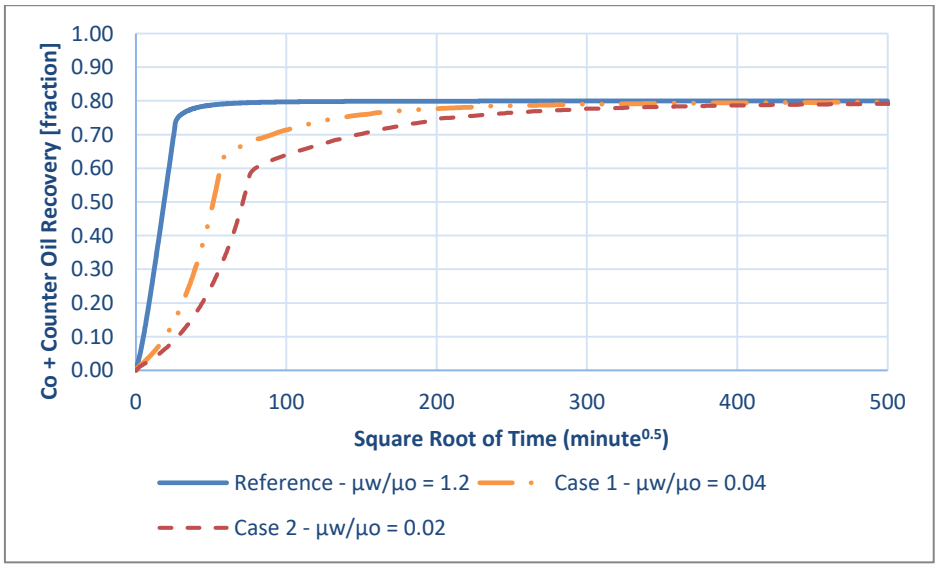

Figure 5-19 Total (Co-Current + Counter-Current) Oil Recovery with Square Root of Time For Different Viscosity Ratio

The simulation result in the Figure 5-19 shows the effect of different viscosity ratio on the oil production with square root of time. The oil recovery deviates from linearity with the square root of time as the oil viscosity rises. The behaviour of non-linearity indicates that some resistance to flow in the wetting phase (water) is vanished by oil. It implies that the resistance to flow exists in both water and oil.

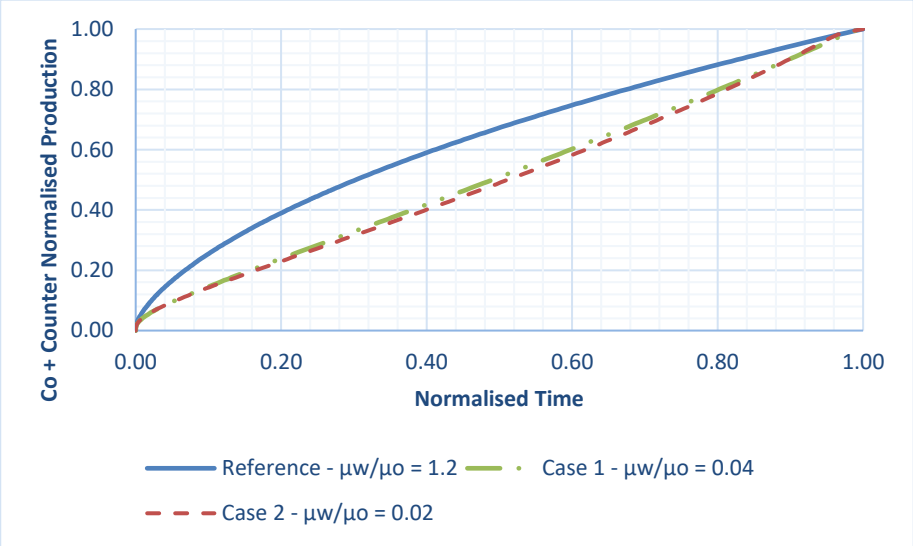

Figure 5-20 Normalized Production versus Normalized Time for Different Viscosity Ratio

Viscosity ratio effect can also be investigated by plotting the normalized production over the normalized time. The trendline of simulation result in the Figure 5.20 is satisfied with hypothesis of the Figure 2-14 (chapter 2) that an increase of viscosity ratio would lead to deacceleration of the interface, while decrease viscosity ratio causes an increase of interface speed. It is absolutely convinced that owing to the high oil viscosity, an increase of interface (low imbibition rate) would lead a decrease of co-current oil production which illustrated by case 1 and case 2.

5.1.5. Parameter study of Imbibition Tube Length

An increase of imbibition tube length is investigated to examine its impact on the oil recovery and oil production rate. In this case, the input reference data for simulation is used where $\mu_w/\mu_o = 1.20$. All the core properties keep constant except the tube length. The tube length is enlarged by two and three times of the reference length which is shown at case 1 and case 2. These number are summarized in the table below, followed by the simulation result.

Table 5-9 The Result of Different Viscosity Ratio Effect on Oil Recovery

Remark	Reference	Case 1	Case 2
Tube Length [cm]	48.3	96.6	144.9

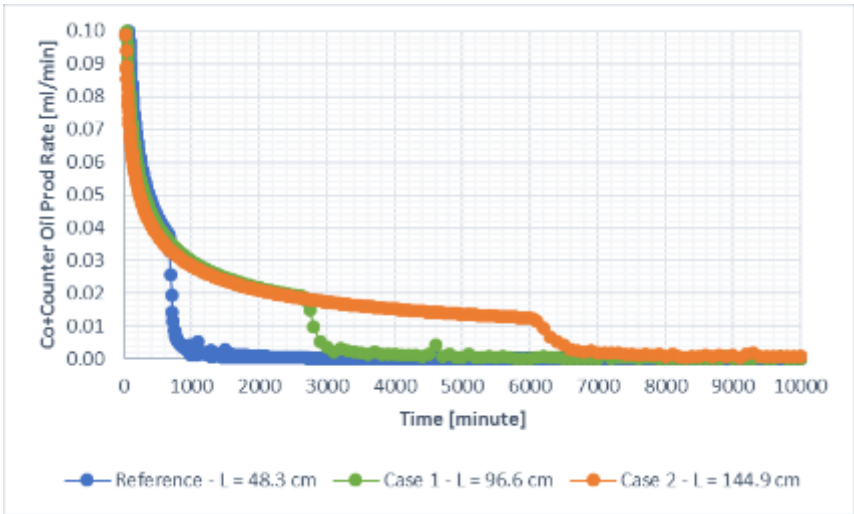

Figure 5-21 Total (Co + Counter Current) Oil Production Rate for Different Tube Length

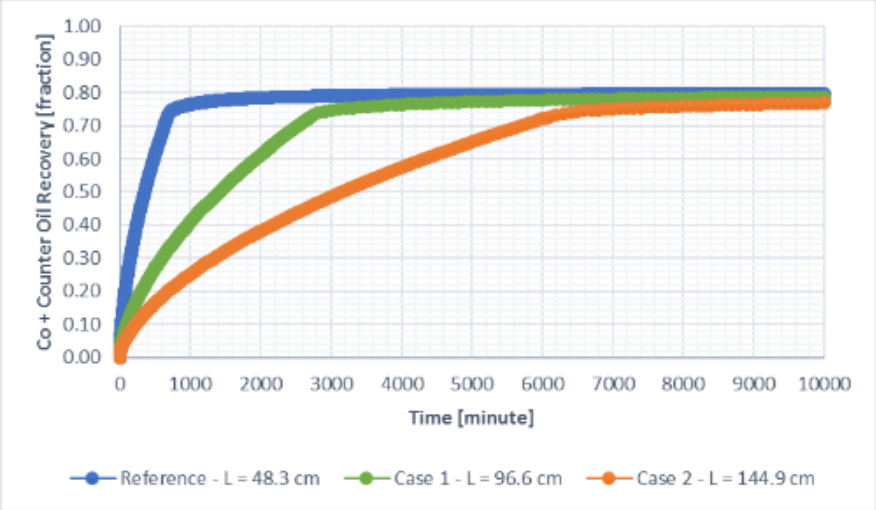

Figure 5-22 Co- & Counter Current Oil Recovery for Different Tube Length

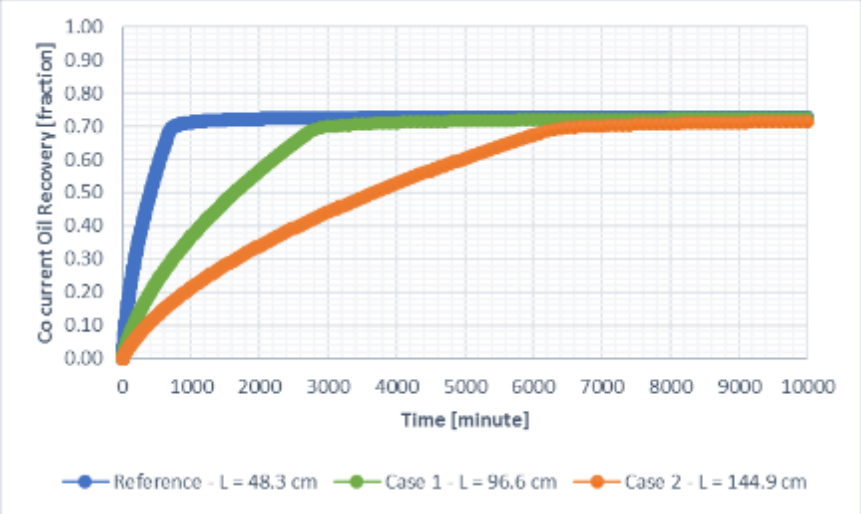

Figure 5-23 Co-Current Oil Recovery for Different Tube Length

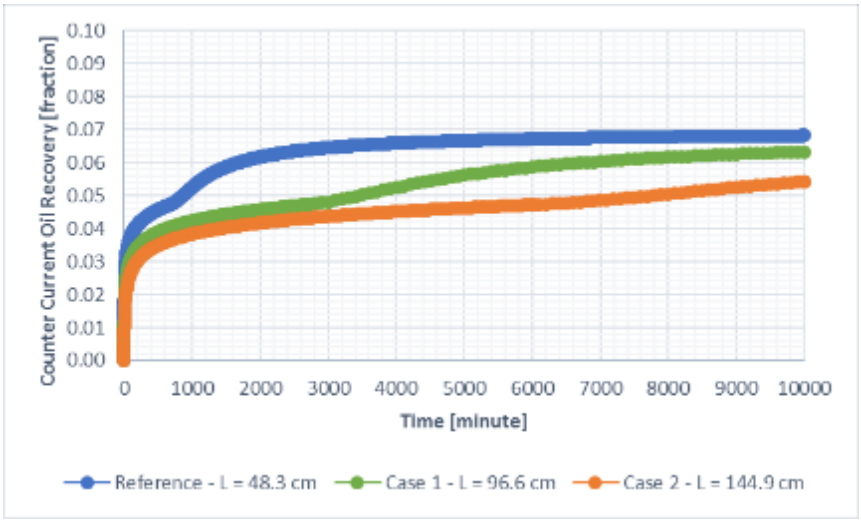

Figure 5-24 Counter Current Oil Recovery for Different Tube Length

An increase of imbibition tube length would delay of production rate reduction in which implies the delay of the breakthrough (see Figure 5-21 and Figure 5-22). During imbibition in the shorter tube length, the production incline faster causes early breakthrough compared to others case. After breakthrough, the oil production still increases gradually until it reaches the maximum oil recovery (RF = 0.8). On the other hand, for case 1 and case 2, as the tube length is increased, the production takes long time to reach the maximum oil recovery.

Figure 5-23 and Figure 5-24 show the co and counter current production decreases at the breakthrough when the length is increased. A decrease of imbibition rate due to an increase of

the imbibition tube length induces a reduction of production. This simulation result has the same issue as the experimental result which conducted by Zhang, et al (1996).

Co current production in the Figure 5-23 shows a decrease of co-current oil production at the breakthrough and somewhat rose afterwards and reach plateau below the maximum oil recovery (RF = 0.8) at residual oil saturation. The co-current oil recovery is below to the maximum recovery due to some oil has been produced counter currently when the water was invaded in the early time. Counter-current oil production in the Figure 5-24 results in significant surge of oil recovery for all cases after the breakthrough. A high capillary pressure over the capillary back pressure lead to an increase of production until reach the maximum of oil recovery is approximately about 0.07. The amount of oil recovery at the breakthrough is summarized in the Table 5-10. Moreover, the linearity of oil recovery with the square root of time in the Figure 5-25 is not given perfect straight line with increasing the tube length. This represent that not all the flow resistance is in the wetting phase (water).

Table 5-10 The Result of Different Tube Length on The Oil Recovery

Remark	**Breakthrough Time [minute]**	**Oil Recovery at Breakthrough [fraction]**			
		Counter Current	**Co Current**	**Total**	**Ratio Counter / Co-Current**
Reference Case (L = 48.3 cm)	762	0.048	0.700	0.749	0.06897
Case 1 (L = 96.6 cm)	2907	0.048	0.696	0.744	0.06872
Case 2 (L = 144.9 cm)	6197	0.047	0.686	0.733	0.06918

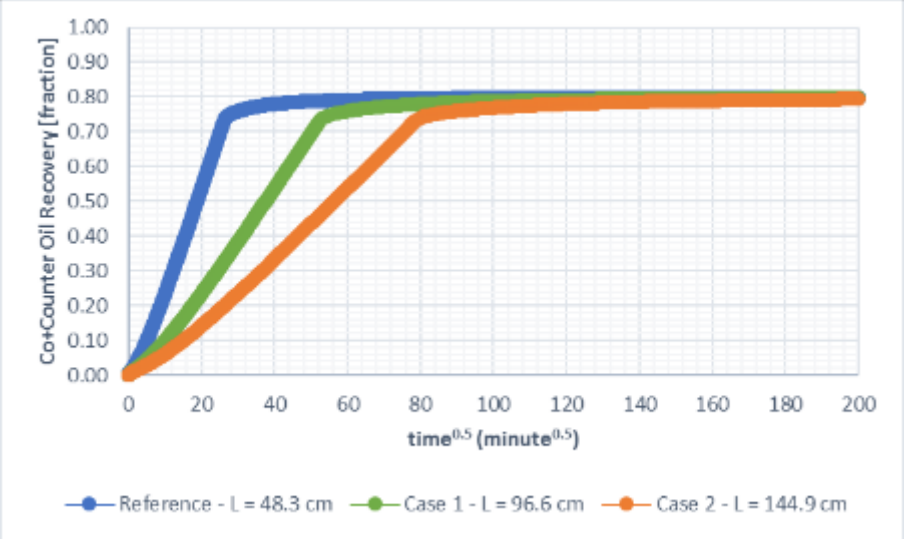

Figure 5-25 Total (Co +Counter Current) Oil Recovery with Square Root of Time for Different Tube Length

5.1.6. Parameter Study of Capillary Pressure

To analysis parameter study of capillary pressure, those parameters of J-function formula in the sub-section 1.7 are adjusted to change the shape of capillary pressure curve. The objective in this parameter study is to investigate the effect of altered capillary pressure shape on the production profile. Since the counter-current production occurs mainly due to the magnitude of capillary back pressure, an investigation of capillary back pressure will be carried out by varying the shape of capillary pressure curve.

Case: Alteration of Capillary Pressure Curve Shape for viscosity ratio (μ_w/μ_o) = 1.2

There are 2 cases will be established in this parameter study, such as decreasing/going down slope (case 1) and increasing slope/high level slope (case 2) compared to the reference capillary pressure (reference case). To form the capillary pressure curve to be, either concave up – slope increasing shape or concave down – slope decreasing shape, E_{R1}, E_{L1} and S_{R1} are adjusted from Table 5-1 (reference case). The other value parameters follow with the change of those parameters, except the S_{L1} since it is kept constant. The result of those capillary pressure is illustrated in the following figure.

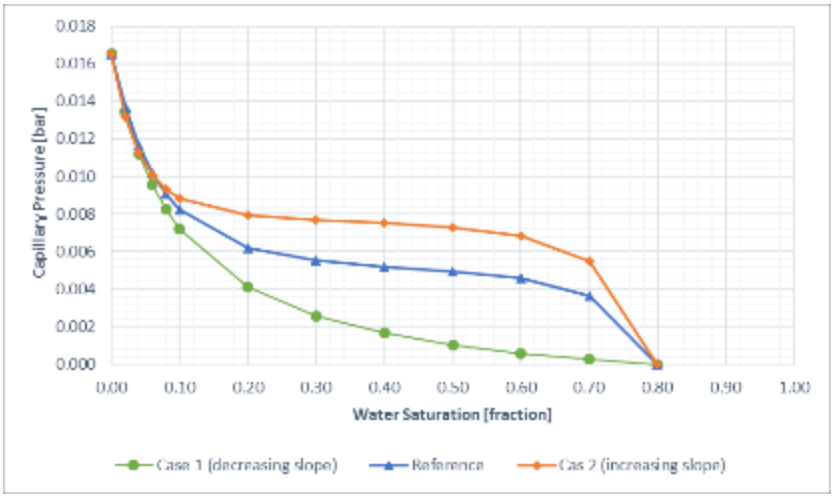

Figure 5-26 Capillary Pressure Curve of Case A (Change Pc Shape)

As the capillary curves are formed (Figure 5-26), In the case A, capillary pressure at initial water saturation and at residual oil saturation remains constant, the only change is the shape of the curve. The reference relative permeability curve is used as the input of relative permeability – capillary pressure table into the model. The results are given as follows:

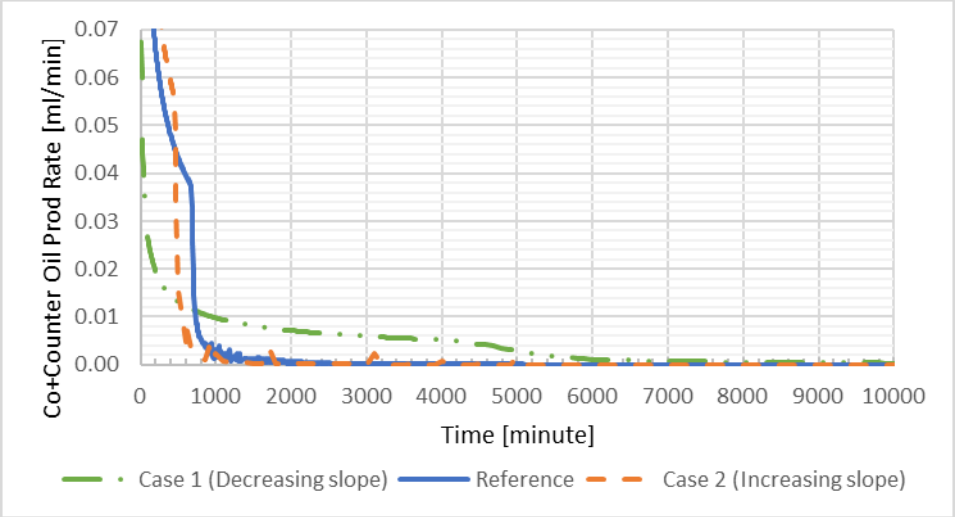

Figure 5-27 Total (Co + Counter Current) Oil Production Rate of Case A (Change Pc Shape)

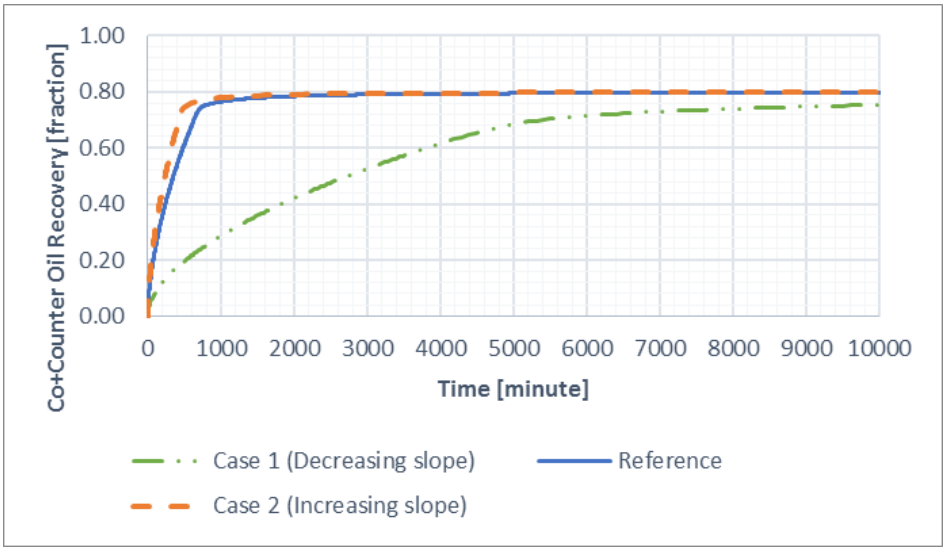

Figure 5-28 Co- & Counter Current Oil Recovery of Case A (Change Pc Shape)

Figure 5-27 shows with decreasing slope of capillary pressure (case 1), it postpones the oil production rate to fall off that it delays the water breakthrough. It can be seen the drop of oil production rate of case 1 occurs 3000 min after the drop of reference production rate. The oil production rate of the case 1 decreases later than that of others case due to low imbibition rate happens in the increased slope of capillary pressure curve (case 1). Owing to that, the oil production at the case 1 is lower than the reference case and case 1 at the breakthrough (see Table 5-11) and it consumes long time to reach the maximum of oil recovery at residual oil saturation which shown in Figure 5-28.

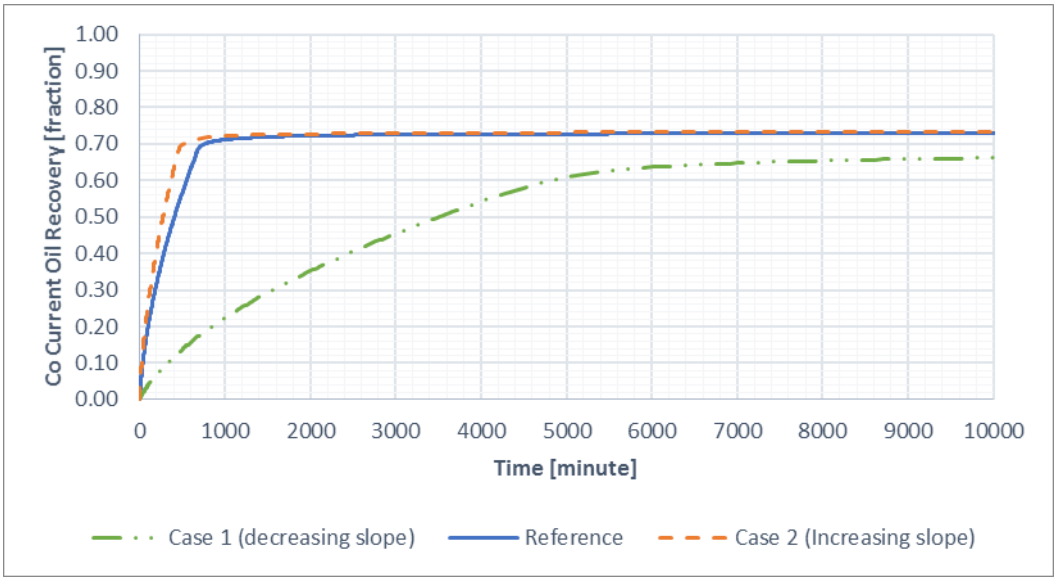

Figure 5-29 Co-Current Oil Recovery of Case A (Change Pc Shape)

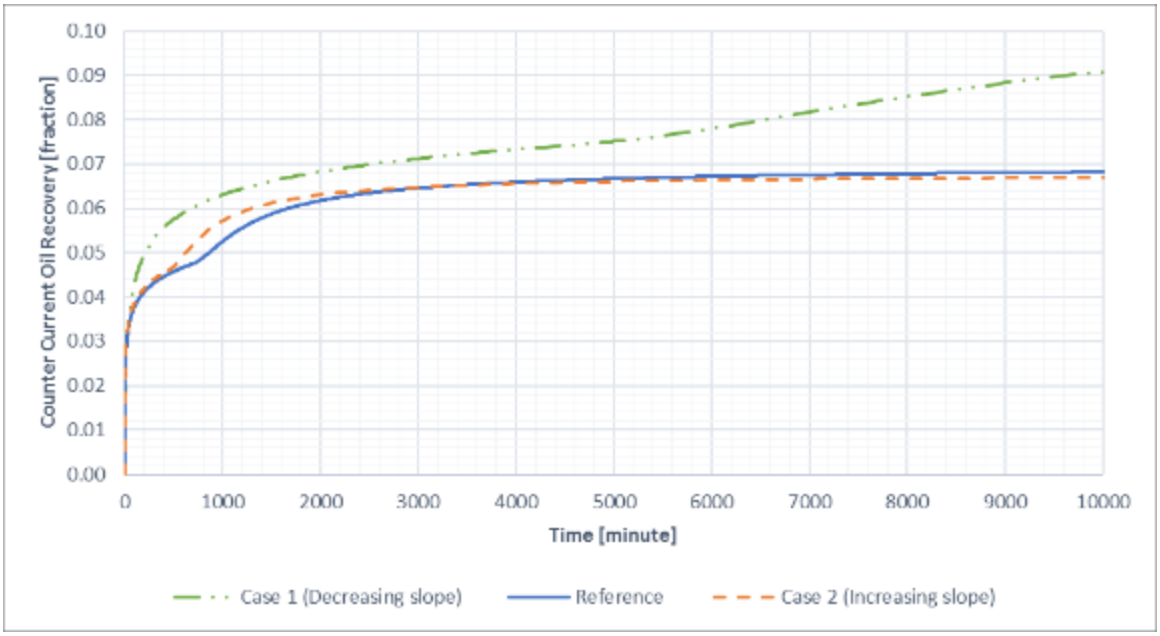

Figure 5-30 Counter Current Oil Recovery of Case A (Change Pc Shape)

Figure 5-29 and Figure 5-30 shows there is a reduction of co current oil production, while an increase of counter current oil production as the shape of capillary pressure curve is a decreased slope (case 1). The increase of counter current oil recovery in the case 1 is caused by very low level of capillary back pressure with decreasing slope of capillary pressure that is pictured in the Figure 5-26. Note that the capillary back pressure has a similar function as the pressure threshold in drainage process.

The capillary back pressure of case 1 is about 0.0005 bar and it is smaller than that of reference case and case 2 where the capillary back pressure is approximately 0.003 bar and 0.005 bar, respectively. This type of capillary pressure can be predicted by monitoring at which water saturation that the counter-current oil is produced constantly (i.e. the cease of counter-current oil production). Since the counter-current production will be ceased when the oil pressure cannot overcome the capillary back pressure. Hence, the low capillary back pressure, the easier for oil to produce counter-currently. The amount of oil recovery co- and counter currently is summarized at the following table. Note that the oil-current production is more dominating than the counter-current production for all the time.

Table 5-11 The Simulation Result of Capillary Pressure – Case A (Change Pc Shape)

Remark	Breakthrough Time [minute]	Oil Recovery at the breakthrough [fraction]			Oil Recovery after the breakthrough [fraction]		
		Counter Current	Co Current	Total	Counter Current	Co Current	Total
Case 1 (Decreasing slope)	5000	0.075	0.609	0.684	0.113	0.686	0.800
Reference Case	762	0.048	0.700	0.749	0.070	0.730	0.800
Case 2 (Increasing slope)	470	0.046	0.690	0.737	0.067	0.733	0.800

Furthermore, by plotting the oil recovery of all cases with the square root of time which is shown in the Figure 5-31, the linearity line of oil recovery of case A represents that all the flow resistance exists in the wetting phase (water).

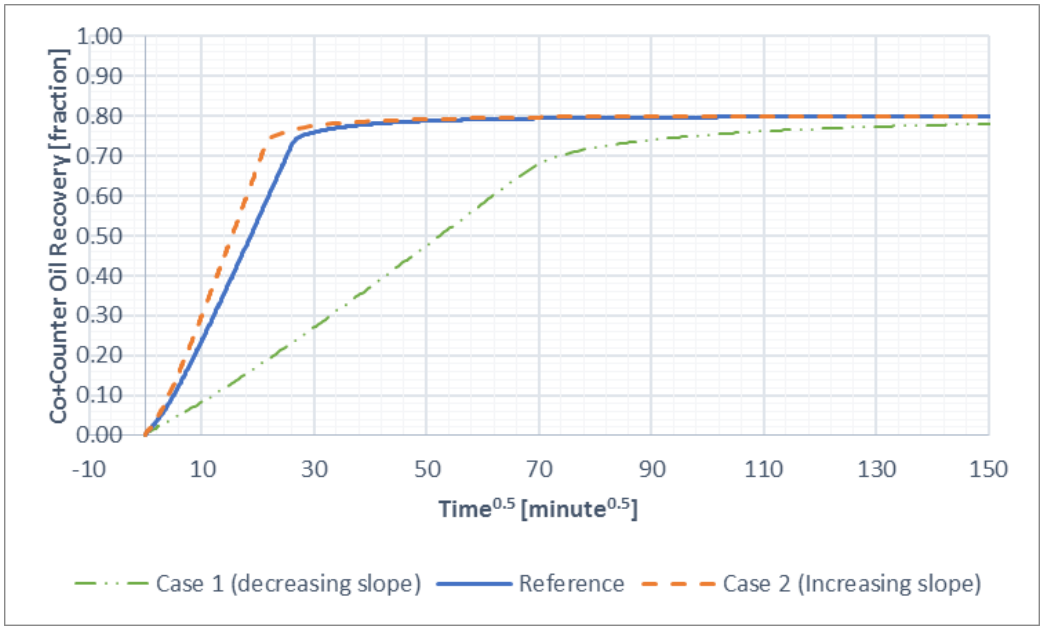

Figure 5-31 Oil Recovery of Case A (Change Pc Shape) with Square Root of Time

5.1.7. Parameter Study of Capillary Back Pressure

Table 5-12 Difference Value of Capillary Boundary Water Pressure for Analysis Capillary Back Pressure

Boundary Pressure in Imbibing Phase (Pcbw) [bar]		
Case 1	**Reference case**	**Case 2**
0.5	1	1.2

By using the reference case relative permeability and the capillary pressure in the Table 5-14, and input a different boundary water pressure that shown in the Table 5-12 into the model, the results are shown in the following figures. The description of play the capillary back pressure in the input data is shown in the Appendix.

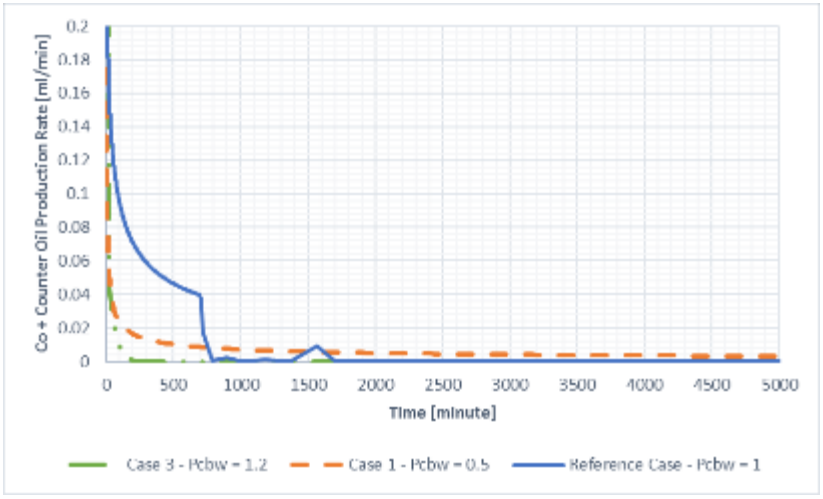

Figure 5-32 Total (Co+Counter) Oil Production Rate for Investigating Capillary Back Pressure

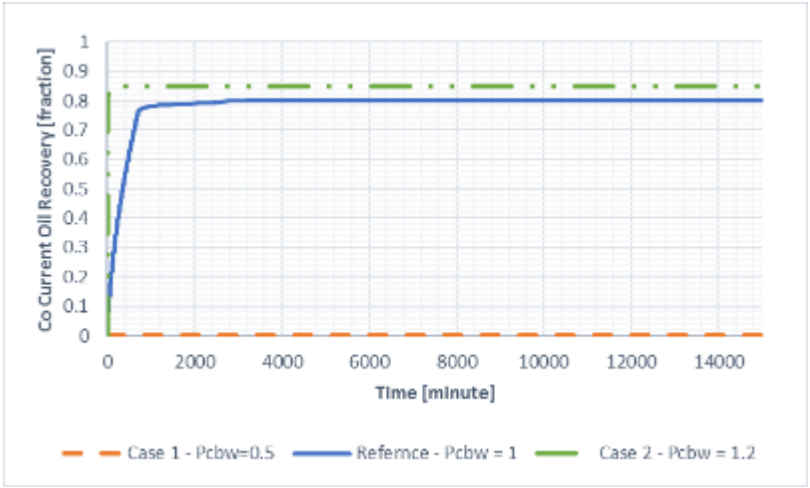

Figure 5-33 Co Current Oil Recovery for Investigating Capillary Back Pressure

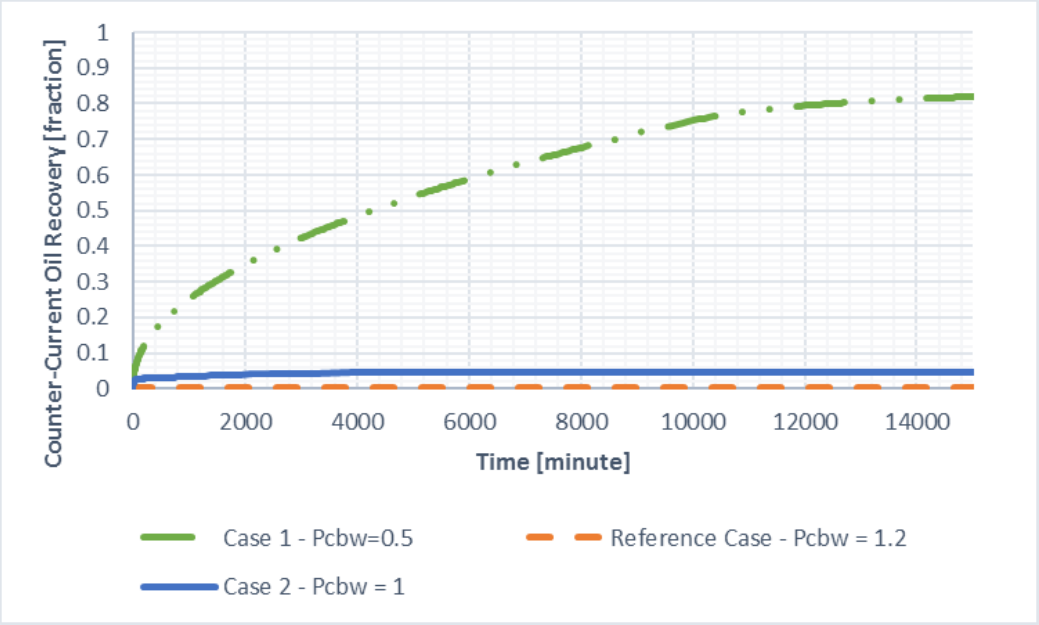

Figure 5-34 Counter Current Oil Recovery for Investigating Capillary Back Pressure

Figure 5-32 shows that delayed water breakthrough occurs as the boundary water pressure decreases. This can be seen at the Figure 5-33 that delayed breakthrough happens for reference case. There is no oil that is produced co-currently when the boundary water pressure is decreased up to 0.5 bar (case 1). This is might because the oil pressure overcomes the boundary water pressure and lead the oil to be produced counter-currently. On the other hand, the counter-current production decreases as the boundary water pressure is higher than the oil pressure. Hence, a little oil is produced counter-currently and most the co-current oil production.

Table 5-13 The Result of Investigating Capillary Back Pressure

	Pcbw [bar]	Average Oil Pressure in the Simulation [bar]	Oil Recovery at Breakthrough [fraction]		
			Counter-Current	Co-Current	Total
Case 1	0.5	0.502	0.848	0.000	0.848
Reference	1	1	0.032	0.765	0.797
Case 2	1.2	1.1	0.002	0.778	0.780

5.2. History Matching (HM)

To obtain acceptable understanding between simulation results and actual data which in this thesis is experimental result, the history matching is required. In this thesis, trial and error approach manually conduct the history matching . The manual tasks for such history matching are adjusting the data input, run the simulation, and plot against to the actual data to improve match. The input data is adjusted based on knowledge and experience. There are 4 experiment result would be matched with the simulation result, for instance experiment SP2, SP3, SP4, and SP7. Note that the experiment SP6 is not included during history matching. It is assumed that the curve match of production profile for SP6 would be similar with the experiment SP7 because of the water viscosity between them is not too different. Hence, the effect might be not far away.

5.2.1. Curve Match of Experiment (SP2) with Viscosity Ratio (μ_w/μ_o) = 1.20

For match the experimental result of SP2 with the simulation result, the different reference case is used.

Table 5-14 HM Reference Kr - Pc Table for Curve Match Experiment SP2

Remark	S_w	k_{rw}	k_{ro}	Pc
S_{iw}	0.000	0.000	1.000	0.00990
	0.020	0.000	0.953	0.00892
	0.040	0.000	0.908	0.00817
	0.060	0.000	0.864	0.00761
	0.080	0.000	0.821	0.00717
	0.100	0.000	0.779	0.00683
	0.200	0.000	0.585	0.00593
	0.300	0.000	0.419	0.00559
	0.400	0.001	0.280	0.00542
	0.500	0.004	0.170	0.00530
	0.600	0.017	0.087	0.00513
	0.700	0.058	0.031	0.00472
	0.800	0.168	0.003	0.00311
$1-S_{or}$	0.850	0.272	0.000	0.00000

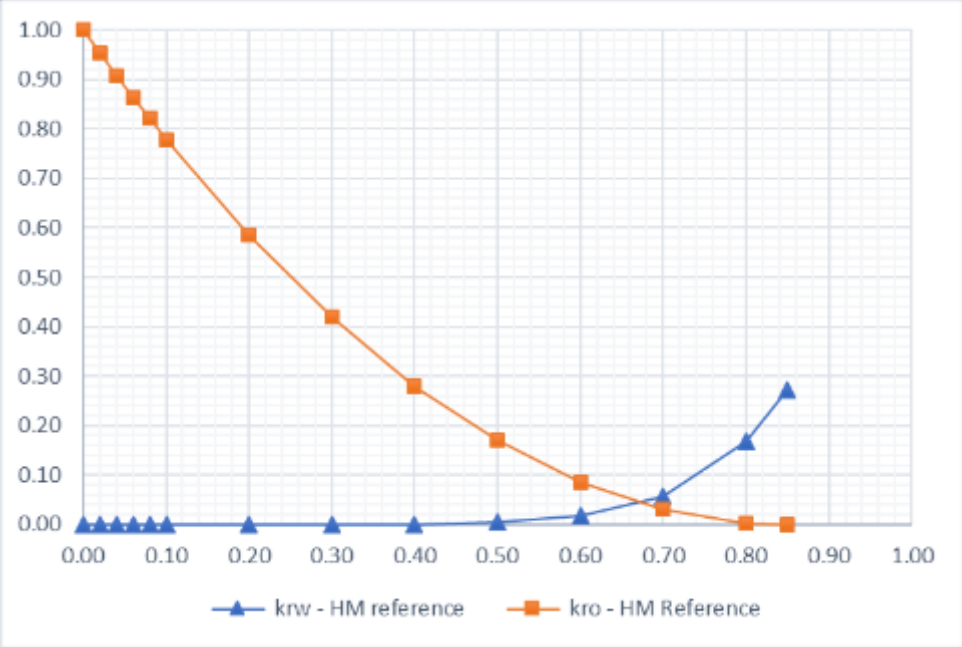

Figure 5-35 HM Reference Relative Permeability For Curve Match Experiment SP2

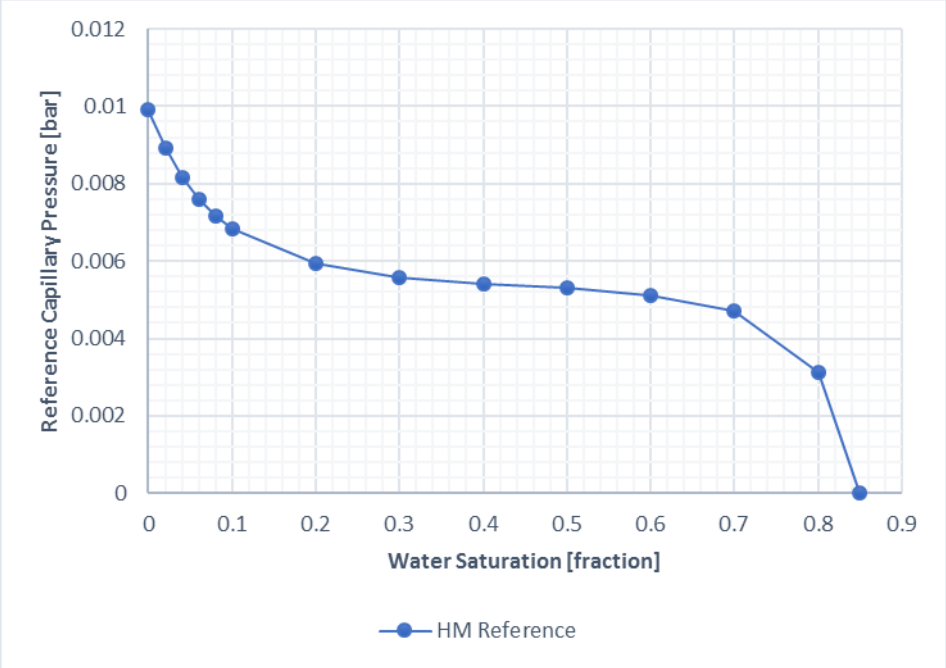

Figure 5-36 HM Refernce Capillary Pressure For Curve Match Experiment SP2

After running simulation with these input data in the model, the result is almost match between the simulation and experimental result in production profile. Figure 5-37 shows that a satisfying result for the matched curves that the oil production rate of counter current is over the co-current in the beginning and reduce to below the co-current production as time elapses.

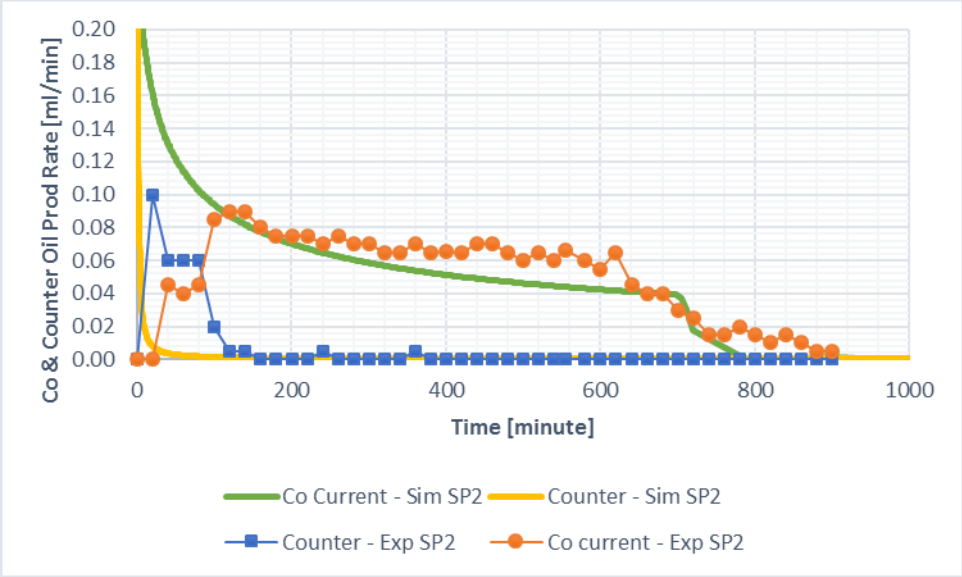

Figure 5-37 Total (Co & Counter Current) Oil Production Rate of Experiment SP2 – History Matching Reference of Simulation SP2

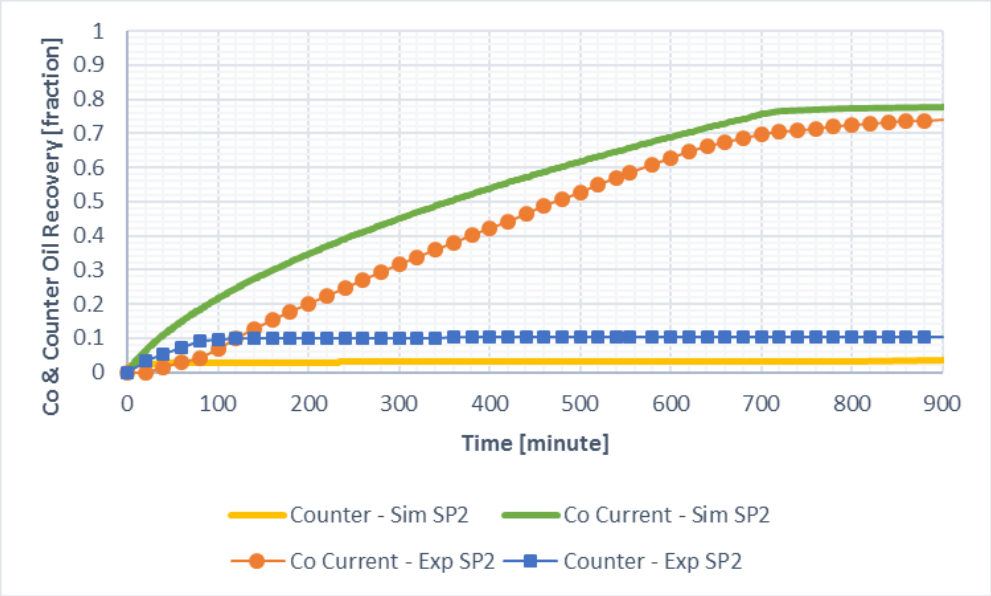

Figure 5-38 Oil Recovery of Experiment SP2 – History Matching Reference of Simulation SP2

The matched curves in the oil production rate lead to the matched curves of oil recovery for both counter current and co-current that is captured in the Figure 5-38. There are similar trendline of counter and co-current production curve between the simulation and the experimental result, similar breakthrough time, however, the values of their oil recovery are slightly divergent at all the time which can be seen in the Table 5-15. The co-current production from the simulation result is over the experimental result at and after the breakthrough due to low water relative permeability that causes an increase of oil recovery. However, the counter-current oil production

of the simulation is lower than the experiment at and after the breakthrough due to the capillary pressure that is input into the model is more concave up and down with the high level of capillary back pressure (as looks in the Figure 5-36). In addition, the shape of oil production curve with square root of time between simulation and experimental results show an identical non linear trendline that means the flow resistance exists in the water and oil (Figure 5-39). Note that, the co-current production is still dominating for all the time.

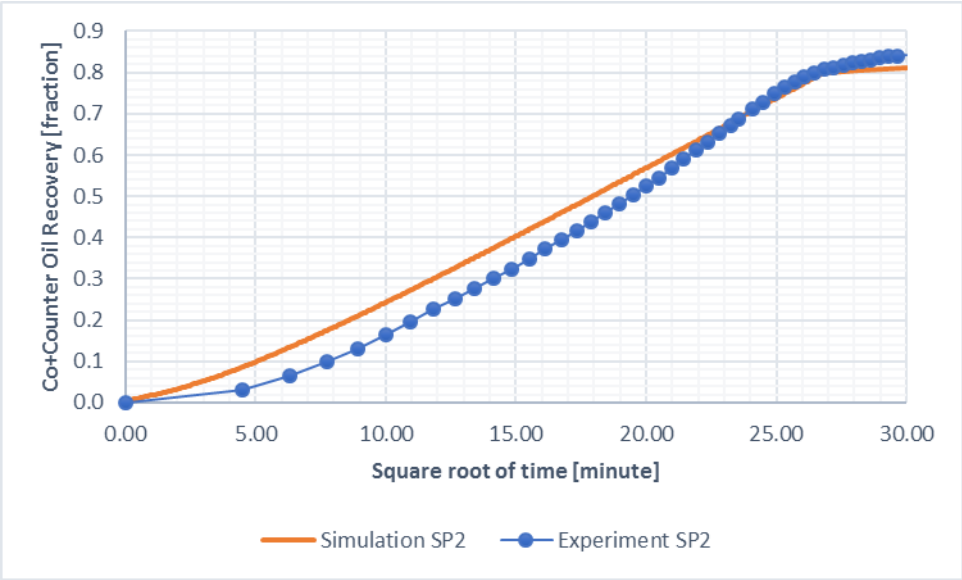

Figure 5-39 Total (Co + Counter Current) Oil Recovery of Experiment – Historty Matching Reference of Simulation SP2 with Square Root of Time

Table 5-15 Comparison of Simulation and Experiment Result of Curve Match SP2

Remark	**Breakthrough Time [minute]**	**Oil Recovery at the breakthrough [fraction]**			**Oil Recovery after the breakthrough [fraction]**		
		Counter Current	**Co Current**	**Total**	**Counter Current**	**Co Current**	**Total**
Simulation	720	0.032	0.765	0.797	0.05	0.80	0.85
Experiment	720	0.10	0.70	0.81	0.10	0.74	0.84

5.2.2. Curve Match of Experiment SP3 with Viscosity Ratio (μ_w/μ_o) = 0.04

For match the experimental result of SP3 with the simulation result, the reference data in the table 5.13 is firstly used. It can be seen from the result (Figure 5-40) that the simulation result does not give the best match with the experiment. The simulation result shows lower production rate and the drop of production rate is more delayed than the experiment. Hence, the reference

data such as capillary pressure and relative permeability are not valid for experiment SP3 and must be changed to approach the best match of production curve. Note that in the experiment SP3 the oil is pure produced co-currently. Therefore, the following oil production profile would be corresponded only to the co-current oil production.

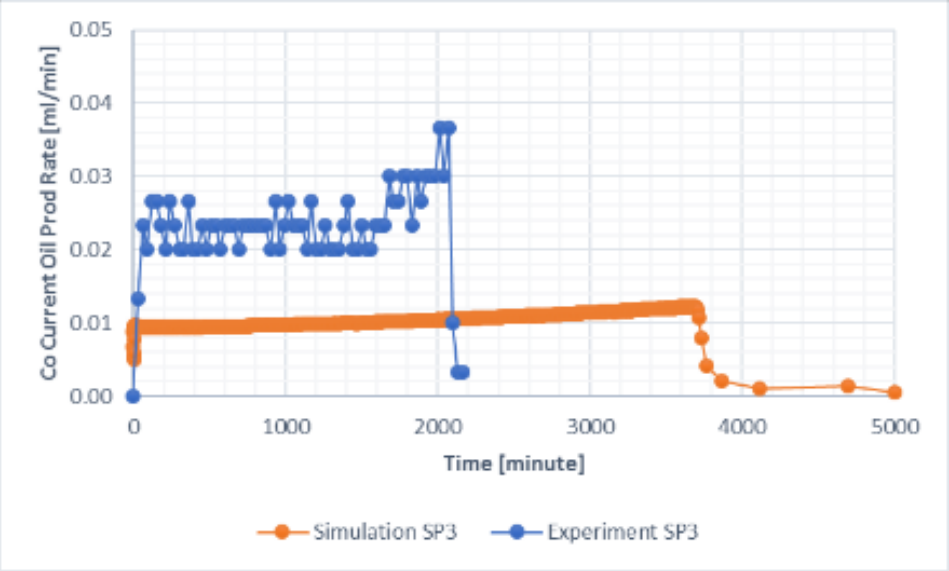

Figure 5-40 Co Current Oil Production Rate of Experiment SP3 – History Matching Reference Case of Simulation SP3

Based on the experience of trial and error, the altered relative permeability and capillary pressure in the Table 5-16 are used to produce the best approach of the production curve match.

Table 5-16 Modified kr - Pc Table for Curve Match Experiment SP3

Remark	S_w	k_{rw}	k_{ro}	Pc
S_{iw}	0.000	0.000	1.000	0.02899
	0.020	0.000	0.953	0.02369
	0.040	0.000	0.908	0.02005
	0.060	0.000	0.864	0.01749
	0.080	0.000	0.821	0.01566
	0.100	0.000	0.779	0.01432
	0.200	0.000	0.585	0.01124
	0.300	0.000	0.419	0.01031
	0.400	0.001	0.280	0.00994
	0.500	0.004	0.170	0.00969
	0.600	0.017	0.087	0.00937
	0.700	0.058	0.031	0.00863
	0.800	0.168	0.003	0.00569
$1-S_{or}$	0.850	0.272	0.000	0.00000

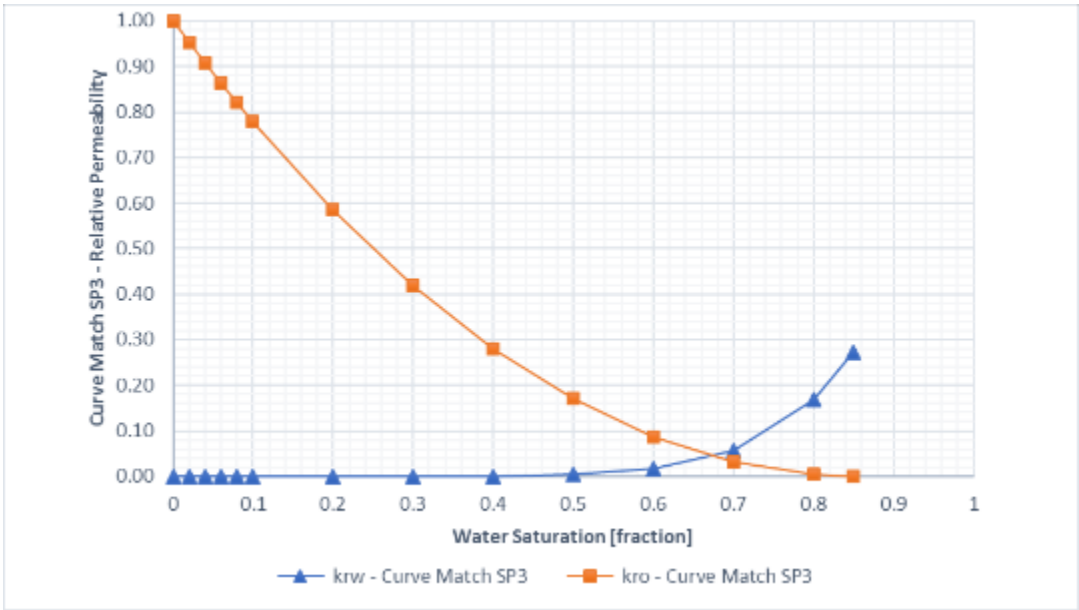

Figure 5-41 Relative Permeability Curve For Curve Match Experiment SP3

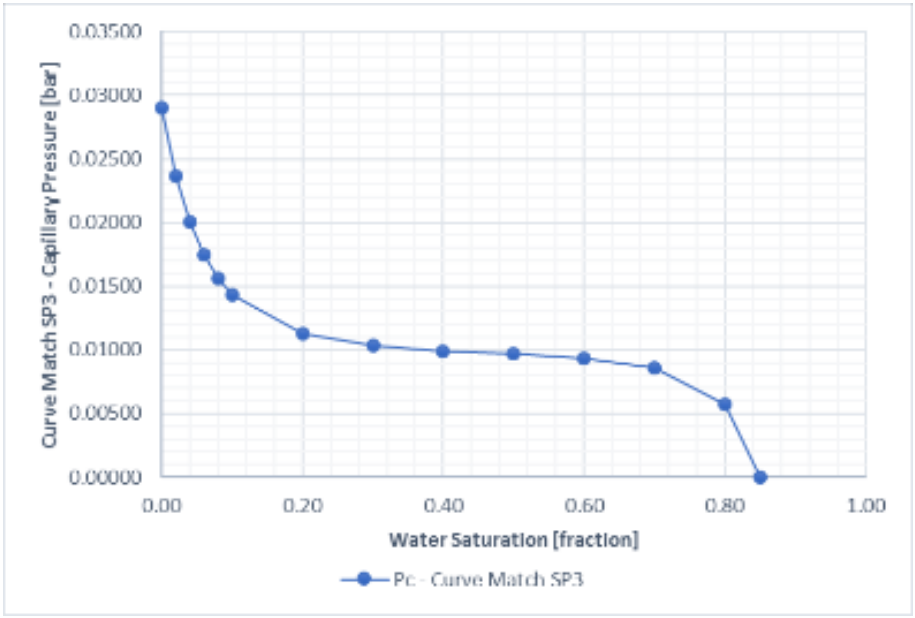

Figure 5-42 Capillary Pressure Curve For Curve Match Experiment SP3

The simulation result in the Figure 5-43 and Figure 5-44 represent imperfect match with the experiment result. The oil recovery at the breakthrough and after that, do not result in the same value. However, the breakthrough shows at the same time and the production curves in the simulation result shows a similar increased trendline with the experimental result that closes to it.

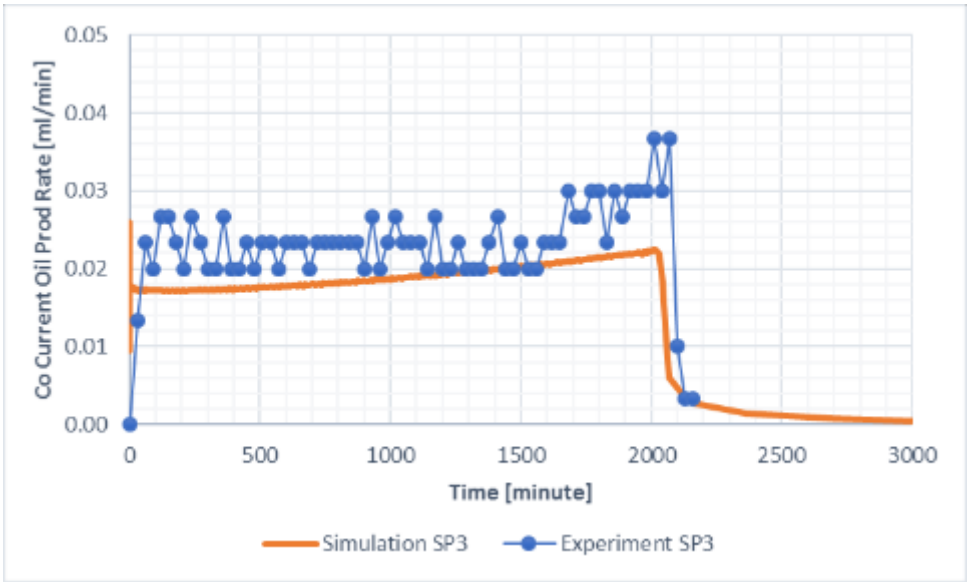

Figure 5-43 Co-Current Oil Production Rate of Experiment – Simulation SP3

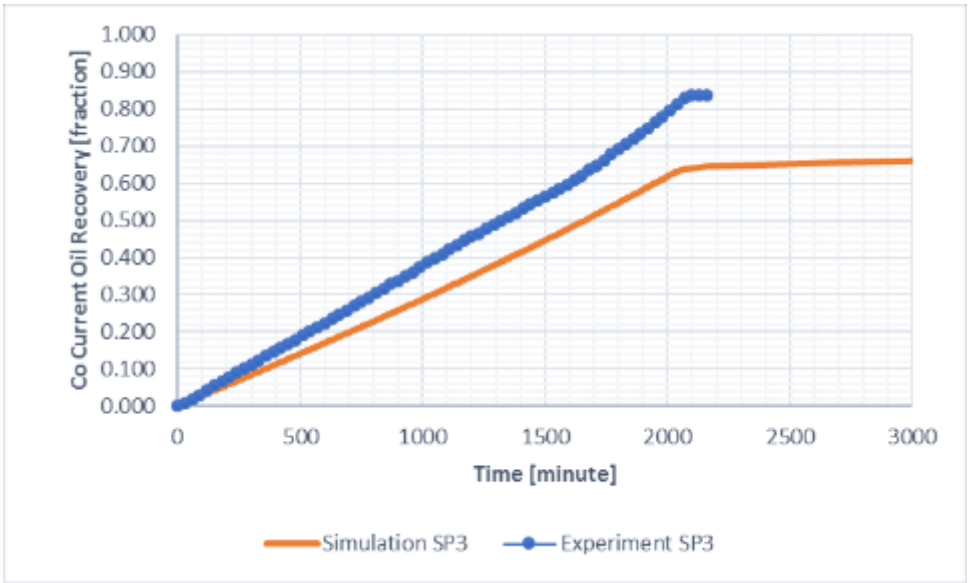

Figure 5-44 Co-Current Oil Recovery of Experiment - Simulation SP3

The Figure 5-44 shows, at and after the breakthrough, the simulation result of co-current oil production has a lower oil recovery than the experimental result. This is because of tuned capillary pressure is not higher enough to force more water imbibes the model. Hence, it causes a reduction of imbibition rate and decreases the oil recovery. The existence of oil recovery in counter-current production from the simulation result due to the low-level of capillary back pressure that the capillary pressure has might induces the low capillary back pressure. Thus, the counter-current oil production still happens. Therefore, to achieve the perfect match with the experimental result, the capillary pressure curve must show high capillary back pressure with

increases capillary pressure. Moreover, the production profile with square root of time in the Figure 5-45 shows an analogous non linear trendline which means the flow resistance exists in the water and oil. Note that oil co-current oil production is still higher than the counter-current for all the time.

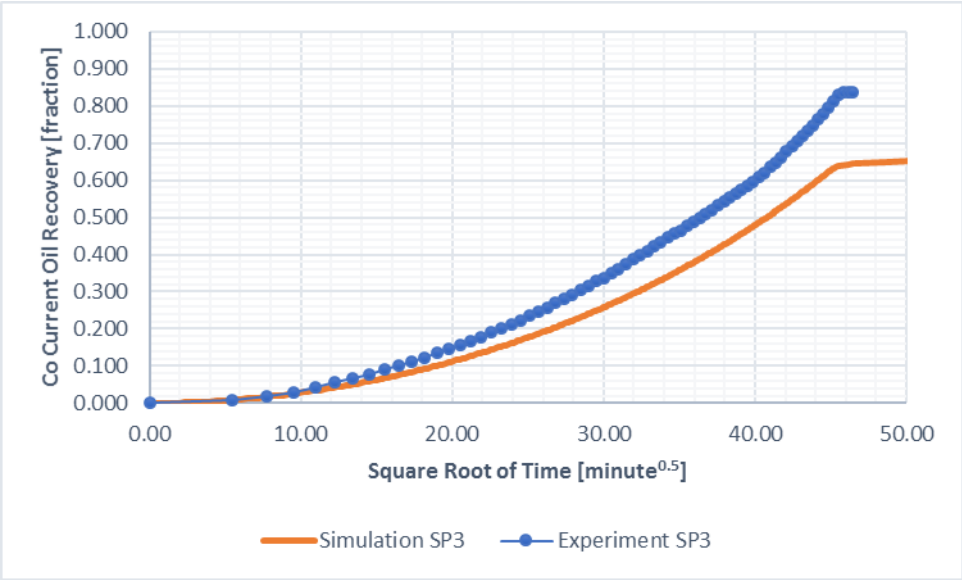

Figure 5-45 Co-Current Oil Recovery of Experiment - Simulation SP3 with Square Root of Time

Table 5-17 Comparison of Simulation and Experiment Result of Curve Match SP3

Remark	Breakthrough Time [minute]	Oil Recovery at the breakthrough [fraction]			Oil Recovery after the breakthrough [fraction]		
		Counter Current	Co Current	Total	Counter Current	Co Current	Total
Simulation SP3	2070	0.056	0.638	0.694	0.118	0.732	0.850
Experiment SP3	2070		0.830	0.830		0.840	0.840

5.2.3. Curve Match of Experiment SP4 with Viscosity Ratio (μ_w/μ_o) = 0.02

For match the experimental result of SP4 with the simulation result, the reference data in the Table 5-15 is firstly used. It has the same explanation as curve match in the experiment SP3 that the simulation result of SP4 does not give the best match with the experimental one (Figure 5-46). The simulation result shows lower production rate than the experimental result. It might be because of low viscosity ratio that experiment SP4 has and the reference data might be credible only for viscosity ratio is about one that lead to a mismatch production profile between

the them. Hence, the reference data such as capillary pressure and relative permeability are not valid for experiment SP4 and must be changed to approach the best match of production curve. Note that in the experiment SP4 the oil is pure produced co-currently. Therefore, the following oil production profile would be corresponded only to the co-current oil production.

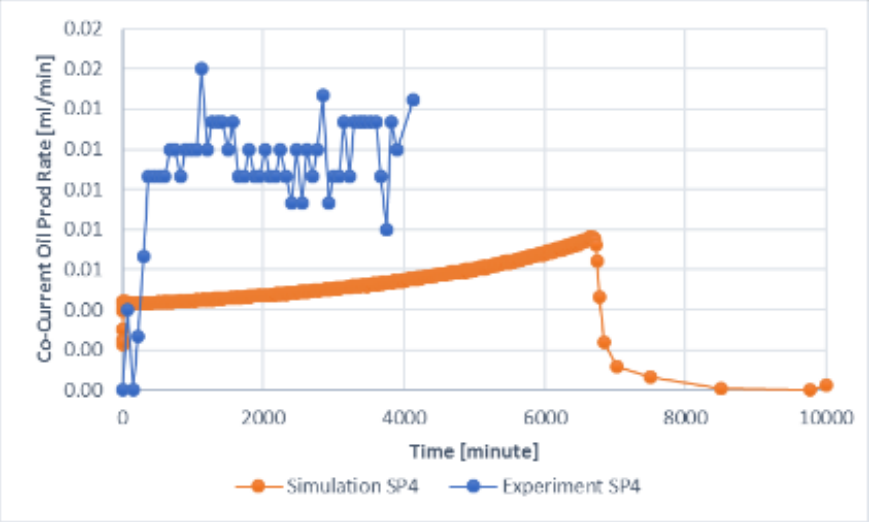

Figure 5-46 Co-Current Oil Production Rate of Experiment SP4 – History Matching Reference Case of Simulation SP4

Based on the experience of trial and error, the altered relative permeability and capillary pressure in the Table 5-18 are used to produce the best approach of the production curve match.

Table 5-18 Modified kr - Pc Table for Curve Match Experiment SP4

Remark	S_w	k_{rw}	k_{ro}	Pc
S_{iw}	0.000	0.000	1.000	0.02837
	0.020	0.000	0.931	0.02307
	0.040	0.000	0.865	0.01943
	0.060	0.000	0.803	0.01688
	0.080	0.000	0.743	0.01505
	0.100	0.000	0.687	0.01371
	0.200	0.000	0.447	0.01063
	0.300	0.000	0.271	0.00971
	0.400	0.001	0.148	0.00933
	0.500	0.004	0.070	0.00909
	0.600	0.017	0.025	0.00879
	0.700	0.058	0.005	0.00809
	0.800	0.168	0.000	0.00534
$1-S_{or}$	0.850	0.272	0.000	0.00000

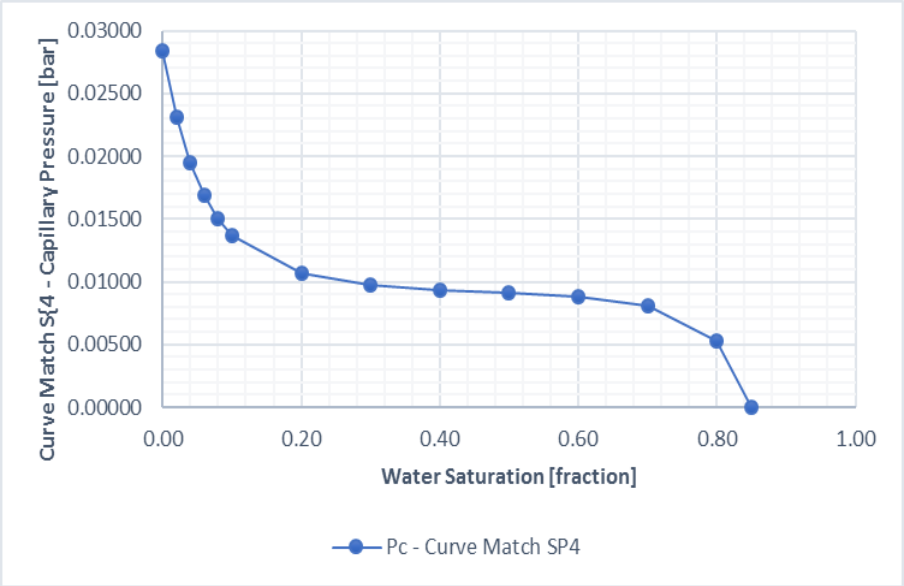

Figure 5-47 Capillary Pressure Curve For Curve Match Experiment SP4

The simulation result in the Figure 5-48 represents imperfect match with the experiment result. The oil production rate curve of the simulation result shows a different trendline with the experimental result that closes to it. However, the breakthrough time of simulation result in the equivalent time as the experimental result. The curve of production profile in the Figure 5-49 shows a similar trendline between the simulation and the experimental one.

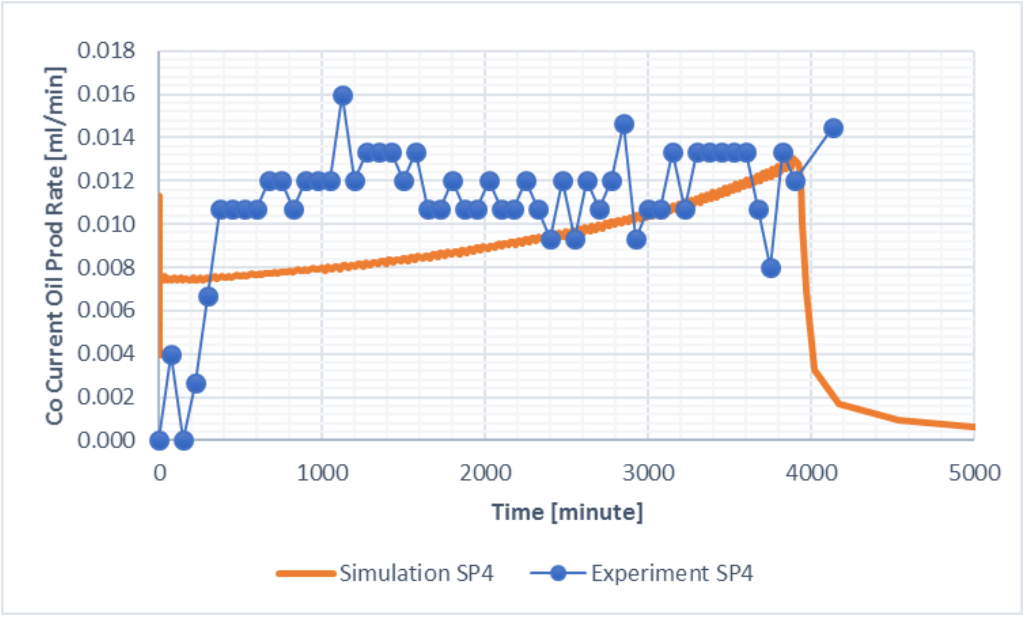

Figure 5-48 Co-Current Oil Production Rate of Experiment – Simulation SP4

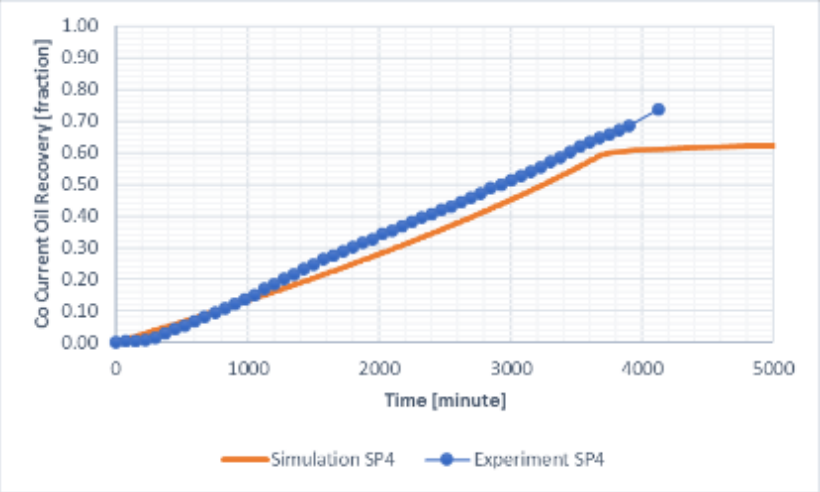

Figure 5-49 Co-Current Oil Recovery of Experiment - Simulation SP4

Figure 5-49 shows similar figure with experiment SP3 (Figure 5-44) that the simulation result of co-current oil production has a lower oil recovery than the experimental result (Table 5-19). The reason is the same that tuned capillary pressure is not higher enough to force more water imbibes the model. Hence, it causes a reduction of imbibition rate and decreases the oil recovery. The level of capillary back pressure in the Figure 5-47 might have low value that oil pressure can overcome it. Therefore, there is a counter-current production from the simulation result. Thus, to achieve the perfect match with the experimental result, the capillary pressure curve must show high capillary back pressure and an increase of capillary pressure. Therefore, the pure co-current production is obtained. Moreover, the production profile with square root of time in the Figure 5-50 shows an analogous non linear trendline which means the flow resistance exists in the water and oil.

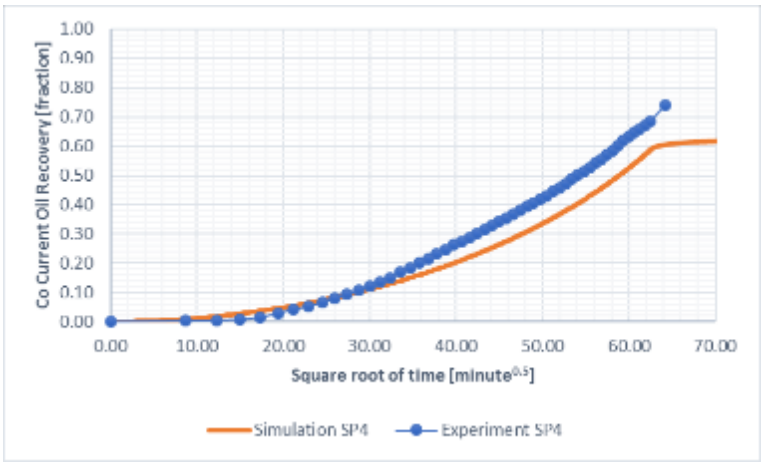

Figure 5-50 Co-Current Oil Recovery of Experiment - Simulation SP4 with Square Root of Time

Table 5-19 Comparison of Simulation and Experiment Result of Curve Match SP4

Remark	Breakthrough Time [minute]	Oil Recovery at the breakthrough [fraction]			Oil Recovery after the breakthrough [fraction]		
		Counter Current	Co Current	Total	Counter Current	Co Current	Total
Simulation SP4	3908	0.061	0.587	0.648	0.136	0.714	0.850
Experiment SP4	3900		0.69	0.69		0.740	0.740

5.2.4. Curve Match of Experiment SP7 with Viscosity Ratio (μ_w/μ_o) = 29.48

For match the experimental result of SP7 with the simulation result, the reference data in the Table 5-15 is firstly used. In the Figure 5-51, the production profile of simulation shows dissimilarity with the experimental result. The simulation result shows a delayed breakthrough, while the experimental result shows a fast decline production rate that is caused by an increase of water viscosity. Hence, the reference data such as capillary pressure and relative permeability are not valid for experiment SP7 and must be changed to approach the best match of production curve. Note that in the experiment SP7 the oil is pure produced co-currently. Therefore, the following oil production profile would be corresponded only to the dominating part such as the co-current oil production.

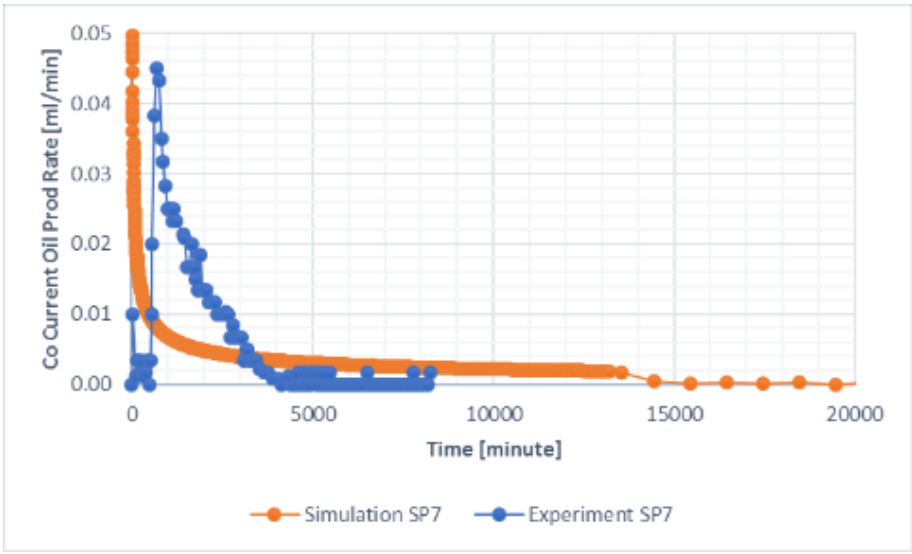

Figure 5-51 Co-Current Oil Production Rate of Experiment SP4 – Reference Case of Simulation SP7

Based on the experience of trial and error, the reference relative permeability and altered capillary pressure in the Table 5-20 are used to produce the best approach of the production curve match.

Table 5-20 Modified kr - Pc Table for Curve Match Experiment SP7

Remark	S_w	k_{rw}	k_{ro}	Pc
S_{iw}	0.000	0.000	1.000	0.06854
	0.020	0.000	0.953	0.05350
	0.040	0.000	0.908	0.04403
	0.060	0.000	0.864	0.03787
	0.080	0.000	0.821	0.03375
	0.100	0.000	0.779	0.03091
	0.200	0.000	0.585	0.02508
	0.300	0.000	0.419	0.02359
	0.400	0.001	0.280	0.02300
	0.500	0.004	0.170	0.02257
	0.600	0.017	0.087	0.02190
	0.700	0.058	0.031	0.02019
	0.800	0.168	0.003	0.01333
$1-S_{or}$	0.850	0.272	0.000	0.00000

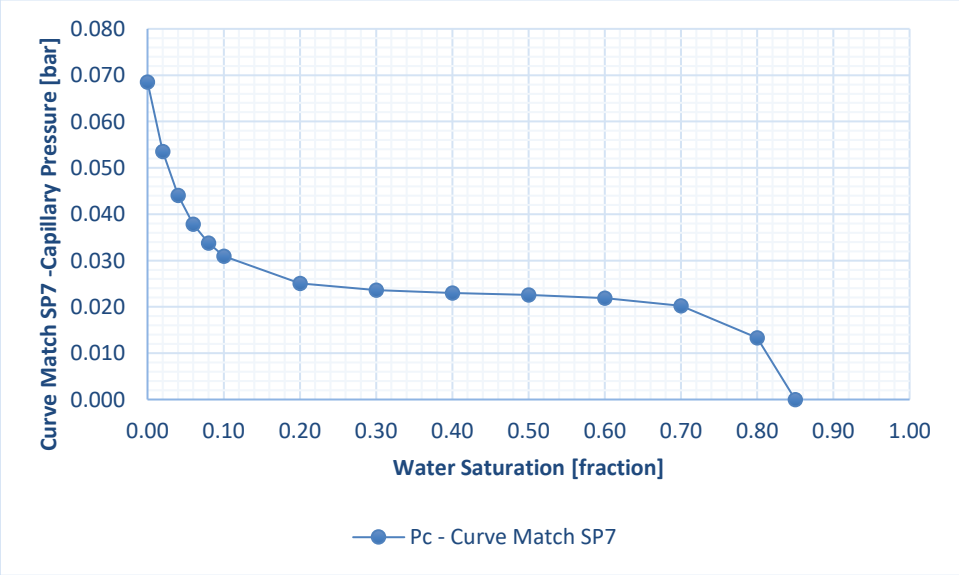

Figure 5-52 Capillary Pressure Curve For Curve Match Experiment SP7

The simulation result in the Figure 5-53 represents imperfect match with the experiment result. The oil production rate curve of the simulation result shows a different trendline with the

experimental result that closes to it. Nevertheless, their production rate decreases gradually during the imbibition and drop at the same time, which indicates the breakthrough time of both them are quite the same. It is shown in the Figure 5-54 that a similar trendline between the simulation and the experimental result happens near the breakthrough time and afterwards.

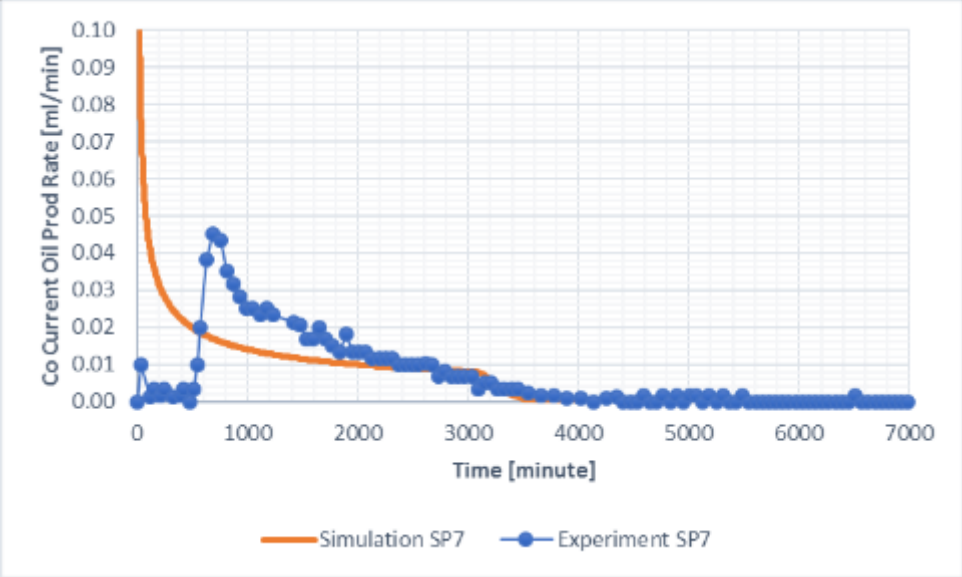

Figure 5-53 Co-Current Oil Production Rate of Experiment – Simulation SP7

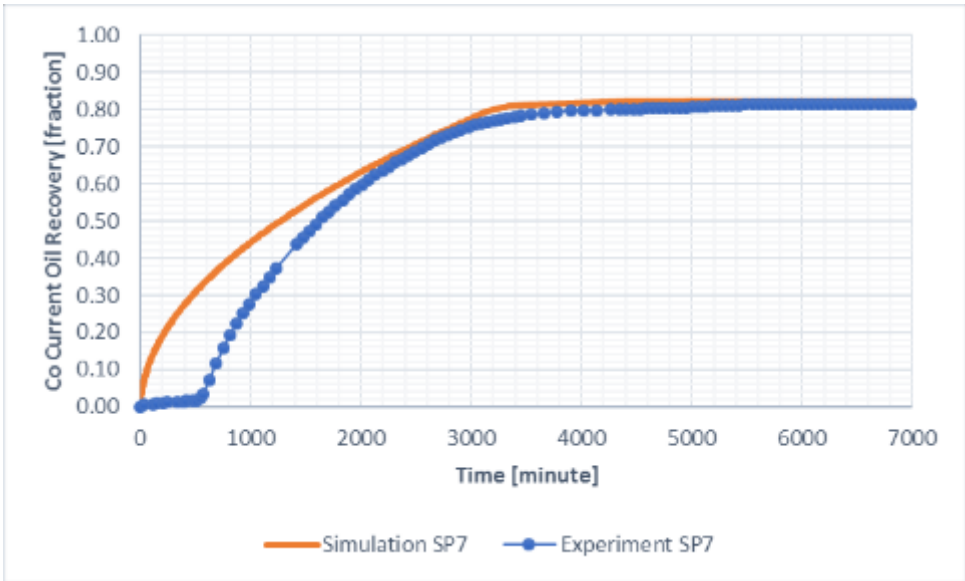

Figure 5-54 Co-Current Oil Recovery of Experiment - Simulation SP7

Figure 5-54 shows, at and after the breakthrough, the simulation result of co-current oil production has a higher oil recovery than the experimental one even though the small counter-current production is still happened in the simulation result (see Table 5-21). An increase of water Corey exponent in the history matching reference leads to high oil mobility that causes an

increase of imbibition rate and thus rises the co-current oil recovery of the simulation. This can be proved by lower counter-current production than the others simulation result. An increase of simulation oil recovery is also caused by a surge of tuned capillary pressure. It can be asMoreover, the production profile with square root of time in the Figure 5-55 shows an dissimilar trendline between the simulation and experimental result. The linear trendline for the simulation result shows the flow resistance exists in the water. Note that the counter-current production is very much lower than the co-current production.

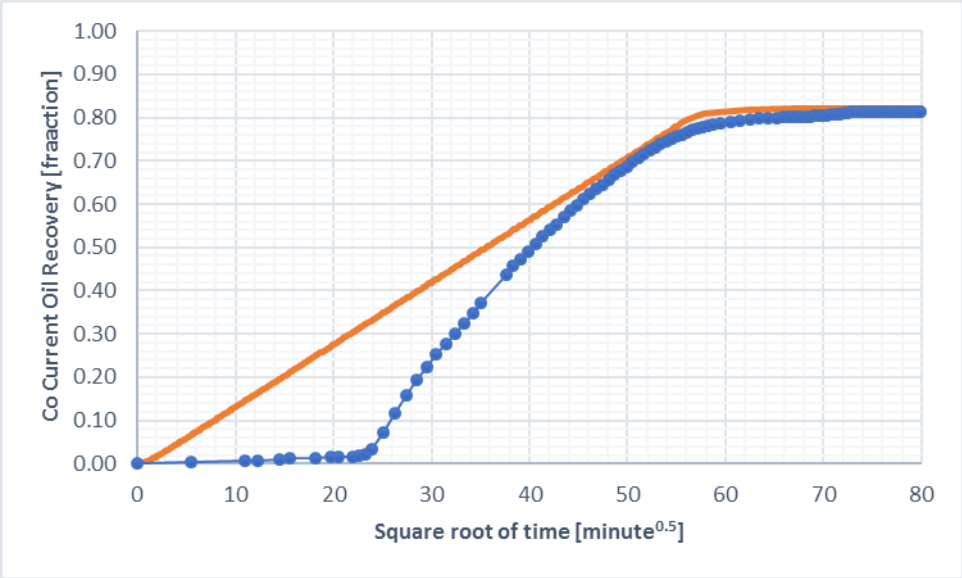

Figure 5-55 Co-Current Oil Recovery of Experiment - Simulation SP7 with Square Root of Time

Table 5-21 Comparison of Simulation and Experiment Result of Curve Match SP7

Remark	Breakthrough Time [minute]	Oil Recovery at the breakthrough [fraction]			Oil Recovery after the breakthrough [fraction]		
		Counter Current	Co Current	Total	Counter Current	Co Current	Total
Simulation SP7	3328	0.02	0.81	0.83	0.03	0.82	0.85
Experiment SP7	3328		0.78	0.78		0.82	0.82

5.2.5. Viscosity Ratio Effect on The Normalised Production of Simulation Result

This section would determine the final validation of the simulation result for all experiment whether it will satisfy the experiment result by investigating the impact of various

viscosity ratio on the normalised production that plotted in the one graph as shown in theFigure 5-56. It can be seen in that figure; the simulation result has a similar trendline with the experimental result and both curves have the same plot as the theory of viscosity effect in the chapter 2 (section 2.5.3). Either the simulation or experimental result, both show when viscosity ratio (μ_w/μ_{nw}) increases, the velocity of the front would be accelerated (shown in the sim SP7 and SP2), while for viscosity ratio that is lower than one, such as sim SP3 and sim SP4 represent a decrease of the front velocity. Note that the experiment SP6 is not included in this investigation because there was a trapped oil behind the front when the experiment was conducted and this is not representative fluid displacement in homogeneous 1D model.

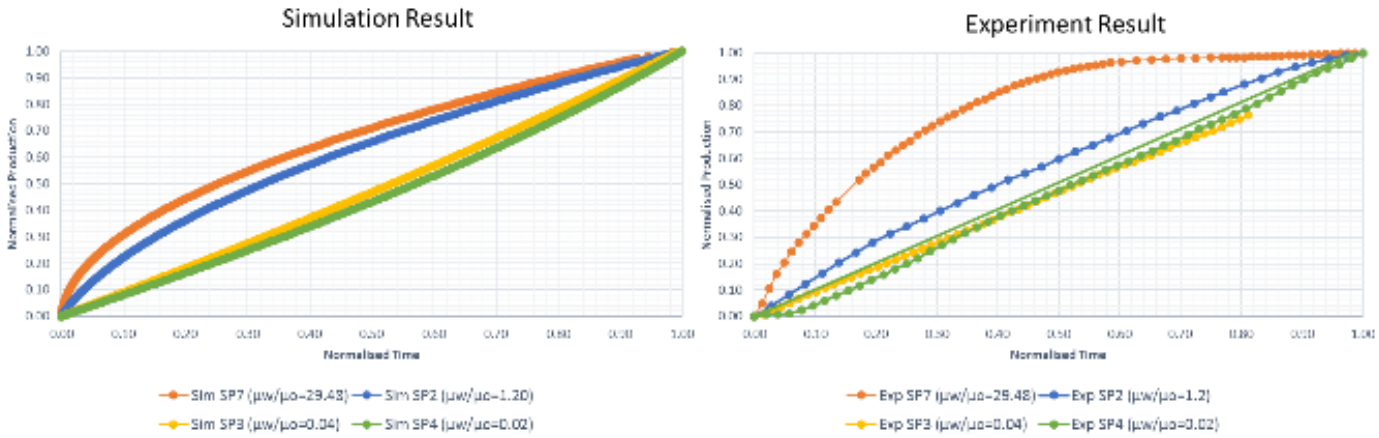

Figure 5-56 Match of Normalised Production Simulation -Experiment Result

6. Conclusion

1D rectangular model (100x1x1) with 48.3 cm x 1.8078 cm x 1.8078 cm has been built with TEOFSI boundary condition where the inlet is in contact with water and the opposite side is in contact the oil. With the initial water saturation is zero and the average of oil residual saturation is 80%, the correlation of relative permeability and capillary pressure is generated. Parameter studies of relative permeability, viscosity ratio, imbibition tube length, and capillary pressure have been investigated by model simulation based on the reference case of relative permeability and capillary pressure. The manual history matching has been done as well by matching the simulation result with the 4 experiments (SP2, SP3, SP4, and SP7). SP6 is not included to the history matching since it is assumed that the curve match of production profile for SP6 would be similar with the experiment SP7. This is because the water viscosity between them is not too different (μ_w/μ_o of SP6 = 30.30 and μ_w/μ_o SP7 = 29.48). When the viscosity ratio effect is being considered on the production, the effect on the production profile in the SP6 might produce the same result as the SP7. All the result in the chapter 5 is summarized in the following list

1. Imbibition rate increases when the mobility oil is higher than the mobility water. This happens when water Corey exponent and water viscosity increases (high viscosity ratio (μ_w/μ_o)). On the other hand, if the water is more mobile than the oil due to low viscosity ratio or increase oil Corey exponent, the imbibition rate decreases.
2. Overall, the co-current production is always more dominating than counter-current production during the imbibition process for all cases at all the time. No counter-current production is higher than the co-current production.
3. An increase of imbibition rate leads to a significant increase of co-current oil production and much less counter-current oil production is obtained. On the contrary, the counter-current production increases, while a decrease of co-current oil recovery with decrease in imbibition rate. The maximum oil recovery that reached by counter-current production from all cases is about 16%, while the co-current oil recovery is about 75%. Hence, the co-current production is always more dominating in process.
4. The imbibition rate is influenced as well by the length of the imbibition tube. From the simulation result, by increasing the tube length triple times, the total oil recovery reduces from 75% of the pore volume to the 73% of the pore volume. This might be because the decrease of imbibition rate with increase in tube length.

5. Another parameter that affect the oil production is a shape of capillary pressure. A concave up-slope increasing of capillary pressure causes a delay of water breakthrough. This type of shape produces a lower co-current oil recovery about 61%, while higher counter-current oil recovery approximately 7.5% than capillary pressure with high level of capillary back pressure. It is because that shape generates low capillary back pressure that induces high oil pressure to overcome it.
6. Counter-current production is controlled by the capillary back pressure. The parameter study of investigating the capillary back pressure effect on the oil production has been done by adjusted the different value of boundary water pressure (Pcbw) at the inlet. This type of pressure controls the counter-current production. When the Pcbw is lower than oil pressure inside the model, the oil will be produced 100% counter currently. On the contrary, most of oil will be produced co-currently when the inside oil pressure is lower than the Pcbw. Both counter-current and co-current production will occurs if the Pcbw has the same value as the oil pressure inside
7. In the manual history matching, the simulation results result in the good match with 4 experimental results. The curve match of simulation-experiment SP2 is the best match in all curves match. There is some curve match result that shows the oil production of simulation result is higher than the experimental result. This might be due to a high-water Corey exponent and high capillary pressure that are used in the simulation causes the production is higher than experiment due to high imbibition rate.
8. By plotting the normalised production over the normalised time from the simulation result, it represents the equivalent trendline with the experiment. This plot also matches with the theory of the viscosity ratio effect on the oil production profile that by increasing the viscosity ratio, the velocity interface will decrease lead to an increase of oil production.
9. In addition, the water breakthrough that occurs during the spontaneous imbibiton defines as the water has reached the outlet. This is because of the involved capillary effect in this process. No water production occurs in the all simulation result.

References

Agnia, A., Algdamsi, H. A., & Al-Mossawy, M. I. (2014). *Oil-Water Relative Permeability Data for Reservoir Simulation Input, Part-I: Systematic Quality Assessment and Consistency Evaluation.* Paper presented at the International Petroleum Technology Conference.

Ahmed, T. (2009). *Working guide to reservoir rock properties and fluid flow*: Gulf Professional Publishing.

Allan, J., & Sun, S. Q. (2003). *Controls on Recovery Factor in Fractured Reservoirs: Lessons Learned from 100 Fractured Fields*. Paper presented at the SPE Annual Technical Conference and Exhibition.

Andersen, P., S. Evje, and A. Hiorth. (2017). Modeling of Spontaneous Imbibition Experiments with Porous Disc - Validity of Exponential Predictions. *SPE 186094*. doi:https://doi.org/10.2118/186094-PA

Anderson, W. G. (1987). Wettability Literature Survey- Part 4: Effects of Wettability on Capillary Pressure. *Society of Petroleum Engineers*. doi:10.2118/15271-PA

Blair, P. (1964). Calculation of oil displacement by countercurrent water imbibition. *Society of Petroleum Engineers Journal, 4*(03), 195-202.

Bourbiaux, B. J. (2009). *Understanding the Oil Recovery Challenge of Water Drive Fractured Reservoirs*. Paper presented at the International Petroleum Technology Conference.

Bourbiaux, B. J., & Kalaydjian, F. J. (1990). Experimental Study of Cocurrent and Countercurrent Flows in Natural Porous Media. *SPE-18283-PA*. doi:10.2118/18283-PA

Brown, R. J. S., & Fatt, I. *Measurements Of Fractional Wettability Of Oil Fields' Rocks By The Nuclear Magnetic Relaxation Method*.

Chen, Z., Huan, G., & Ma, Y. (2006). *Computational methods for multiphase flows in porous media*: SIAM.

Corey, A. T. (1954). The interrelation between gas and oil relative permeabilities. *Producers Monthly, 19*(1), 38-41.

Craig, F. F. (1971). *The reservoir engineering aspects of waterflooding* (Vol. 3): HL Doherty Memorial Fund of AIME.

Dong, M., Dullien, F. a. L., & Zhou, J. (1998). Characterization of waterflood saturation profile histories by the 'complete'capillary number. *Transport in Porous Media, 31*(2), 213-237.

Donnez, P. (2012). *Essentials of reservoir engineering* (Vol. 2): Editions Technip.

Foley, A. Y., Nooruddin, H. A., & Blunt, M. J. (2017). The Impact of Capillary Backpressure on Spontaneous Counter-current Imbibition in Porous Media. *Advances in Water Resources*.

Green, D. W., & Willhite, G. P. (1997). *Enhanced Oil Recovery*. Richardson, UNITED STATES: Society of Petroleum Engineers.

Hamon, G., & Vidal, J. (1986). *Scaling-up the capillary imbibition process from laboratory experiments on homogeneous and heterogeneous samples.* Paper presented at the European Petroleum Conference.

Handy, L. (1960). Determination of effective capillary pressures for porous media from imbibition data. *Trans. AIME, 219*(7).

Haugen, Å., Fernø, M. A., Mason, G., & Morrow, N. R. (2014). Capillary pressure and relative permeability estimated from a single spontaneous imbibition test. *Journal of Petroleum Science and Engineering, 115*, 66-77. doi:http://doi.org/10.1016/j.petrol.2014.02.001

Haugland, H. K. (2016). *Spontaneous Imbibition in Sand-Viscosity Effects on Oil Recovery and Flow Using Polymer and Glycerol.* The University of Bergen.

Honarpour, M. M., Koederitz, F., & Herbert, A. (1986). Relative permeability of petroleum reservoirs.

Kazemi, H., Gilman, J., & Elsharkawy, A. (1992). Analytical and numerical solution of oil recovery from fractured reservoirs with empirical transfer functions (includes associated papers 25528 and 25818). *SPE Reservoir Engineering, 7*(02), 219-227.

Killins, C., Nielsen, R., & Calhoun, J. (1953). Capillary desaturation and imbibition in porous rocks. *Producers Monthly, 18*(2), 30-39.

Leverett, M. C. (1941). Capillary Behavior in Porous Solids. *SPE-941152-G*. doi:10.2118/941152-G
Lohne, A. (2013). *Bugsim manual - an MEOR simulator (Version 1.2)*. Retrieved from IRIS:
Lomeland, F., Ebeltoft, E., & Thomas, W. H. (2005). *A new versatile relative permeability correlation.* Paper presented at the International Symposium of the Society of Core Analysts, Toronto, Canada.
Lyons, W. C. (1996). *Standard handbook of petroleum & natural gas engineering : Vol. 2*. Houston, Tex. Gulf.
Ma, S., Morrow, N. R., & Zhang, X. (1999). Influence of fluid viscosity on mass transfer between rock matrix and fractures. *Journal of Canadian Petroleum Technology, 38*(07).
Mason, G., Fischer, H., Morrow, N. R., Johannesen, E., Haugen, Å., Graue, A., & Fernø, M. A. (2010). Oil production by spontaneous imbibition from sandstone and chalk cylindrical cores with two ends open. *Energy & Fuels, 24*(2), 1164-1169.
Mason, G., Fischer, H., Morrow, N. R., & Ruth, D. W. (2009). Spontaneous counter-current imbibition into core samples with all faces open. *Transport in Porous Media, 78*(2), 199-216.
Mason, G., & Morrow, N. R. (2013). Developments in spontaneous imbibition and possibilities for future work. *Journal of Petroleum Science and Engineering, 110*, 268-293.
Mattax, C. C., & Kyte, J. (1962). Imbibition oil recovery from fractured, water-drive reservoir. *Society of Petroleum Engineers Journal, 2*(02), 177-184.
McPhee, C., Reed, J., & Zubizarreta, I. (2015). *Core Analysis: A Best Practice Guide* (Vol. 64): Elsevier.
Morrow, N. R. (1976). Capillary pressure correlations for uniformly wetted porous media. *Journal of Canadian Petroleum Technology, 15*(04).
Morrow, N. R. (1990). Wettability and Its Effect on Oil Recovery. *Society of Petroleum Engineers*. doi:10.2118/21621-PA
Morrow, N. R., & Mason, G. (2001). Recovery of oil by spontaneous imbibition. *Current Opinion in Colloid & Interface Science, 6*(4), 321-337.
Nelson, R. (2001). *Geologic analysis of naturally fractured reservoirs*.
Qasem, F. H., Nashawi, I. S., Gharbi, R., & Mir, M. I. (2008). Recovery performance of partially fractured reservoirs by capillary imbibition. *Journal of Petroleum Science and Engineering, 60*(1), 39-50. doi:http://doi.org/10.1016/j.petrol.2007.05.008
Saidi, A. (1983). *Simulation of naturally fractured reservoirs.* Paper presented at the SPE Reservoir Simulation Symposium. Society of Petroleum Engineers.
Shouxiang, M., Morrow, N. R., & Zhang, X. (1997). Generalized scaling of spontaneous imbibition data for strongly water-wet systems. *Journal of Petroleum Science and Engineering, 18*(3-4), 165-178.
Stiles, J. (2013). Using special core analysis in reservoir engineering. *Imperial College course notes*.
Tavassoli, Z., Zimmerman, R. W., & Blunt, M. J. (2005). Analytic analysis for oil recovery during counter-current imbibition in strongly water-wet systems. *Transport in Porous Media, 58*(1-2), 173-189.
Unsal, E., Mason, G., Morrow, N., & Ruth, D. (2007). Co-current and counter-current imbibition in independent tubes of non-axisymmetric geometry. *Journal of colloid and interface science, 306*(1), 105-117.
Unsal, E., Mason, G., Morrow, N. R., & Ruth, D. W. (2009). Bubble snap-off and capillary-back pressure during counter-current spontaneous imbibition into model pores. *Langmuir, 25*(6), 3387-3395.
Washburn, E. W. (1921). The dynamics of capillary flow. *Physical review, 17*(3), 273.
Zhang, X., Morrow, N. R., & Ma, S. (1996). Experimental verification of a modified scaling group for spontaneous imbibition. *SPE Reservoir Engineering, 11*(04), 280-285.

APPENDIX

An Example of Input Model For Parameter Study and History Matching

```
title
1D spontaneous imbibition co current flow/
griddim
*nx   ny nz irad
 100  1  1  0 /

nrock
1 /
phases
 1 1 0 / w o g (0/1 flags)

units
* L t Q      K  P   V    rho    (properties)
* m d m**3/d mD bar m**3 g/cc   (units)
* 1 0 3      0  3   2    0 /
* cm min ml/min mD bar ml g/ml
  0  2   1      0  3   0  0 /

components
-- type name /    Defining components
water WAT1 /
oil   OIL1 /
/


nwells
 2 /

tabdim
200 /

krflag
-- mdirkr  iKrMode  mKrSet (max directional curve sets)
       kcKrMod (interpolating component)
   1       0        1  / defaults

------------------------------------------------------------
gridsect
------------------------------------------------------------

dxc
0.483 /

dzc
 1.8078 /  constant dz (cm)

dyc
```

```
1.8078 /

permxc
14500  /  constant permx (mD)

copy
permx permz 1 /  permz=1*permx
permx permy /
/

poroc
0.39 /  constant porosity

rocktypec
1 /


dtop
--Dtop anglex angley (decreasing depth)
  0     0      0 /   horizontal core (flow in z-dir)


------------------------------------------------------------
propsect
------------------------------------------------------------
pref
1 /  make sure reference pressure 1 bar is used

cmpprop
* Name Prefc Bw density   Cw    PrefV TrefV°C visc  BTw
       TC(°C)  BPw
  WAT1 1    1.0  1.102  0    1    25.    1.15    570.6 133.15
       /
  OIL1 1    1.0  0.775  0    1    25.    0.96    0     273.15
       0.0016 / (similar input as wat)
/ -empty slash - terminates the keyword cmpprop

rockprop
--Pref Crock
1  0 / check

--Relative permeabilities
krpctab1
--ir js j1 j2 jpc id ik vint
  1  1  2  3  4   1   / rock 1
--Sw       krw       kro      Pcow
0.000  0.000   1.000     0.00990
0.020  0.000   0.953     0.00892
0.040  0.000   0.908     0.00817
0.060  0.000   0.864     0.00761
0.080  0.000   0.821     0.00717
```

```
0.100  0.000   0.779     0.00683
0.200  0.000   0.585     0.00593
0.300  0.000   0.419     0.00559
0.400  0.001   0.280     0.00542
0.500  0.004   0.170     0.00530
0.600  0.017   0.087     0.00513
0.700  0.058   0.031     0.00472
0.800  0.168   0.003     0.00311
0.850  0.272   0.000     0.00000
/ end table
/ end keyword

jscale
--JscaleF IFTow IFTgo   Turn on J-scaling of Pc
0        22 /

----------------------------------------------------------------
initsect
----------------------------------------------------------------

swinitc
0 / constant initial Sw

pinitd
* p   depth
  1   0 /

phaseconc-w
1  0 /  initial water phase concentration

phaseconc-o
0 1  / initial oil phase concentration


tinit
* T0 zT0 Tgrad
  25 0   0 /
/end
----------------------------------------------------------------
compsect
----------------------------------------------------------------
gravity
0 /


PrintKey
Pr_S 110
Pr_P 100
--Pr_CT 1
Pr_C  100
Pr_Vis 110
```

```
Pr_kr 110
  /
--PrintCF
--0 0 10*1  /  water concentrations
--0  /   oil concentrations

---PrintCTF
---1 1 1 /   total concentrations

Pr_Pcow

history
10  1000  / history print frequency minimum of every 100
       timestep or every 100 day

timestep
*dt0 (days)  qxmax dsmax dtfmax dtmax
  1e-08       60   0.01   1.5      /

tollit
*tollit itmax  seq_tol seq_itmax
1e-13   1000    1e-12    200 /

solver
seq /

--Turn on implicit transport algorithm
--ctransport
-- 1  /
------------------------------------------------------------
wellsect
------------------------------------------------------------
welldef
*name pcflag
 winj1  1 / (primary boundary)
*dir i1  j1   k1  k2   rw  open
  4  -1 /
/ terminates keyword

welldef
*name pcflag
 wprod1  1   / (secondary boundary)
*dir i1   j1   k1  k2   rw  open
 -4  -1 /
/ terminates keyword

wimb
*name   phase  plim hz0: boundary for counter-current flow (SI)
 winj1    w     1    0 /
1/  concentration of water
/   Vimbcell, Temper
```

```
/ terminates keyword

wprod
*name   r/p  rlim  plim Hz0
wprod1   p   500    1  0 / boundary for co-current production
/

pcwell
setting boundary capillary pressure for produced phase
*name  Pcboil  Pcbwater   SwPcbo  SwPcbw
 winj1 0.005     0         0.9       0.1    /
/ terminate keyword

time
0 60 120 240 600 720 900 1000 5000 10000 50000 100000 200000
       250000 600000/ cumulative time to report in hr
end
/
```

An Example of Input Model for Investigating Capillary Back Pressure

```
title
1D spontaneous imbibition co current flow/
griddim
*nx   ny nz irad
 100  1  1  0 /

nrock
1 /
phases
 1 1 0 / w o g (0/1 flags)

units
* L t Q      K  P   V    rho    (properties)
* m d m**3/d mD bar m**3 g/cc   (units)
* 1 0 3      0  3   2    0 /
* cm min ml/min mD bar ml g/ml
  0  2   1      0  3   0  0 /

components
-- type name /    Defining components
water WAT1 /
oil   OIL1 /
/


nwells
 2 /

tabdim
200 /

krflag
```

```
-- mdirkr  iKrMode  mKrSet (max directional curve sets)  kcKrMod
(interpolating component)
   1       0        1  / defaults

------------------------------------------------------------
gridsect
------------------------------------------------------------

dxc
0.483 /

dzc
 1.8078 /  constant dz (cm)

dyc
1.8078 /

permxc
14500  /  constant permx (mD)

copy
permx permz 1 /  permz=1*permx
permx permy /
/

poroc
0.39 /  constant porosity

rocktypec
1 /


dtop
--Dtop anglex angley (decreasing depth)
  0     0      0 /   horizontal core (flow in z-dir)


------------------------------------------------------------
propsect
------------------------------------------------------------
pref
1 /  make sure reference pressure 1 bar is used

cmpprop
* Name Prefc Bw density   Cw    PrefV TrefV°C visc  BTw   TC(°C)  BPw
  WAT1 1    1.0  1.102  0    1    25.    1.15    570.6 133.15  /
  OIL1 1    1.0  0.775  0    1    25.    0.96    0     273.15 0.0016
/ (similar input as wat)
/ -empty slash - terminates the keyword cmpprop

rockprop
--Pref Crock
1  0 / check

--Relative permeabilities
krpctab1
```

```
--ir js j1 j2 jpc id ik vint
  1  1  2  3  4   1   / rock 1
--Sw      krw          kro       Pcow
0.000 0.000 1.000 0.00990
0.020 0.000 0.953 0.00892
0.040 0.000 0.908 0.00817
0.060 0.000 0.864 0.00761
0.080 0.000 0.821 0.00717
0.100 0.000 0.779 0.00683
0.200 0.000 0.585 0.00593
0.300 0.000 0.419 0.00559
0.400 0.001 0.280 0.00542
0.500 0.004 0.170 0.00530
0.600 0.017 0.087 0.00513
0.700 0.058 0.031 0.00472
0.800 0.168 0.003 0.00311
0.850 0.272 0.000 0.00000
/ end table
/ end keyword


jscale
--JscaleF IFTow IFTgo   Turn on J-scaling of Pc
0        22 /

------------------------------------------------------------
initsect
------------------------------------------------------------

swinitc
0 / constant initial Sw

pinitd
* p   depth
  1   0 /

phaseconc-w
1  0 /  initial water phase concentration

phaseconc-o
0 1  / initial oil phase concentration



tinit
* T0 zT0 Tgrad
  25 0   0 /

/end

------------------------------------------------------------
compsect
------------------------------------------------------------
gravity
0 /
```

```
PrintKey
Pr_S 110
Pr_P 100
--Pr_CT 1
Pr_C  100
Pr_Vis 110
Pr_kr 110
  /

--PrintCF
--0 0 10*1  /  water concentrations
--0  /   oil concentrations

---PrintCTF
---1 1 1 /   total concentrations

Pr_Pcow

history
10  1000  / history print frequency minimum of every 100 timestep or
every 100 day

timestep
*dt0 (days)  qxmax dsmax dtfmax dtmax
  1e-08       60   0.01   1.5      /

tollit
*tollit itmax  seq_tol seq_itmax
1e-13   1000    1e-12    200 /

solver
seq /

--Turn on implicit transport algorithm
--ctransport
-- 1  /

------------------------------------------------------------
wellsect
------------------------------------------------------------
welldef
*name pcflag
 winj1  1 / (primary boundary)
*dir i1  j1   k1  k2   rw  open
  4  -1 /
/ terminates keyword

welldef
*name pcflag
 wprod1  1   / (secondary boundary)
*dir i1   j1   k1  k2   rw  open
 -4  -1 /
/ terminates keyword

wimb
```

```
*name   phase  plim hz0: boundary for counter-current flow (SI)
 winj1    w     0.5    0 /
1/  concentration of water
/   Vimbcell, Temper
/ terminates keyword

wprod
*name   r/p  rlim  plim Hz0
wprod1   p   500    1  0 / boundary for co-current production
/

pcwell
setting boundary capillary pressure for produced phase
*name  Pcboil  Pcbwater   SwPcbo  SwPcbw
 winj1 0.05     0.09         0.5       0.5    /
/ terminate keyword


time
0 60 120 240 600 720 900 1000 5000 10000 50000 100000 200000 250000
600000/ cumulative time to report in hr


end
/
```